

UNCLASSIFIED

AD NUMBER
ADB804447
NEW LIMITATION CHANGE
TO Approved for public release, distribution unlimited
FROM Distribution authorized to DoD only; Administrative/Operational Use; 03 MAR 1999. Other requests shall be referred to Air Force Materiel Command, Wright-Patterson AFB, OH 45433.
AUTHORITY
WHS ltr dtd Apr 2009

THIS PAGE IS UNCLASSIFIED

Reproduced by



CENTRAL AIR DOCUMENTS OFFICE

WRIGHT-PATTERSON AIR FORCE BASE - DAYTON, OHIO

AD-B804447

REEL-C

3045 B

A.T.I

5248

The
U.S. GOVERNMENT

IS ABSOLVED

FROM ANY LITIGATION WHICH MAY ENSUE FROM ANY
INFRINGEMENT ON DOMESTIC OR FOREIGN PATENT RIGHTS
WHICH MAY BE INVOLVED.

UNCLASSIFIED

Reproduced

FROM

LOW CONTRAST COPY.

ORIGINAL DOCUMENTS
MAY BE OBTAINED ON
LOAN

FROM

CADDO

UNCLASS.

JUN 25

1

SECURITY

DATE OF INITIATION

PRIORITY

680447

AUTHOR(S) Freberg, C. R. Hardy, J. A.	DIVISION(S): Power Plants, Reciprocating (6) SECTION(S): Components Induction, & Supercharging	ATI No. 5248 G.A. No. FR/31-10-44 (2)
---	---	---

CROSS REFERENCES: Manifolds, Intake (59655)

AMER. TITLE: Final Report on Study of Multi-Cylinder Engine Manifolds

FORG'N. TITLE:

ORIG. AGENCY: Purdue University, Engineering Experiment Station,
LaFayette, Indiana

TRANSLATION:

REMARKS:

COUNTRY	LANGUAGE	FOR. CLASS.	DATE	PAGES	ILLUS.	FEATURES
US.	English	—	Oct 1944	132	68	Photos, tables, diagrs, graphs, Graphs, Photos, Diagrams, Tables

ABSTRACT

Investigation shows technique and methods developed using electrical analogue for studying complex engine manifold problems. Equipment was developed for analyzing manifolds having any number of cylinders to obtain maximum volumetric efficiency. In manifold studied, peak efficiency was reached at 2900 rpm. By various changes in diameter and length of pipes, volumetric efficiency increased to 3300 rpm. Experiments show performance of properly designed individual pipes give better results than multi-cylinder manifold. Test results included.

ICM

EDITOR CHECK	AUTHOR CHECK	TRANSL. CHECK	TITLE CHECK	ABSTR. CHECK	CR. REF. CHECK	MX DATA CHECK	OK FOR TYPING	OK FOR FILMING
LG	AEW	AEW			AEW	AEW.	HS	

PURDUE UNIVERSITY
ENGINEERING EXPERIMENT STATION
LAFAYETTE, INDIANA

1161
MAY 28 1947

FINAL REPORT ON
STUDY OF MULTI-CYLINDER ENGINE MANIFOLDS

ATI No. 5248

by
C. R. Freberg
J. A. Hardy
E. N. Kemler

AIR DOCUMENTS DIVISION, T-2
AMC, WRIGHT FIELD
MICROFILM No.
R C-137 F 5248

ARMY AIR FORCES COOPERATIVE RESEARCH PROJECT

M-125-1

Contract No. W-535 ac-38886

PURDUE UNIVERSITY

OFFICE OF THE DEAN OF ENGINEERING
LAFAYETTE, INDIANA

A

November 24, 1944

Commanding General
Army Air Forces
Materiel Command
Wright Field
Dayton, Ohio

Subject: Letter of Transmittal for Report on "Final Report on Study of Multi-Cylinder Engine Manifolds", Contract No. W-535 ac-38886, Engineering Experiment Station Project M-125-1.

Gentlemen:

I am sending you under separate cover three copies of report on "Final Report on Study of Multi-Cylinder Engine Manifolds", which has been prepared by my colleagues Messrs. Freberg, Hardy and Kenler. This completes Item 1 of Contract No. W-535 ac-38886.

We have in previous reports to you discussed in considerable detail both the experimental and theoretical phases in the investigation of single pipe manifolds. The multi-cylinder engine manifold being considerably more complex cannot be handled by mathematical methods so that recourse must be made to experimental methods for its analysis. An experimental study of many manifolds failed to show how they could be dependably designed except by cut-and-dry method. This method is very long and expensive and not entirely satisfactory. In order to develop some shorter and more rational method, the possibilities of the

electrical-mechanical-acoustical analogue were investigated. This study showed that it is practical to analyze a manifold in the design stage by this method. In this analogue the air in the manifold and cylinders is replaced by equivalent lumped springs and masses of a mechanical system, which in turn is replaced by inductances and capacitances in an electrical circuit. Measurements can then be made in the electrical circuit which can be interpreted to give indications of the relative volumetric efficiency of the actual manifold system. The principal advantage of this method is that the equivalent of changes in pipe diameters and lengths can be easily made in the electrical system and their effects studied rather hurriedly once the analogue has been set up.

While this investigation was carried far enough to show that the use of the analogue for this purpose will work and has certain very definite advantages, further work should be done on it in order to reduce it to a point where it can be more simply and easily applied. This report has been concerned with determining whether or not such a method has possibilities and not with the reduction of this method to its simplest form.

The experimental work on actual manifolds indicates that the performance of manifolds which have individual pipes from a common source will give better results than any other type of multi-cylinder manifold. These conclusions are based on a limited number of tests. Because of the many possibilities with regard to individual cylinder pipe sizes and lengths, size

and length of common pipe, cylinder spacing, timing, etc. it is impossible to draw any general conclusions from a limited number of tests. The tests to date do, however, give some general trends and indicate some future factors which could be studied particularly in connection with the analogue. It is probable that the maximum amount of information can be obtained by carrying out a limited amount of experimental work in connection with a further study of the analogue as applied to manifold problems.

Respectfully submitted,



A. A. Potter
Dean of the Schools of Engineering and
Director of the Engineering Experiment Station

PURDUE UNIVERSITY
Engineering Experiment Station

FINAL REPORT ON
STUDY OF MULTI-CYLINDER ENGINE MANIFOLDS

by

C. R. Freberg
J. A. Hardy
E. N. Kemler

Army Air Forces Cooperative Research Project
M-125-1
Contract No. W-535 ac-38886

October 31, 1944

7

TABLE OF CONTENTS

SUMMARY	Page
	1
PART I	
I. Purpose	4
II. Electrical-Mechanical Analogies	4
III. Analogy for Acoustical Systems	20
IV. Determination of Acoustical Values	24
V. Apparatus	28
VI. Test Results	32
VII. Conclusions	38
PART II	
I. Purpose	40
II. Experimental Apparatus	40
III. Theory	41
IV. Experimental Results	47
V. Conclusions	57

Figures

LIST OF FIGURES (PART I)

Fig. No.

1. One Mass Mechanical System
2. One Inductance Electrical System
3. Velocity Impressed on One Mass System
4. Voltage Impressed on One Inductance System
5. Two Mass System
6. Two Inductance System
7. Simple System in the Indirect Analogue
8. Indirect Analogue Comparison of Elements
9. Two Mass System and Indirect Analogue
10. One Cylinder System - One Mass
11. One Cylinder System - Two Masses
12. Two Cylinder System
13. Three Cylinder System
14. Schematic Diagram of Analogous Manifold System
15. Electric Circuit of Analogous Manifold System
16. Rotating Condensers
17. Rotating Contactor
18. Complete Setup
19. Six Cylinder Manifold
20. Measuring Method Diagram
- 20-A Three Cylinder Results
21. Results for Six Cylinder with No Damping
22. Results for Six Cylinder with 2000 ohms Damping

Fig. No.

- 23. Results on Six Cylinder Manifold Without Large End Pipe
- 24. Results on Six Cylinder Manifold Without Pipe Between Front and Rear Cylinders
- 25. Results on Six Cylinder Manifold With 5000 ohms Damping
- 26. Manifold With Larger Pipe Between Front and Rear Cylinders
- 27. Results for Larger Pipe Between Front and Rear Cylinders
- 28. Results for Larger Pipe With End Pipe Removed
- 29. Changed Length of Pipe Between Front and Rear Cylinders
- 30. Results for Changed Length of Pipe Between Front and Rear Cylinders
- 31. Manifold with Individual Pipe Diameters Changed
- 32. Results With Individual Pipe Diameters Changed
- 33. Results With End Pipe Removed

LIST OF FIGURES (PART II)

Fig. No.

1. Engine Data
2. Experimental Engine
3. Diagram of Three Cylinder Manifold
4. Diagram of Three Cylinder Manifold
5. Compression Pressures, Single Cylinder Manifolds
6. Pressure Diagrams, Single Cylinder Manifolds
7. Compression Pressures, Two Cylinder Manifolds
8. Compression Pressures, Two Cylinder Manifolds
9. Pressure Diagrams, Two Cylinder Manifold
10. Compression Pressures, 1" Diameter, Three Cylinder Manifold, 25" Branch Pipes, 3" Inlet Pipe
11. Pressure Diagrams, 1" Diameter, Three Cylinder Manifold, 25" Branch Pipes, 3" Inlet Pipe
12. Compression Pressures, 1" Diameter, Three Cylinder Manifold, 25" Branch Pipes, 13" Inlet Pipe
13. Pressure Diagrams, 1" Diameter, Three Cylinder Manifold, 25" Branch Pipes, 13" Inlet Pipe
14. Compression Pressures, 1" Diameter, Three Cylinder Manifold, 25" Branch Pipes, 33" Inlet Pipe
15. Pressure Diagrams, 1" Diameter, Three Cylinder Manifold, 25" Branch Pipes, 33" Inlet Pipe
16. Compression Pressures, 1" Diameter, Three Cylinder Manifold, 15" Branch Pipes, 3" Inlet Pipe
17. Pressure Diagrams, 1" Diameter, Three Cylinder Manifold, 15" Branch Pipes, 3" Inlet Pipe
18. Compression Pressures, 1" Diameter, Three Cylinder Manifold, 15" Branch Pipes, 13" Inlet Pipe
19. Pressure Diagrams, 1" Diameter, Three Cylinder Manifold, 15" Branch Pipes, 13" Inlet Pipe
20. Compression Pressures, 1" Diameter, Three Cylinder Manifold, 4" Branch Pipes, 13" Inlet Pipe

Fig. No.

21. Pressure Diagrams, 1" Diameter, Three Cylinder Manifold, 4" Branch Pipes, 13" Inlet Pipe
22. Compression Pressures, 1" Diameter, Three Cylinder Manifold, 4" Branch Pipes, 33" Inlet Pipe
23. Pressure Diagrams, 1" Diameter, Three Cylinder Manifold, 4" Branch Pipes, 33" Inlet Pipe
24. Compression Pressures, 1-1/4" Diameter, Three Cylinder Manifold, 3" Branch Pipes, 2-1/2" Inlet Pipe
25. Pressure Diagrams, 1-1/4" Diameter, Three Cylinder Manifold, 3" Branch Pipes, 2-1/2" Inlet Pipe
26. Compression Pressures, 1-1/4" Diameter, Three Cylinder Manifold, 3" Branch Pipes, 19" Inlet Pipe
27. Pressure Diagrams, 1-1/4" Diameter, Three Cylinder Manifold, 3" Branch Pipes, 19" Inlet Pipe
28. Compression Pressures, 1-1/4" Diameter, Three Cylinder Manifold, 14" Branch Pipes, 2-1/2" Inlet Pipe
29. Pressure Diagrams, 1-1/4" Diameter, Three Cylinder Manifold, 14" Branch Pipes, 2-1/2" Inlet Pipe
30. Compression Pressures, Six Cylinder Manifold Without Carburetor
31. Pressure Diagrams, Six Cylinder Manifold Without Carburetor
32. Pressure Diagrams, Six Cylinder Manifold Without Carburetor
33. Compression Pressures, Six Cylinder Manifold With Carburetor
34. Pressure Diagrams, Six Cylinder Manifold With Carburetor
35. Pressure Diagrams, Six Cylinder Manifold With Carburetor

SUMMARY

The general study of engine manifolds started with the analysis of the simple single pipe manifold or induction pipe which would be used on a single cylinder engine. Previous reports have considered both the experimental and theoretical phases of the single pipe manifold. After considerable experimental work reasonable agreement between a simplified theory and experimental results was obtained. The study of multicylinder manifolds is too difficult to undertake mathematically. The experimental study of such manifolds is difficult because of the many variables involved. A considerable study of many manifolds failed to show how they could be dependably designed. The cut and try method for manifolds is of course a long and expensive procedure. In an attempt to develop some shorter and more rational method, the possibilities of the electrical-mechanical-acoustical analogue has been investigated.

Since this report involves two different approaches to the multi-cylinder problem, it has been divided into two distinct and independent parts. The first discusses the work done in adapting the analogue or electrical model to the study of the manifold problem, and the second to further experimental work. The following gives a brief summary of each Part.

Part I.

This section of the report shows that an engine manifold may be analyzed while in the proposed design stage to determine the speed at which a particular manifold will give peak efficiency. The

analysis is carried out on a six cylinder manifold and shows the effect of changing pipe diameters and lengths.

The air in the manifold and cylinders has both mass and elasticity so it is first replaced by an equivalent system of lumped springs and masses. The first part of the report shows how this mechanical system of weights and springs can be replaced by electrical elements in an electrical circuit according to the principles of electrical-mechanical analogies. Measurements can then be made on this electrical circuit which may be interpreted to give the volumetric efficiency of the original manifold system.

The main value in this method of analysis lies in the fact that the effect of changes in diameter and length may be determined quickly and easily.

In the particular manifold studied the peak efficiency was reached at about 2900 rpm. By various changes in diameter and length the peak speed was raised to about 3300 rpm.

Part II.

The experimental work which has been done to date indicates that the performance of properly designed individual pipes from a common source will give better results than any other type of multi-cylinder manifold. The study indicated that for reasonable designs the common pipe in a six cylinder manifold shows practically steady flow and is, therefore, not much of a factor in the performance of the manifold. This permits symmetrical manifolds of the six or twelve cylinder type to be broken down into three cylinder units (for the commonly used types).

The air motion in the three cylinder manifold can be divided into (1) a ramming effect and (2) resonant vibrations. The total ramming effect includes the entire air column. The ramming effect of the branch columns is of greater importance than the common inlet pipe. Resonance vibrations in the inlet pipe to a three cylinder section are not, in general, effective in increasing the volumetric efficiency.

-4-

PART I.

I. Purpose

This part of the report has two purposes; the first purpose is to give a thorough discussion of electrical-mechanical-acoustical analogues and the second is to show that they may be adapted to solve engine manifold problems. Techniques and equipment were developed so that manifolds for any number of cylinders could be analyzed for maximum volumetric efficiency.

II. Electrical-Mechanical Analogies

Electrical-mechanical analogies can be set up in a variety of ways depending upon the conditions of the problems. That is, some mechanical systems have constant forces applied to them to make them vibrate, others have constant velocity or displacement. The choice of the type of analogy then depends mostly upon the electrical circuit requirements. Fundamentally, there are two types of analogies, the direct and the indirect. These will be described separately in succeeding pages.

Direct Analogue for Simple Mechanical System

In a simple mechanical system consisting of a mass, a spring, a damper, and a harmonic disturbing force such as shown in Fig. 1, the equation of motion is given as

$$\frac{W}{g} \frac{d^2x}{dt^2} + r \frac{dx}{dt} + kx = P \sin \nu t \quad (1)$$

where W = weight of the mass - lb

g = acceleration due to gravity - 386 in/sec²

x - displacement - inches

t - time - sec

r - damping coefficient - lb sec/in.

k - spring constant - lb/in.

F - amplitude of force - lb

ν - forced frequency - radians/sec

This equation may be put in dimensionless form by changing the variable x and t by making the following substitutions:

$$X = \frac{x}{l} \quad \text{and} \quad T = \omega t \quad (2)$$

where l is some characteristic length or displacement and ω is some frequency such as the natural frequency. (See Freberg and Kemler - "Elements of Mechanical Vibration" Chapter VIII - John Wiley & Sons for more detailed discussion).

If these dimensionless quantities are differentiated, they give

$$\frac{dx}{dt} = \omega l \frac{dX}{dT}$$

and

$$\frac{d^2x}{dt^2} = \omega^2 l \frac{d^2X}{dT^2}$$

When these terms are substituted in equation (1), the result is

$$\frac{W}{g} \omega^2 l \frac{d^2X}{dT^2} + r \omega l \frac{dX}{dT} + k l X = F_0 \sin \left[\frac{\nu}{\omega} \right] T$$

When this expression is divided by $\frac{W}{g} \omega^2 l$, it becomes

$$\frac{d^2X}{dT^2} + \left[\frac{rg}{W\omega} \right] \frac{dX}{dT} + \left[\frac{kg}{W\omega^2} \right] X = \left[\frac{F_0 g}{Wl\omega^2} \right] \sin \left[\frac{\nu}{\omega} \right] T$$

The first term is dimensionless since it involves only the dimensionless factors T and X, so all others must be dimensionless. Since X, T, and their derivatives are dimensionless, all terms in the brackets are also dimensionless. These terms involve only the physical characteristics and applied force of the system. Therefore, if any two systems have identical values for these dimensionless terms, the two systems will have identical motion and frequencies.

If the equation for an electrical circuit such as shown in Fig. 2 consisting of an inductance, resistance, capacitance, and an alternating voltage in series is written on the basis of Kirchoff's law, it is

$$L \frac{d^2q}{dt^2} + R \frac{dq}{dt} + \frac{1}{C} q = E_0 \sin \phi t \quad (4)$$

where L = inductance - henries

q = charge - coulombs

t = time - seconds

R = resistance - ohms

C = capacitance - farads

E₀ = amplitude of voltage - volts

φ = forced frequency - radians/sec

If equations (1) and (4) are compared it will be noted that they have the same form with

$\frac{W}{g}$	corresponding to	L
x	"	q
r	"	R
k	"	$\frac{1}{C}$

F_0 corresponding to E_0

" "

$\frac{dx}{dt}$ " " $\frac{dq}{dt}$

$\frac{d^2x}{dt^2}$ " " $\frac{d^2q}{dt^2}$

Equation (4) may be reduced to dimensionless form just as equation (1) was by substituting

$$Q = \frac{q}{Q_0} \text{ and } T = \Omega t \quad (5)$$

The resulting equation that corresponds to equation (3) is

$$\frac{d^2Q}{dT^2} + \left[\frac{R}{L \Omega} \right] \frac{dQ}{dT} + \left[\frac{1}{C L \Omega^2} \right] Q = \left[\frac{E_0}{L \Omega_2 \Omega^2} \right] \sin \left[\frac{\phi}{\Omega} \right] T \quad (6)$$

From this it may be seen that the terms in the brackets are dimensionless and determine the characteristics and applied voltage of the circuit. In fact since equations (3) and (6) are identical except for notation, the resulting motion and frequencies will behave the same for both systems if the dimensionless terms of one system are equal to the corresponding terms in the other system.

In some types of problems a constant displacement or velocity is impressed upon the mechanical system. A simple one mass system of this kind is shown in Fig. 3. If a harmonic velocity V_1 is impressed at the top of the spring, two equations may be written both based on the equation

$$V_1 \sin \nu t = V_2 + V_{1,2} \quad (7)$$

The velocity of V_2 can be expressed in terms of both the damping or inertia forces, that is

$$F_1 = V_2 r \quad \text{or} \quad V_2 = \frac{F_1}{r} \quad (8)$$

and

$$F_2 = \frac{W}{g} \frac{dV}{dt} \quad \text{or} \quad V_2 = \int \frac{F_2 g}{W} dt \quad (9)$$

The two equations are therefore

$$V_1 \sin \nu t = \frac{F_1}{r} + V_{1,2} = \frac{F}{r} + \frac{1}{k} \frac{dF_3}{dt}$$

$$V_1 \sin \nu t = \int \frac{F_2 g}{W} dt + \frac{1}{k} \frac{dF_3}{dt}$$

To reduce these to a dimensionless form, the dimensionless quantities

$$\mathcal{F}_1 = \frac{F}{F_0} \quad \text{and} \quad \mathcal{T} = \omega t$$

may be substituted to give

$$V_1 \sin \frac{\nu}{\omega} \mathcal{T} = \frac{\mathcal{F}_1 F_0}{r} + \frac{\omega F_0}{k} \frac{d\mathcal{F}_3}{d\mathcal{T}}$$

and

$$V_1 \sin \frac{\nu}{\omega} \mathcal{T} = \int \frac{F_0 \mathcal{F}_2 g}{W \omega} d\mathcal{T} + \frac{\omega F_0}{k} \frac{d\mathcal{F}_3}{d\mathcal{T}}$$

Dividing both equations by $\omega F_0/k$ gives the dimensionless forms

$$\left[\frac{V_1 k}{\omega F_0} \right] \sin \left[\frac{\nu}{\omega} \right] \mathcal{T} = \left[\frac{k}{r \omega} \right] \mathcal{F}_1 + \frac{d\mathcal{F}_3}{d\mathcal{T}} \quad (10a)$$

and

$$\left[\frac{V_1 k}{\omega F_0} \right] \sin \left[\frac{\nu}{\omega} \right] \mathcal{T} = \left[\frac{k g}{W \omega^2} \right] \mathcal{F}_2 + \frac{d\mathcal{F}_3}{d\mathcal{T}} \quad (10b)$$

These dimensionless terms are the same as those previously found for the other mechanical system where a force was applied.

The term $\left[\frac{V_1 k}{F_0} \right]$ differs from $\left[\frac{F_0 g}{\pi \omega^2 l} \right]$ only in form but may be made similar by combining two dimensionless terms as

$$\left[\frac{V_1 k}{\omega F_0} \right] \left[\frac{\pi \omega^2}{k g} \right] = \left[\frac{V_1 \pi \omega}{F_0 g} \right] = \left[\frac{\pi l \omega^2}{F_0 g} \right]$$

Since the system has simple harmonic motion velocity V is equal to the product of the displacement l and the angular velocity or

$$V_1 = l \omega$$

This can be explained physically by assuming that l is the maximum displacement. Then V is the maximum velocity. The dimensionless equations then are expressed in percentage of maximum displacement or velocity. The quantity $\frac{k}{r \omega}$ also corresponds to $\frac{r g}{\pi \omega}$ because when $\frac{k}{r \omega}$ is multiplied by the other dimensionless term, that is

$$\left[\frac{k}{r \omega} \right] \left[\frac{\pi \omega^2}{k g} \right] = \frac{\pi \omega}{r g}$$

the original value obtained by the first analysis is obtained.

The equivalent electrical circuit is shown in Fig. 4.

From Kirckhoffs law it is known that

$$I_1 = I_2 + I_{1,2} \quad (11)$$

The values of $I_{1,2}$ and I_2 are therefore

$$I_{1,2} = C \frac{dE_1}{dt} \quad (12)$$

$$I_2 = \frac{1}{L} \int E_2 dt \quad (13)$$

$$I_2 = \frac{E_1}{R} \quad (14)$$

These terms when substituted above give for I_1

$$I_1 = \frac{E_1}{R} + C \frac{dE_2}{dt}$$

$$I_1 = \frac{1}{L} \int E_2 dt + C \frac{dE_2}{dt}$$

Dimensionless terms of the form

$$\mathcal{E} = \frac{E}{E_0} \text{ and } T = \Omega t$$

may be used to give the equations

$$\left[\frac{r_1}{C \Omega E_0} \right] \sin \left[\frac{\phi}{\Omega} \right] T = \left[\frac{1}{C R \Omega} \right] \mathcal{E}_1 + \frac{d\mathcal{E}_2}{dT} \quad (15a)$$

and

$$\left[\frac{I_1}{C \Omega E_0} \right] \sin \left[\frac{\phi}{\Omega} \right] T = \left[\frac{1}{C L \Omega^2} \right] \mathcal{E}_2 + \frac{d\mathcal{E}_2}{dT} \quad (15b)$$

These terms are analogous to those in the mechanical system where a force was impressed on the system.

Direct Analogue for Multi-Mass Systems

Usually problems involve several masses, dampers, and springs. These two may be represented by analogous electrical circuits. The general relations may be conveniently inferred from a two mass system such as shown in Fig. 5.

For this system two force equations can be written. They

are

$$\frac{W_1}{g} \frac{d^2 x_1}{dt^2} + r_1 \frac{dx_1}{dt} + k_1 x_1 + k_2 (x_1 - x_2) = F_1 \sin \nu_1 t \quad (16)$$

and

$$\frac{W_2}{g} \frac{d^2 x_2}{dt^2} + r_2 \frac{dx_2}{dt} + k_2 (x_2 - x_1) = F_2 \sin \nu_2 t \quad (17)$$

By using dimensionless quantities of the form

$$X = \frac{x}{l} \quad \text{and} \quad T = \omega t$$

these force equations reduce to

$$\frac{W_1}{g} l_1 \omega^2 \frac{d^2 X_1}{dT^2} + r_1 l_1 \omega \frac{dX_1}{dT} + k_1 l_1 X_1 + k_2 (l_1 X_1 - l_2 X_2) = F_1 \sin \frac{\nu_1}{\omega} T$$

and

$$\frac{W_2}{g} l_2 \omega^2 \frac{d^2 X_2}{dT^2} + r_2 l_2 \omega \frac{dX_2}{dT} + k_2 (l_2 X_2 - l_1 X_1) = F_2 \sin \frac{\nu_2}{\omega} T$$

Dividing by the first coefficients gives

$$\frac{d^2 X_1}{dT^2} + \left[\frac{r_1 g}{W_1 \omega} \right] \frac{dX_1}{dT} + \left[\frac{k_1 g}{W_1 \omega^2} \right] X_1 + \left[\frac{k_2 g}{W_1 \omega^2} \right] X_1 - \left[\frac{k_2 l_2 g}{W_1 l_1 \omega^2} \right] X_2 = \left[\frac{F_1 g}{W_1 l_1 \omega^2} \right] \sin \left[\frac{\nu_1}{\omega} \right] T \quad (18a)$$

and

$$\frac{d^2 X_2}{dT^2} + \left[\frac{r_2 g}{W_2 \omega} \right] \frac{dX_2}{dT} + \left[\frac{k_2 g}{W_2 \omega^2} \right] X_2 - \left[\frac{k_1 l_1 g}{W_2 l_2 \omega^2} \right] X_1 - \left[\frac{F_2 g}{W_2 l_2 \omega^2} \right] \sin \left[\frac{\nu_2}{\omega} \right] T \quad (18b)$$

Since l_1 and l_2 are some length or displacement, taking them equal will mean that x_1 and x_2 are being measured to the same scale. This is desirable to facilitate measurements. Under these conditions then the dimensionless constants are

$$\frac{r_1 g}{\pi_1 \omega} \quad \text{and} \quad \frac{r_2 g}{\pi_2 \omega}$$

$$\frac{k_1 g}{\pi_1 \omega^2}, \quad \frac{k_1 g}{\pi_2 \omega^2}, \quad \frac{k_2 g}{\pi_1 \omega^2}, \quad \text{and} \quad \frac{k_2 g}{\pi_2 \omega^2}$$

$$\frac{F_1 g}{\pi_1 l \omega^2}, \quad \frac{F_2 g}{\pi_2 l \omega^2}, \quad \frac{V_1}{\omega}, \quad \frac{V_2}{\omega}$$

The equivalent electrical circuit is shown in Fig. 6. Each mesh is made to include all the elements needed to give voltage drop terms corresponding to each term in each force equation. The voltage equations then are

$$L_1 \frac{d^2 q_1}{dt^2} + R_1 \frac{dq_1}{dt} + \frac{1}{C_1} q_1 + \frac{1}{C_2} (q_1 - q_2) = E_1 \sin \phi_1 t \quad (20a)$$

and

$$L_2 \frac{d^2 q_2}{dt^2} + R_2 \frac{dq_2}{dt} + \frac{1}{C_2} (q_2 - q_1) = E_2 \sin \phi_2 t \quad (20b)$$

By using the dimensionless forms

$$q = \frac{q}{Q_0} \quad \text{and} \quad T = \Omega t$$

the dimensionless terms are found to be

$$\frac{R_1}{L_1 \Omega} \quad \text{and} \quad \frac{R_2}{L_2 \Omega}$$

$$\frac{1}{C_1 L_1 \Omega^2}, \quad \frac{1}{C_1 L_2 \Omega^2}, \quad \frac{1}{C_2 L_1 \Omega^2}, \quad \text{and} \quad \frac{1}{C_2 L_2 \Omega} \quad (21)$$

$$\frac{E_1}{I_1 \omega_0 \Omega^2}, \frac{E_2}{I_2 \omega_0 \Omega^2}, \frac{\phi_1}{\Omega}, \frac{\phi_2}{\Omega}$$

These correspond term for term with those of the mechanical system.

The close correlation of terms in the electrical and mechanical system suggests the possibility of setting up an electrical circuit on which measurements could be made. These measurements would not only represent answers to the electrical problems but could be correlated with answers in a mechanical system as long as the dimensionless quantities for the two systems are made equal.

The correlation needed in setting up a system depends upon the answers desired. If the points of maximum response, that is the natural frequencies, are wanted, the terms involving only masses and spring constants are needed.

When dealing with a large number of masses, spring constants, etc. the calculations may be simplified by choosing one mass, one spring constant, one damper, one force, etc. and the corresponding quantities in the electrical system. Thereafter, all other electrical elements are directly or indirectly proportional to their mechanical counterpart according to the basic analogy. This may be demonstrated using the terms of the two mass system. Combining two or more dimensionless quantities gives

$$\left[\frac{1}{C_1 I_1 \Omega^2} \right] \left[\frac{C_1 I_2 \Omega^2}{1} \right] = \left[\frac{k_1 \epsilon}{W_1 \omega^2} \right] \left[\frac{W_2 \omega^2}{k_1 \epsilon} \right] \quad \text{or} \quad \frac{I_2}{I_1} = \frac{W_2}{W_1}$$

$$\left[\frac{R_1}{I_1 \Omega} \right] \left[\frac{I_2 \Omega}{R_2} \right] = \left[\frac{r_1 \epsilon}{W_1 \omega} \right] \left[\frac{W_2 \omega}{r_2 \epsilon} \right] \quad \text{or} \quad \frac{R_1}{R_2} = \frac{r_1}{r_2}$$

$$\left[\frac{1}{C_1 L_1 \Omega^2} \right] \left[\frac{C_2 L_1 \Omega^2}{1} \right] = \left[\frac{k_1 g}{W_1 \omega^2} \right] \left[\frac{W_1 \omega^2}{k_2 g} \right] \quad \text{or} \quad \frac{C_2}{C_1} = \frac{k_1}{k_2} \quad (22)$$

$$\left[\frac{E_1}{L_1 Q_0 \Omega^2} \right] \left[\frac{L_2 Q_0 \Omega^2}{E_2} \right] = \left[\frac{F_1 g}{W_1 l \omega^2} \right] \left[\frac{W_2 l \omega^2}{F_2 g} \right] \quad \text{or} \quad \frac{E_1}{E_2} = \frac{F_1}{F_2}$$

$$\left[\frac{v_1}{\omega} \right] \left[\frac{\omega}{v_2} \right] = \left[\frac{\phi_1}{\Omega} \right] \left[\frac{\Omega}{\phi_2} \right] \quad \text{or} \quad \frac{v_1}{v_2} = \frac{\phi_1}{\phi_2}$$

The elements of the direct analogy may be summed up in a table such as Table I. The analogous quantities and the dimensionless quantities are listed in Table II.

Indirect Analogy for Simple Mechanical System

In the inverted analogy the approach is essentially the same, that is, through differential equations. In this case the force is made analogous to the current and the velocity analogous to the voltage. The expressions for each type of element, both mechanical and electrical, are listed in Table III with the analogous quantities directly opposite one another.

To begin with let us take the same example as used previously, that is, Fig. 1. The equation must be a force equation because a force is applied so that one writes

$$\frac{W}{g} \frac{dv}{dt} + r v + k \int v dt = F_0 \sin \nu t \quad (23)$$

This may be reduced to dimensionless form by substituting

$$s = \frac{\nu}{\Omega} \quad \text{and} \quad T = \Omega t$$

and their derivatives into equation (23). The result is

$$\frac{dz}{dT} + \left[\frac{Fk}{W\omega} \right] z + \left[\frac{kg}{W\omega^2} \right] \int z dT = \left[\frac{F_0 g}{W V \omega} \right] \sin \left[\frac{\nu}{\omega} \right] T \quad (24)$$

These terms in the brackets are dimensionless and determine the characteristics of the system.

If in an electrical circuit we put all the elements in parallel with the disturbing current as shown in Fig. 7, it is necessary to supply a constant amplitude current because it is analogous to the force. Also it is necessary to write a current equation. The supplied must equal the sum of the other currents so that we can write

$$C \frac{dE}{dt} + \frac{E}{R} + \frac{1}{L} \int E dt = I_0 \sin \phi t \quad (25)$$

Now this equation is the same as equation (23) term for term with

C	corresponding to	$\frac{W}{g}$
E	"	v
$\frac{1}{R}$	"	r
$\frac{1}{L}$	"	k
I_0	"	F_0
ϕ	"	ν
$\frac{dE}{dt}$	"	$\frac{dv}{dt}$
$\int E dt$	"	$\int v dt$

The electrical equation may be put in dimensionless form by substituting

$$Y = \frac{E}{E_0} \quad \text{and} \quad T = \Omega t$$

and the derivative so that the result is

$$\frac{dY}{dT} + \left[\frac{1}{RC\Omega} \right] Y + \left[\frac{1}{LC\Omega^2} \right] \int Y dt = \left[\frac{I_0}{C E_0 \Omega} \right] \sin \left[\frac{\phi}{\Omega} \right] T \quad (26)$$

Thus all the terms in the brackets are dimensionless and they along determine the characteristics of the circuit. Since equations (24) and (26) are the same, except for notation for an electric circuit with the same dimensionless constants as for the mechanical system, the resulting motion will be the same.

In the inverted system it should be noted that the diagrams are similar as shown by the adapted diagrams of Fig. 8 wherein parallel elements are equivalent to parallel elements and series elements are equivalent to series elements. In comparing the direct analogy with the inverted analogy, it is found that the dimensionless constants are different in most cases as shown in Table IV.

When damping is neglected in a free vibration system, the two systems become identical.

Indirect Analogies for Multi-Mass Systems

It is necessary to develop certain generalities for multi-mass systems in order to deal with manifold problems. A two mass system will be used to illustrate the principles for an inverted analogy. A similar analysis was used for the direct analogy. (See Freberg and Kemler, "Elements of Mechanical Vibration").

A two mass system such as Fig. 9a can be drawn schematically as shown in Fig. 9b. The equivalent electrical circuit of an inverted analogy takes on the same form as the mechanical system as

shown in Fig. 9c. The analogous quantities given in Table III help in drawing up this diagram. From this the equations for velocity and voltage may be written as follows:

$$\begin{aligned}
 V &= V_1 + \frac{1}{k_1} \frac{dF_1}{dt} & E &= E_1 + L_1 \frac{dI_1}{dt} \\
 V_1 &= \frac{F_2}{W_1} \int F_2 dt & E_1 &= \frac{1}{C_1} \int I_2 dt \\
 V_1 &= \frac{F_3}{r_1} & E_1 &= R_1 I_3 \\
 V_1 &= V_2 + \frac{1}{k_2} & E_1 &= E_2 + L_2 \frac{dI_4}{dt} \\
 V_2 &= \frac{F_5}{W_2} \int F_5 dt & E_2 &= \frac{1}{C_2} \int I_5 dt \\
 V_2 &= \frac{F_6}{r_2} & E_2 &= R_2 I_6
 \end{aligned} \tag{27}$$

These equations may be combined to give various forms which can be made non-dimensional by changing variables. If the first and second are considered the equation is

$$V = \frac{F_2}{W_1} \int F_2 dt + \frac{1}{k_1} \frac{dF_1}{dt} \tag{28}$$

For the first and third

$$V = \frac{F_3}{r_1} + \frac{1}{k_1} \frac{dF_1}{dt} \tag{29}$$

For the first, fourth, and fifth

$$V = \frac{F_5}{W_2} \int F_5 dt + \frac{1}{k_2} \frac{dF_4}{dt} + \frac{1}{k} \frac{dF_1}{dt} \tag{30}$$

For the first, fourth, and sixth

$$V = \frac{F_6}{r_2} + \frac{1}{k_2} \frac{dF_4}{dt} + \frac{1}{k_1} \frac{dF_1}{dt} \quad (31)$$

These may be reduced to dimensionless forms just as a single mass system by substituting terms of the form

$$Z = \frac{V}{V_0}, \quad T = \omega t, \quad \mathcal{F} = \frac{F}{F_0} \quad (32)$$

The dimensionless forms of equations 28 through 31 become

$$\frac{Z V_0 k_1}{\omega F_{01}} = \frac{k_1 \epsilon F_{02}}{W_1 \omega^2 F_{01}} \int \mathcal{F}_2 dT + \frac{d \mathcal{F}_1}{dT} \quad (33)$$

$$\frac{Z V_0 k_1}{\omega F_{01}} = \frac{k_1 F_{03}}{r_1 \omega F_{01}} \mathcal{F}_3 + \frac{d \mathcal{F}_1}{dT} \quad (34)$$

$$\frac{Z V_0 k_1}{\omega F_{01}} = \frac{k_1 \epsilon F_{05}}{W_2 \omega^2 F_{01}} \int \mathcal{F}_5 dT + \frac{k_1}{k_2} \frac{F_{04}}{F_{01}} \frac{d \mathcal{F}_4}{dT} + \frac{d \mathcal{F}_1}{dT} \quad (35)$$

$$\frac{Z V_0 k_1}{\omega F_{01}} = \frac{k_1 F_{06}}{r_2 F_{01}} \mathcal{F}_6 + \frac{k_1}{k_2} \frac{F_{04}}{F_{01}} \frac{d \mathcal{F}_4}{dT} + \frac{d \mathcal{F}_1}{dT} \quad (36)$$

Similar changes may be made in the electrical equations so that dimensionless terms may also be determined. On the other hand the analogous terms may be substituted in the mechanical terms that are dimensionless to obtain the equivalent terms directly.

They are

$$\frac{k_1 \epsilon}{W_1 \omega^2} = \frac{1}{L_1 C_1 \Omega^2}$$

$$\frac{k_1}{r_1 \omega} = \frac{R_1}{L_1 \Omega}$$

$$\frac{k_1}{k_2} = \frac{L_2}{L_1}$$

$$\frac{k_1}{W_2} = \frac{g}{\omega^2} = \frac{1}{L_1 C_2 \Omega^2} \quad (37)$$

$$\frac{k_1}{r_2} = \frac{R_2}{L_1}$$

$$\frac{V_0 k_1}{\omega F_{ol}} = \frac{E_0}{L_1 \Omega I_{ol}}$$

These are set up on the assumption that the ratio of various forces as indicated are equal to analogous ratios in the electrical circuits. Equation (37) are not in a generally convenient form for actually using them with the greatest ease. One equality may be divided by another in several instances so that the basic relations are

$$\frac{k_1 g}{W_1 \omega^2} = \frac{1}{L_1 C_1 \Omega^2}$$

$$\frac{k_1}{r_1 \omega} = \frac{R_1}{L_1 \Omega}$$

$$\frac{k_1}{k_2} = \frac{L_2}{L_1}$$

$$\frac{r_1}{r_2} = \frac{R_2}{R_1}$$

$$\frac{W_1}{W_2} = \frac{C_1}{C_2}$$

$$\frac{V_0 k_1}{\omega F_{ol}} = \frac{E_0}{L_1 \Omega I_{ol}}$$

(38)

These equations show that the whole system is determined once the first set of values are determined. The remaining quantities are proportional to those in the original system.

This analysis can be repeated for 3, 4, or any other number of masses. The result, however, will be the same as the two mass system. After one inductance, one resistance, and one capacitance have been chosen to correspond to the mechanical quantities, all others will bear the same relative proportions as the mechanical quantities, that is, either directly or indirectly proportional as shown in Table IV. This is a generality for either the direct or inverted analogy keeping in mind which quantities are analogous and whether they are directly or indirectly proportional. The diagram for the final electrical circuit is shown in Fig. 9d.

III. Analogy for Acoustical System

In an acoustical system the problems and analysis is very nearly the same as an ordinary mechanical system except the mass, spring, and resistance are distributed. This is ordinarily handled by partial differential equations. The equation of motion in a pipe is then given as (See Morse - Vibration & Sound - McGraw-Hill)

$$d_0 \frac{\partial^2 y}{\partial t^2} + r \frac{\partial y}{\partial t} - p_0 \gamma \frac{\partial^2 y}{\partial x^2} \quad (39)$$

where d_0 = mass density - lb sec²/in.⁴

y = particle displacement

t = time - sec

r = damping coefficient per unit volume - lb sec/in.⁴

p_0 = equilibrium pressure - lb/in.²

γ = 1.4

x = distance along the pipe - in.

The analogous electrical circuit would have to be supplied by a transmission line. The transmission line equation is

$$L \frac{\partial^2 Q}{\partial t^2} + R \frac{\partial Q}{\partial t} = \frac{i}{C} \frac{\partial^2 Q}{\partial x^2} \quad (40)$$

where L = inductance - henries

Q = charge - coulombs

t = time - seconds

R = resistance - ohms

C = capacitance - farads

X = distance along wire - inches

This shows that the two are identical in the direct analogy. They could also be made identical in the inverted analogy by writing a force equation in terms of the velocity and a current equation in terms of the voltage.

This approach is possible with a simple system consisting of a single cylinder and its intake pipe. With the addition of more cylinders the pipe becomes branched and the analysis and equations becomes extremely difficult to set up. Therefore, a simpler approach is desirable.

Usually in acoustical problems branched pipes are approximated by lumping masses, damping and elasticity. When the lumps are very small, the system approaches the distributed system very closely.

It was necessary to choose between the direct and inverted analogy. Several reasons led us to try the inverted analogy first among which were considerations of possible electrical circuits. Subsequent trials indicated that the reasoning for the direct analogy was easier and that measurements could be made to indicate volumetric efficiency almost directly. In the indirect system no satisfactory means of measuring volumetric efficiency was found. This was mainly because the volumetric efficiency depends upon the displacement. However, the displacement has no counterpart in the electrical system except $\int E dt$. Normally no interpretation is placed upon this term in electrical work so reasoning becomes difficult.

After a number of preliminary tests and trials the direct analogy was then adopted. A one cylinder system is shown in Fig. 10a and its direct equivalent electrical system is shown in Fig. 10b. No attention will be devoted to valve action as yet in order to simplify the explanation. The piston moves with nearly sinusoidal motion and acts on the cylinder and pipe volumes. The air in the cylinder moves so slowly compared with that in the pipe that its mass effects may be neglected. It does act as a spring, however. The pipe acts both as a mass and a spring. Therefore, some means must be adopted to allow for the distributed mass and spring effects of the pipe. If the air in the pipe were divided into small lumps we would have a close approximation of a distributed system. Actually relatively few lumps are needed. Figures 11a and 11b show a single pipe system represented by two springs and two masses.

When there are two cylinders jointed by a common intake pipe, the diagram changes slightly due to the new conditions at the point of branching. The system is shown in Fig. 12a. The weights are concentrated at the middle of pipe length they represent and if the lengths were divided into more than one lump the lumps should be equal to give a better distribution of harmonics in pipe.

The equivalent electrical circuit is shown in Fig. 12b. It indicates that the method of handling branched pipe systems requires the introduction of a new concept. The displacement of a mass of air in one pipe equals the sum of the displacements in its branches. This is the law of continuity. This is analogous to the electrical principle that the electricity flowing in one wire equals the sum of that flowing in its branches. To correlate this principle in the two systems the one pipe may be considered in series with each branch simultaneously. In the electrical system then each of the branch condensers is in parallel with the main condenser individually. That is, each branch condenser is in a mesh by itself with the main condenser. This makes all condensers in parallel.

The branched system involving three cylinders connected to a common pipe such as shown in Fig. 13 forms the basis for the six cylinder investigation. The lumping of masses and elasticities is as indicated. The electrical circuit using the direct analogy is shown in Fig. 13

In all these cases, the method of determining the equivalent values is basically the same as for a one mass-one spring system.

The analogous terms given in Table II must be made equal. When multi-mass systems are involved, one value of inductance, capacitance, and resistance are determined; from then on the rest of the values are directly or indirectly proportional to the analogous terms depending upon which terms are being considered.

IV. Determination of Acoustical Values

It has been shown that the air in the pipe acts as a mass. The air in the pipe also acts as a spring so there is some limit to the volume that can be assumed to act as a concentrated mass. Our investigations indicated that a manifold system could be represented by relatively few masses. The weight of these masses is dependent upon the volume and specific weight so that it may be expressed analytically as

$$W = d_o \frac{\pi d^2}{4} l \quad (41)$$

where W = weight in pounds

d_o = weight density - lb/cu in. = $\frac{0.0765}{1728}$ lb/cu in. for air

d = pipe diameter - in.

l = pipe length - in.

The spring constant of the cylinder is given by the expression usually used for Helmholtz resonators and gives the force necessary to move the air in the pipe one inch. It is expressed as

$$k = \frac{d_o}{g} \frac{d^2 (\pi d^2)^2}{16 V} \quad (42)$$

where k = spring constant - lb/in.

d_0 = specific weight in lb/cu in.

c = velocity of sound in air (1100 x 12) in./sec

d = pipe diameter - in.

g = acceleration due to gravity

V = volume of air acting as a spring - cu in.

Since the mass may be concentrated at the mid-section of lumps the spring volumes are taken between centers.

It is necessary to modify the above results so that all pipes or masses and springs are such as to represent only one diameter of pipe. The reason for this is that the electrical circuits have no way of representing pipe areas. Thus, changes in velocities and displacements due to changes in area in the pipe would not be represented in the equivalent electrical circuits.

Fortunately, this can be overcome by setting up equivalent pipe systems having only one diameter pipe. This is done by maintaining the same potential and kinetic energy capacities of the air in the pipe. This method is used in other engineering problems to simplify the solutions.

To retain the potential energy capacity the original pipe may be replaced by another having the desired diameter and another length. Thus, the potential energy capacity in the original pipe may be set equal to that of the equivalent pipe or

$$P.E. = 1/2 F x = 1/2 F_0 x_0$$

where the force F and the displacement are

$$F = \text{pressure} \left(\frac{\pi d^2}{4} \right) \times \sim L$$

$$F_0 = \text{pressure} \left(\frac{\pi d_0^2}{4} \right) \times \sim L_0$$

so that the equivalent length of a pipe of the required diameter is

$$L_0 = L \left(\frac{d}{d_0} \right)^2 \quad (43)$$

For the kinetic energy we have that

$$KE = 1/2 M V^2 = 1/2 M_0 V_0^2$$

where the mass M and the velocity V are

$$M = \rho L \frac{\pi d^2}{4} \quad V = \frac{\text{Volume}}{\pi d^2/4}$$

$$M_0 = \rho L_0 \frac{\pi d_0^2}{4} \quad V_0 = \frac{\text{Volume}}{\pi d_0^2/4}$$

so that the equivalent length of pipe to maintain the kinetic energy is

$$L_0 = L \left(\frac{d_0}{d} \right)^2 \quad (44)$$

This method is somewhat confusing in that the lengths for the potential energy or k may be increased but the lengths may be decreased to maintain equivalent masses.

Fortunately there is a less confusing method. First, find the values of the spring constants k and the masses M . Then make the change to equivalent values of k and M . The potential energy is given by the equation

$$P.E. = 1/2 k x^2 = 1/2 k_0 x_0^2$$

where x is the displacement. Since the volume passing any point remains the same we have that

$$xA = x_0 A_0$$

so that the equivalent spring constant k_0 is

$$k_0 = k \left(\frac{A_0}{A} \right)^2 = k \left(\frac{d_0}{d} \right)^4 \quad (45)$$

The kinetic energy gives the relation for the masses. It is

$$KE = 1/2 M V^2 = 1/2 M_0 V_0^2$$

where V is the velocity given by the relations

$$V = \frac{\text{Volume}}{A}; V_0 = \frac{\text{Volume}}{A_0}$$

so that

$$M_0 = M \frac{A_0^2}{A^2} \quad (46)$$

Thus, both the masses and the spring constants are corrected in the same direction. This is as would be expected for the natural frequency of a simple system would then be the same as evidenced by the equation for the natural frequency

$$f = \frac{1}{2\pi} \sqrt{\frac{k}{M}}$$

Since damping is comparatively difficult to evaluate only approximate values can be used for the present. These were determined in a general way based on critical damping and by test.

V. Apparatus

A number of tests were run on one cylinder to develop the equipment and technique. Then a three cylinder manifold was reduced to an equivalent electrical circuit and the technique refined until the results were comparable with the test data from the actual manifold. A sample result of this test work is included in part VI.

The apparatus to be described is that for a six cylinder manifold. It will illustrate all the calculation and test details needed for any manifold.

The apparatus used on the six cylinder investigation has to duplicate the motions of the piston, the valves, and their influence on the intake system. The piston motion produces nearly a sinusoidal force or pressure which the valve allows to act on the intake system for a definite period of the complete cycle. The piston velocity was simulated by a motor driven generator consisting of rotating condenser plates that produce a constant sinusoidal voltage. In this way six sets of rotating condensers could be spaced to introduce the crank angle phase relationship for the pressures in the different cylinders. These voltages, after going through an amplifier and output power supply, emerge as constant amplitude currents which are now fed to a rotating contactor switch that reproduces the valve action. The switches connect the pipe circuit to the cylinder condensers only for the time the valves are open. These switches are on the same shaft as the rotating condensers so valve timing was maintained. A schematic diagram of this unit is shown in Fig. 14 with the electric

shown in Fig. 15a. The actual units are shown in separate pictures. The rotating condensers are shown in Fig. 16, the rotary contactor in Fig. 17, and the power supply with the rest of the setup in the background in Fig. 18.

The manifold system for the engine is as shown in Fig. 19. This was divided into lumped masses as shown. Indications were that the supercharger volume was great enough to act as a very weak spring so would not be important in this investigation. The electrical circuit is shown in Fig. 19. The switching is also shown in this diagram. The piston motion is always applied to the cylinder volume so the one condenser remains with the generating unit at all times. The rest of the circuit is switched in and out to simulate valve action.

The calculation of masses and elasticities will be illustrated to show the general procedure. Using the dimensions of the pipes as given, the volume of air in the pipe running from cylinder 3 to the point where it joins the pipe from cylinder 2 is 34 cu in. This volume was divided into two equal parts each having a volume of 17 cu in. because it was felt these masses should be kept reasonably small since they were close to the cylinder and therefore quite effective in the manifold. The weight of these two lumps of air is then

$$W = 17 \times \frac{.076}{1728} = 0.00075 \text{ lb}$$

The spring constant of the cylinder is given by equation 26 as

$$k = \frac{d_2}{g} \frac{e^2 (\pi d^2)^2}{16 V}$$

where d = pipe diameter = 1.92 in.

V = cylinder volume = 75.71 cu in.

The diameter of 1.92 inches represented approximately the pipe diameter over the region concerned. Small variations from this had negligible results in the test data and would have been difficult to handle in setting up the system. This gives the spring constant as

$$k = \frac{0.076}{1728 \times 386} \frac{(13,450)^2 (\pi 1.92^2)^2}{16 \times 75.71} = 2.29 \text{ lb/in.}$$

In determining the spring constant of a certain length of pipe, the only difference is that V represents the volume between ends of the spring. Thus, the spring constant is

$$k = \frac{0.076 (13,450)^2 (\pi 1.92^2)^2}{1728 \times 386 \times 16 \times 8.5} = 20.4 \text{ lb/in.}$$

where 8.5 is the volume of air between the valve and the first lump.

Since the pipes were not all the same size, it was necessary to reduce the manifold to an equivalent system in which voltage could be measured and made to represent pressures. That is, we are dealing with total forces when we measure voltages. Therefore, to be able to indicate pressures, we must reduce it to an equivalent constant diameter pipe. This also takes care of the current flow which cannot easily be made to change along the circuit as the velocity changes when the pipe size changes. This change to an equivalent system involves maintaining the same energy storage capacities as explained earlier. As such, only the ratio of areas needs to be considered.

Thus, in the large pipe leading from the supercharger, the area is 5.6 sq in. and the volume of each lump of air is 52.5 cu in. The weight is, therefore,

$$W = 52.5 \left(\frac{0.076}{1728} \right) = 0.0023 \text{ lb}$$

Since the basic area was taken as 2.9 sq in. for the pipe near the cylinder, the above mass must be corrected by the ratio

$$W' = W \left(\frac{\text{Basic Area}}{\text{Actual Area}} \right)^2$$

so that the equivalent weight must be

$$W' = 0.0023 \left(\frac{2.9}{5.6} \right)^2 = 0.00062$$

The spring constant must also be corrected in the same direction

$$k' = k \left(\frac{\text{Basic Area}}{\text{Actual Area}} \right)^2$$

The remainder of the quantities can be determined using these procedures.

In setting up the electrical quantities we must maintain the dimensionless terms given in Table II. Since we will not need the force quantities, we can omit any consideration of them. Further, the resistance is such an unknown quantity in the actual manifold that we cannot justify any more than just approximate values of resistance in the electrical circuit. This leaves us only two terms that must be maintained

$$\frac{kx}{W\omega^2} = \frac{1}{LC \Omega^2}$$
$$\frac{v}{\omega} = \frac{e}{\Omega}$$

By making all frequencies in the mechanical system in the same ratio as in the electrical, we eliminate the last quantity so we have really only one term that determines the equivalent values. The values for one condenser and one coil are found from this equation. The rest are proportional to those according to the analogy.

To illustrate this procedure, let us take the values already determined for the pipe above. The cylinder spring constant was $k = 2.29$ lb/in. and the mass of the first lump was 0.00075 lb. A ratio of 2 was maintained between the analogous systems, that is, all electrical frequencies were twice those in the mechanical. This gives

$$\frac{2.29 \times 386}{0.00075 \times (1)^2} = \frac{1}{LC (2)^2}$$

so that

$$LC = 0.212 \times 10^{-6}$$

Now if C is chosen as 0.25 mfd

$$L = 0.85 \text{ henry}$$

Since in the direct analogy all inductances are directly proportional to the mass, the other inductances are

$$L_x = 0.85 \frac{W_x}{0.00075}$$

VI. Test Results

A number of preliminary tests were made on single cylinder manifolds to develop the technique and procedure for the more elaborate manifolds described in the main report. These results checked well

with data from the actual manifold and cylinder.

After this more extensive tests were made on a three cylinder manifold for which actual results were known. Those results are shown in Fig. 20a.

The important thing to note is that the peak volumetric efficiency comes at about the same speed. The difference in values is not particularly significant except that it indicates that the amount of damping or resistance in the electrical circuit is not great enough. This one handicap that is hard to overcome, not because the equivalent circuit can not handle it but because the value of friction thru the valve and pipe is unknown. Since it is not known, the equivalent resistance can not be determined. Even values reasonably close are not known. No efforts were made on this manifold to increase the electrical resistance and thereby make the results check more closely. However, some other cases were tried with different amounts of resistance. Some were higher as that shown above while others with more resistance fell below. An intermediate value showed close correlation.

Using the above methods and apparatus a number of tests were made to find the volumetric efficiency for different intake systems for the six cylinder engine. After trying several methods, one was found that checked for single and three cylinder investigations very closely. It was, therefore, adopted and used for all the tests on six cylinder manifolds.

The method of measuring is easiest understood by referring to Fig. 20. In Fig. 20 the broken line curve represents the current which is analogous to the piston velocity. The driving circuit produces a fixed current which is proportional to piston velocity and independent of the circuit connected to it. The total charge that flows into the engine is equal to the sum of the charge that would flow due to this current and the charge that is stored on the cylinder condenser at the time of valve closing. A measure of the charge that will flow due to the fixed current of the driving circuit can be obtained by disconnecting the pipe circuit. Under these conditions all of this charge will come from the cylinder condenser. The charge that flows during the intake stroke from T.C. to B.C. (not during the entire valve opening period) is the charge that would flow for 100% volumetric efficiency. Since the charge on a condenser is given by

$$Q = EC$$

the voltage E_1 Fig. 20 is proportional to the charge for 100% volumetric efficiency. The charge that would flow into the driving circuit during the entire valve opening period is proportional to E_1' . With simple harmonic piston motion and 60° valve timing, E_1' would be 75% of E_1 . The volumetric efficiency of the engine with no inertia or friction in the intake system would also be 75%. Since the charge flowing into the driving circuit is independent of the pipe that is connected to the circuit, this charge will always flow into the driving circuit. When a pipe with no inductance (mass) and no

resistance is connected to the cylinder condenser, this charge will flow from the pipe into the driving circuit may come from the cylinder condenser or, on the other hand, some excess charge may flow from the pipe and be stored in the cylinder condenser. The total charge flowing from the pipe to the cylinder would be equal to the charge measured by E_1' plus the charge stored in the cylinder condenser at the time of valve closing. This charge that is stored in the cylinder condenser is proportional to E_2 Fig. 20. Since E_1' is equal to $.75E_1$, the total charge flowing from the pipe to the cylinder is proportional to $.75 E_1 + E_2$. The volumetric efficiency is

$$\text{Vol. eff.} = \frac{.75 E_1 + E_2}{E_1} \quad (47)$$

Therefore, only two voltages must be measured to find the volumetric efficiency.

Proposed Engine Manifold

The dimensions of the proposed engine manifold were taken from a set of drawings and from these the volumes and areas of different parts of the manifold were calculated. These were converted to lumped masses and springs. After this, the electrical elements were determined and connected up.

After the circuits were set up with no damping the test was run and the curves shown in Fig. 21 were obtained. These indicated quite definitely that the maximum volumetric efficiency was obtained at about 3000 or 3100 rpm. All cylinders seemed to be reasonably

well balanced. This test did not include sufficient damping to provide a set of curves with the general trend that would be expected.

A second test was run with 2000 ohms introduced at the valve. The results are plotted in Fig. 22. These curves show the peak volumetric efficiency somewhat below 3000 rpm. Cylinders 1 and 6, 2 and 5, and 3 and 4 occupy similar positions in the manifold so should follow the same tendencies. The sets seem to be about correct. There was a slight lowering of the point of maximum volumetric efficiency when these results are compared with the case with no damping. It was of interest to find out what effect the large end pipe had on the rest of the system so another set of readings was taken with the big pipe elements grounded. This had the effect of removing this pipe from the manifold. The test results are plotted in Fig. 23. The variation between cylinders is less but the general trend is the same as before with the maximum at about 2900 rpm. It was further decided to run a test with the common pipe between the front and rear three cylinders as removed. This was done by grounding at the corresponding point in the manifold. The results on the first three cylinders are shown in Fig. 24. It shows that the peak efficiency is above 4500 rpm so the common pipe mentioned above is very important in determining peak efficiencies. It suggests the possibility of designing this pipe and the individual cylinder pipes in such a way that their effects may be combined to give the peak where it is desired. The next section will describe some of these investigations.

A further test was made using 5000 ohms resistance at the valve. These results Fig. 25 show the peaks have generally shifted to lower speeds. It shows that friction has the effect of raising the volumetric efficiency at low speeds and lowers it at higher speeds.

Revised Manifolds

The present manifold would peak at too low a speed to get best results at peak speed. Therefore, several attempts were made to modify the present manifold. The first attempt was to increase the diameter of the pipe connecting the manifolds of the front and rear three cylinders as indicated in Fig. 26 because Fig. 23 showed that the large pipe had little effect in shifting the peak. The test results for this manifold are shown in Fig. 27. The maximum peak now comes at about 3300 rpm. Again the pairs of cylinders agree quite closely. The removal of the end pipe was also tried with this setup. These results are shown in Fig. 28. There is possibly some lowering of the speed at which maximum volumetric efficiency occurs. The variation also is somewhat less between the cylinders.

Another pipe modification is shown in Fig. 29. The pipes were retained at their original diameters. Under these conditions, the test results yielded the curves shown in Fig. 30. The average peak volumetric efficiency seems to be at about 3300 rpm. For some reason, the curves are irregular but the cylinder pairs agree very well.

A third modification is a modification on the previous manifold with the pipe to cylinder 1 and 6 being made 1.67" in diameter

as shown in Fig. 31. The test results are shown in Fig. 32. The average speed for peak volumetric efficiency is about 3300 rpm. At the same time, the circuit was grounded at the point corresponding to the point where the manifold for three cylinders enters a common pipe so that the common pipe was in effect removed. Under these conditions, the test results are shown in Fig. 33. The peak values occur here at about 4000 rpm.

VII. Conclusions

This investigation has shown the techniques and methods developed to use the electrical analogue for analyzing complex engine manifolds and their effect on volumetric efficiency.

The design of manifold furnished for the engine shows that the peak volumetric efficiency occurred at approximately 2800 or 2900 rpm. This is somewhat below the desired peak which was 3400 or 3600 rpm. Therefore, several modifications were tried. By increasing the diameter of the pipe connecting the front and rear groups of three cylinders to 2.38 inches, the peak efficiency was reached at about 3300 rpm. However, this resulted in reduction of the velocity in the pipe to about 140 ft/sec. If this same pipe were brought in between cylinders 2 and 3, and between 4 and 5 the pipe is shortened. The effect on the efficiency is about the same, that is, the peak is reached at about 3300 rpm. With this same manifold and the individual pipes to the cylinders reduced to 1.67 inches, the same peak was still reached at about the same speed but the performance of cylinders 1, 2, 5, and 6 was increased at other speeds.

By changing the diameters or lengths of certain individual or common pipes, it is possible to show marked improvement in the volumetric efficiency. By careful test, it should be possible to shift the curves so as to give the desired characteristics for the individual cylinders as well as for the whole engine. Consideration of distribution and velocity are factors in determining which design is best.

Further work could be done to find more effective designs which would raise the peak speed even more. More could be learned about balancing the volumetric efficiencies for the individual cylinders. General rules for improvement of a manifold could probably be formulated after a number of further tests. They would indicate the effect of the diameter and length of each pipe.

DIRECT MECHANICAL AND ELECTRICAL ANALOGY

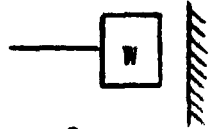
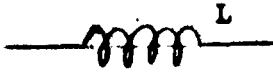
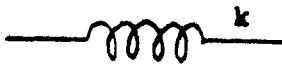
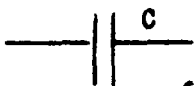
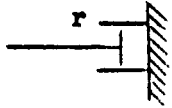
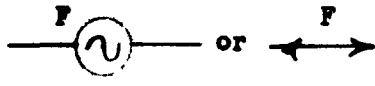
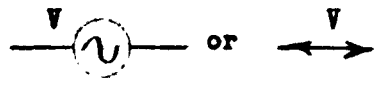
 $F = M \frac{d^2x}{dt^2} = M \frac{dy}{dt}$ $V = \frac{1}{2} \int P dt$	 $E = L \frac{dq}{dt} = L \frac{di}{dt}$ $i = \frac{1}{L} \int E dt$
 $F = kx = k \int v dt$ $v = \frac{1}{k} \frac{dF}{dt}$	 $E = \frac{1}{C} q = \frac{1}{C} \int i dt$ $i = C \frac{dE}{dt}$
 $F = r \frac{dx}{dt} = rv$ $v = \frac{F}{r}$	 $E = R \frac{dq}{dt} = Ri$ $i = \frac{E}{R}$
	
	

TABLE II.

Direct Mechanical and Electrical Analogydisplacement - x velocity - $v = \frac{dx}{dt}$ acceleration - $a = \frac{dv}{dt} = \frac{d^2x}{dt^2}$ mass - $\frac{W}{g}$ damping factor - r spring constant - k force - F natural frequency - ω forced frequency - ν

$$\frac{k_1 g}{W_1 \omega^2}$$

$$\frac{r_1 g}{W_1 \omega} \quad \text{or} \quad \frac{k}{r \omega}$$

$$\frac{F_0 g}{W l \omega^2} = \frac{F_0 g}{W v \omega} \quad \text{or} \quad \frac{V_1 k}{F \omega}$$

$$\frac{\nu_1}{\omega}$$

$$W_1/W_n$$

$$k_1/k_n$$

$$r_1/r_n$$

$$F_1/F_n$$

$$\nu_1/\nu_n$$

$$V_1/V_n$$

charge - q current - $i = \frac{dq}{dt}$

$$\frac{di}{dt} = \frac{d^2q}{dt^2}$$
inductance - L resistance - R

$$\frac{1}{C} = 1/C$$
voltage - E natural frequency - Ω forced frequency - ϕ

$$\frac{1}{C_1 L_1 \Omega^2}$$

$$\frac{R}{L \Omega} \quad \text{or} \quad \frac{1}{C R \Omega}$$

$$\frac{E_0}{L C_0 \Omega^2} = \frac{E_0}{L I \Omega} \quad \text{or} \quad \frac{I_1}{C E_0 \Omega}$$

$$\frac{\phi_1}{\Omega}$$

$$L_1/L_n$$

$$C_n/C_1$$

$$R_1/R_n$$

$$E_1/E_n$$

$$\phi_1/\phi_n$$

$$I_1/I_n$$

TABLE III.

INVERTED ELECTRICAL ANALOGY

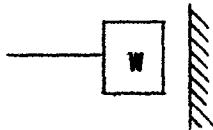
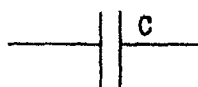
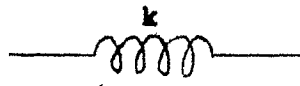
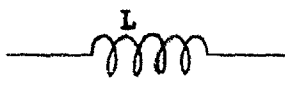
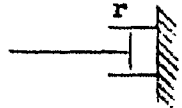
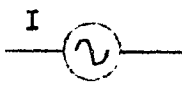
 $F = \frac{W}{g} \frac{dy}{dt}$ $V = \frac{1}{k} \int F dt$	 $I = C \frac{dE}{dt}$ $E = \frac{1}{C} \int I dt$
 $F = k \int V dt$ $V = \frac{1}{k} \frac{dF}{dt}$	 $I = \frac{1}{L} \int E dt$ $E = L \frac{dI}{dt}$
 $F = rV$ $V = \frac{F}{r}$	 $I = \frac{E}{R}$ $E = RI$
	
	

TABLE IV.

<u>Mechanical</u>	<u>Direct</u>	<u>Inverted</u>
$\frac{r_1 g}{W_1 \omega}$ or $\frac{k}{r \omega}$	$\frac{R}{L \Omega}$ or $\frac{1}{C R \Omega}$	$\frac{1}{RC \Omega}$ or $\frac{R}{L \Omega}$
$\frac{kr}{k \omega^2}$	$\frac{1}{C L \Omega^2}$	$\frac{1}{C L \Omega^2}$
$\frac{F_0 g}{W l \omega^2}$ or $\frac{F_0 g}{W \omega V}$	$\frac{E_0}{L Q_0 \Omega^2}$ or $\frac{E_0}{L I \Omega}$	$\frac{I_0}{C E_0 \Omega}$
$\frac{v_1}{\omega}$	$\frac{\phi_1}{\Omega}$	$\frac{\phi_1}{\Omega}$
$\frac{W_1}{W_n}$	$\frac{L_1}{L_n}$	$\frac{C_1}{C_n}$
$\frac{k_1}{k_n}$	$\frac{C_n}{C_1}$	$\frac{L_n}{L_1}$
$\frac{r_1}{r_n}$	$\frac{R_1}{R_n}$	$\frac{R_n}{R_1}$
$\frac{F_1}{F_n}$	$\frac{E_1}{E_n}$	$\frac{I_1}{I_n}$
$\frac{v_1}{v_n}$	$\frac{\phi_1}{\phi_n}$	$\frac{\phi_1}{\phi_n}$
$\frac{V_1}{V_n}$	$\frac{I_1}{I_n}$	$\frac{E_1}{E_n}$

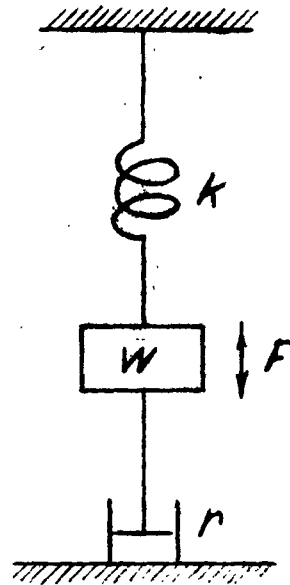


Figure 1

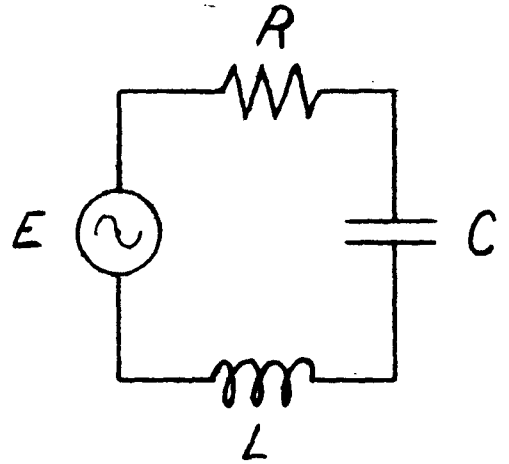


Figure 2

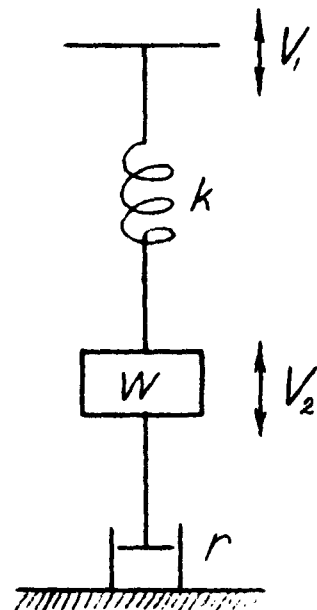


Figure 3

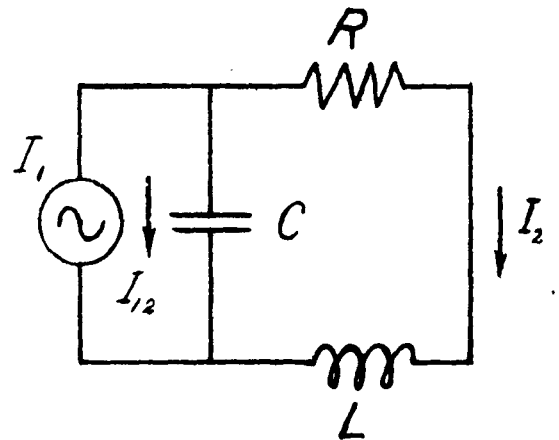


Figure 4

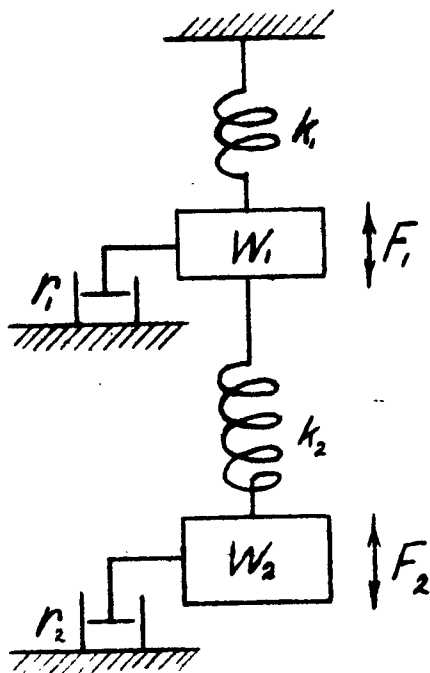


Figure 5

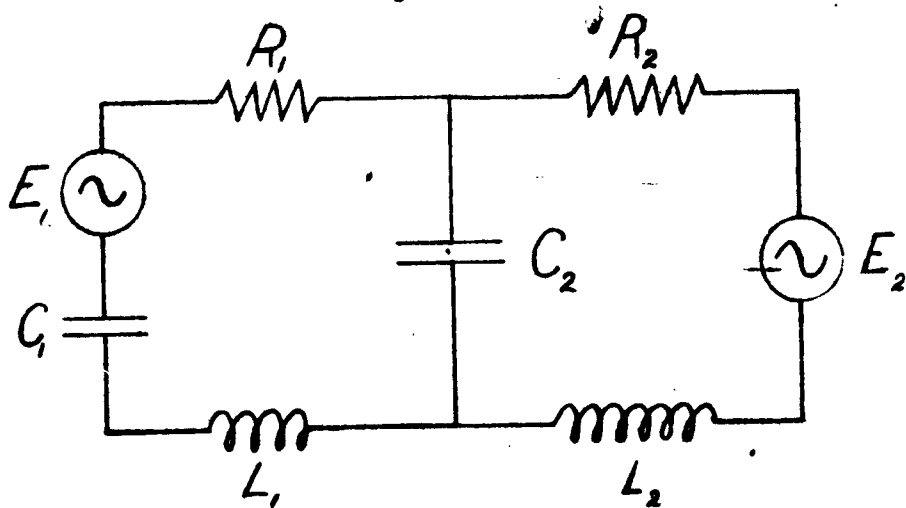


Figure 6

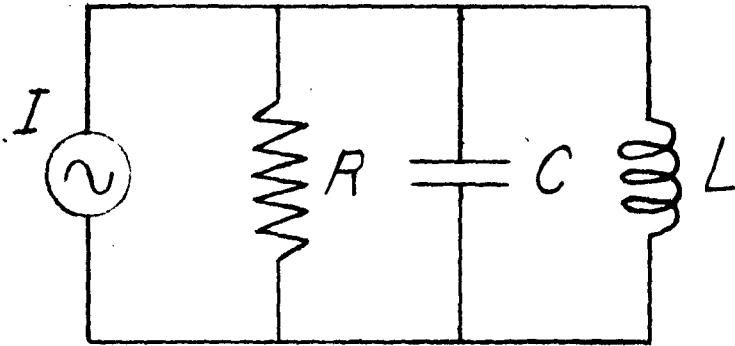


Figure 7

Mechanical

Electrical

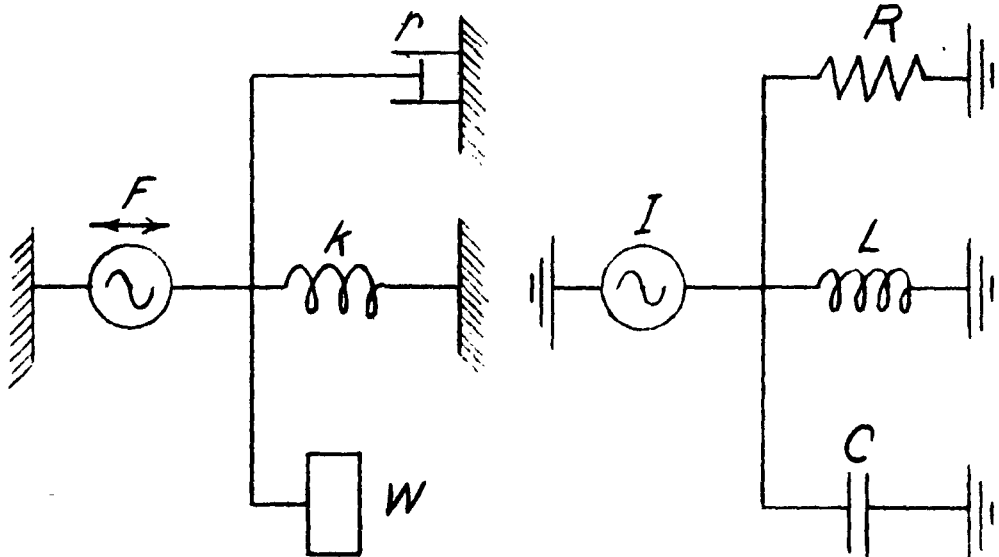


Figure 8

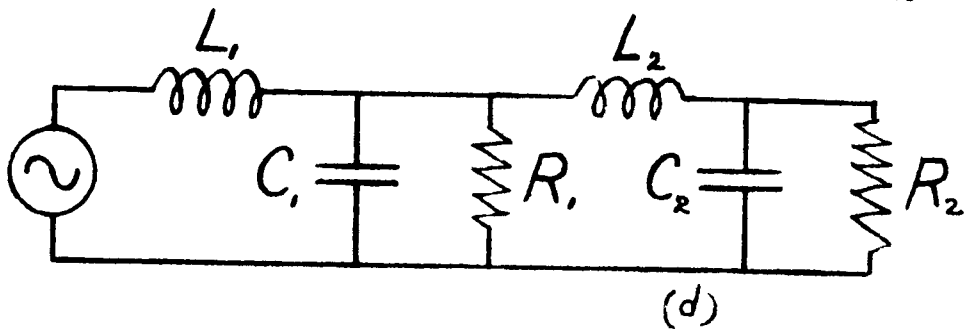
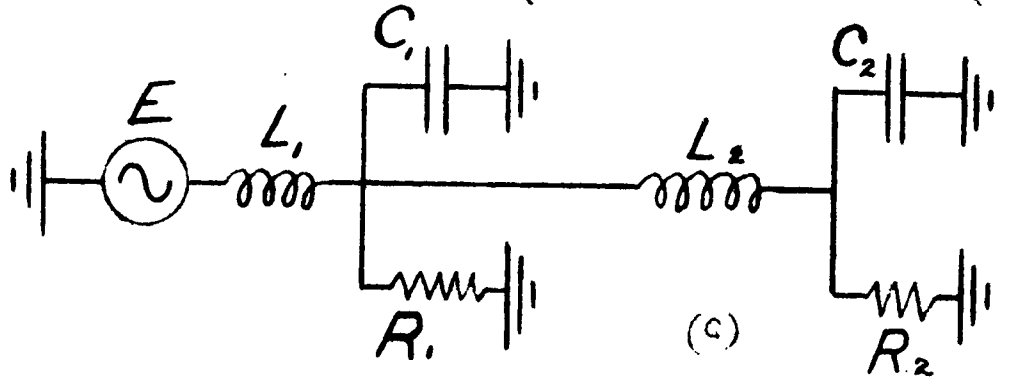
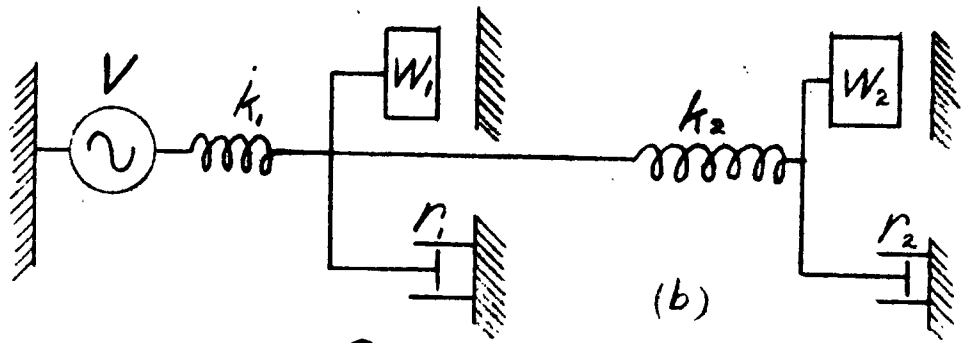
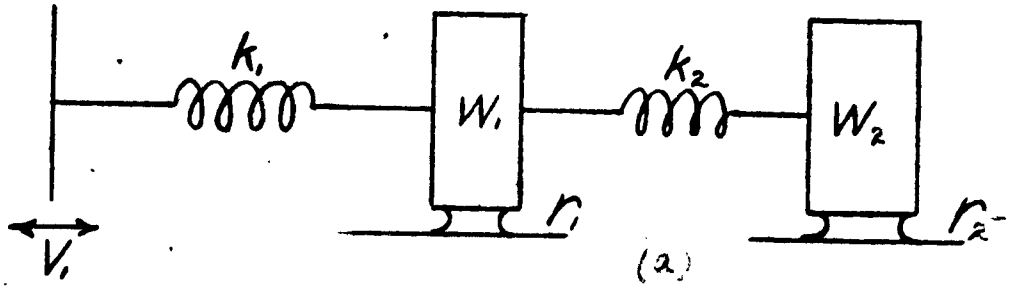


Figure 9

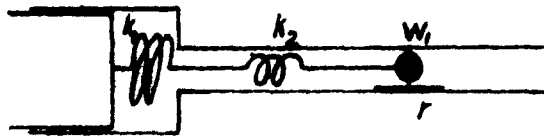


Fig. 10(a)

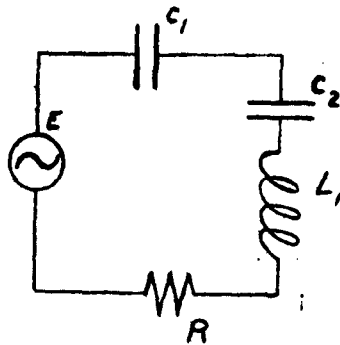


Fig. 10(b)

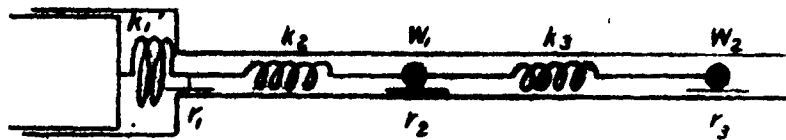


Fig. 11(a)

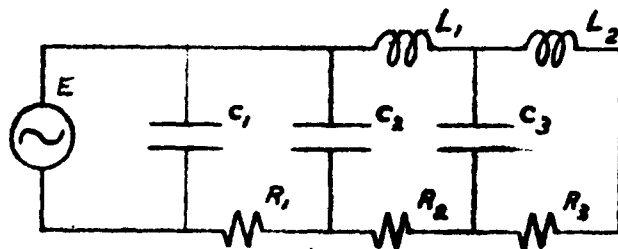


Fig. 11(b)

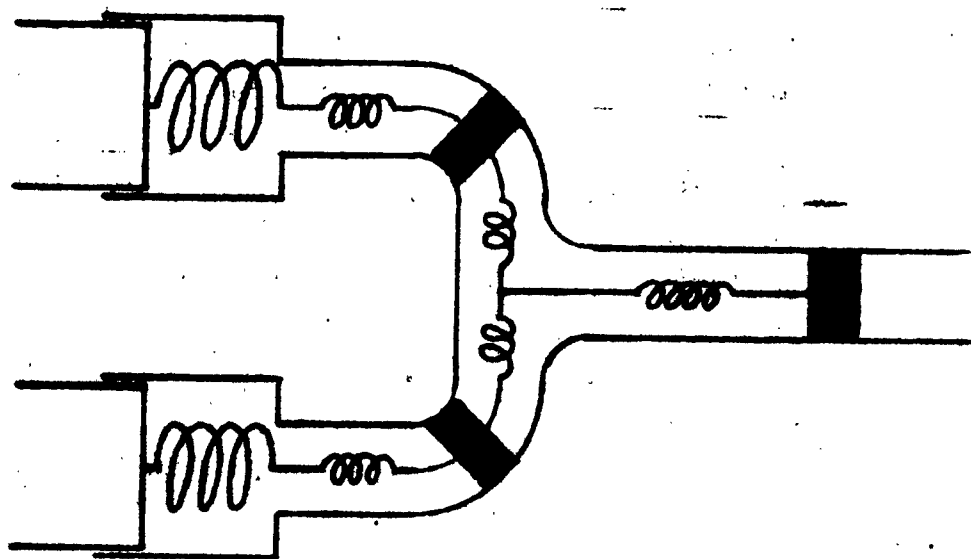


Fig. 12(a)

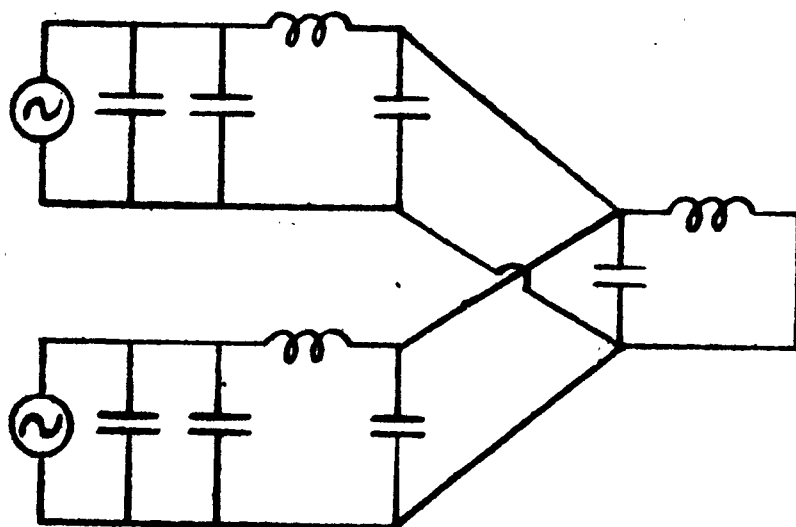


Fig. 12(b)

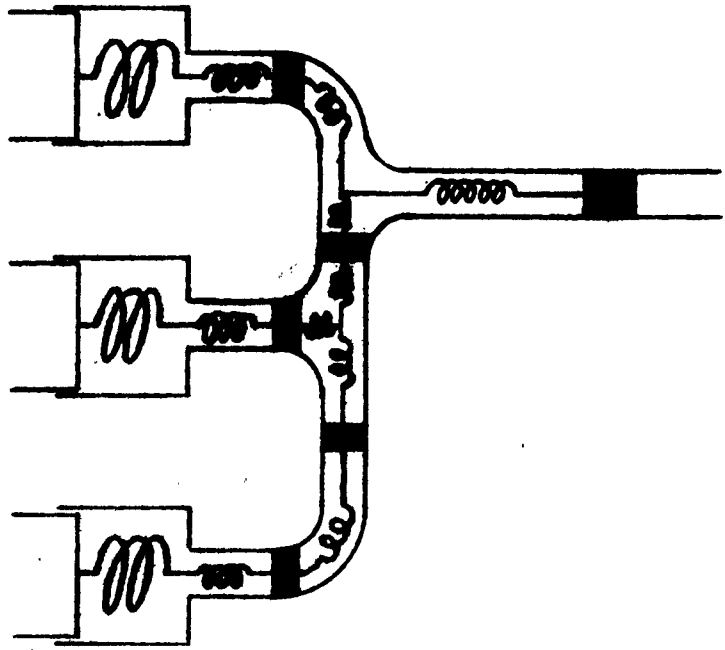


Fig. 13(a)

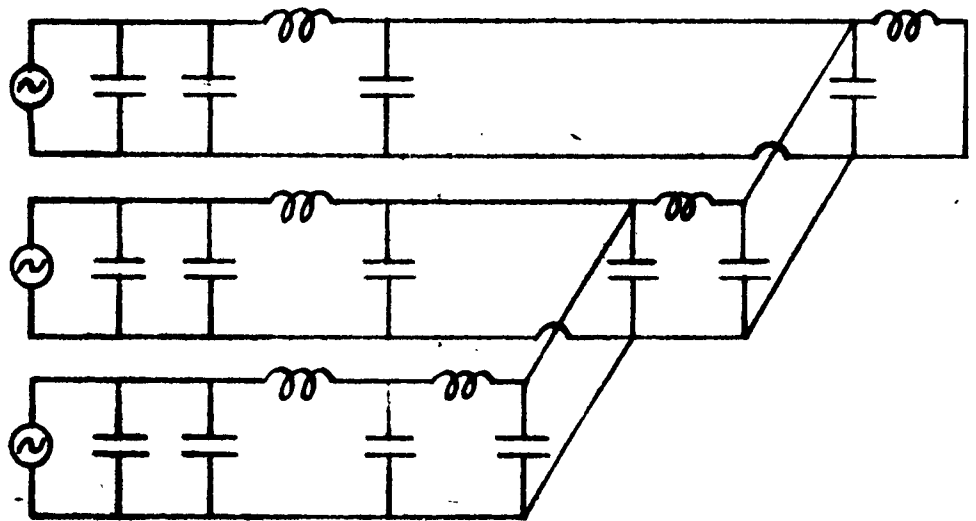


Fig. 13(b)

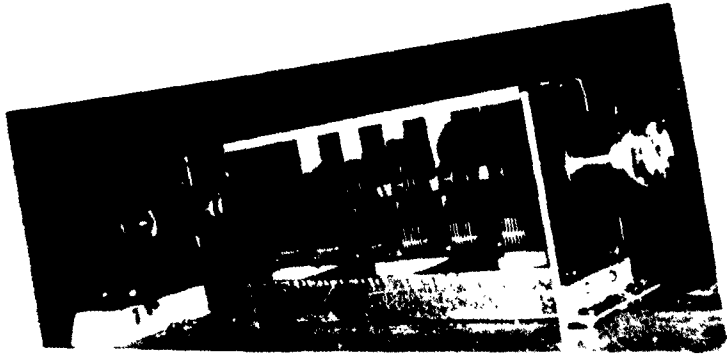


Fig. 16

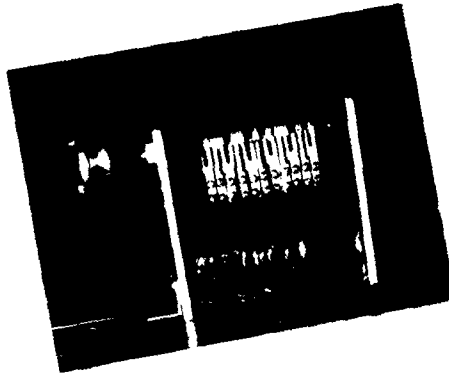


Fig. 17

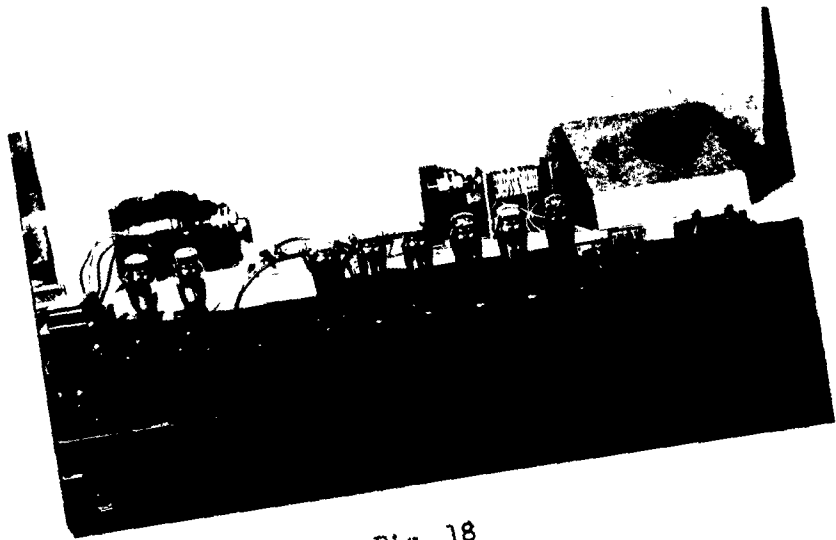


Fig. 18

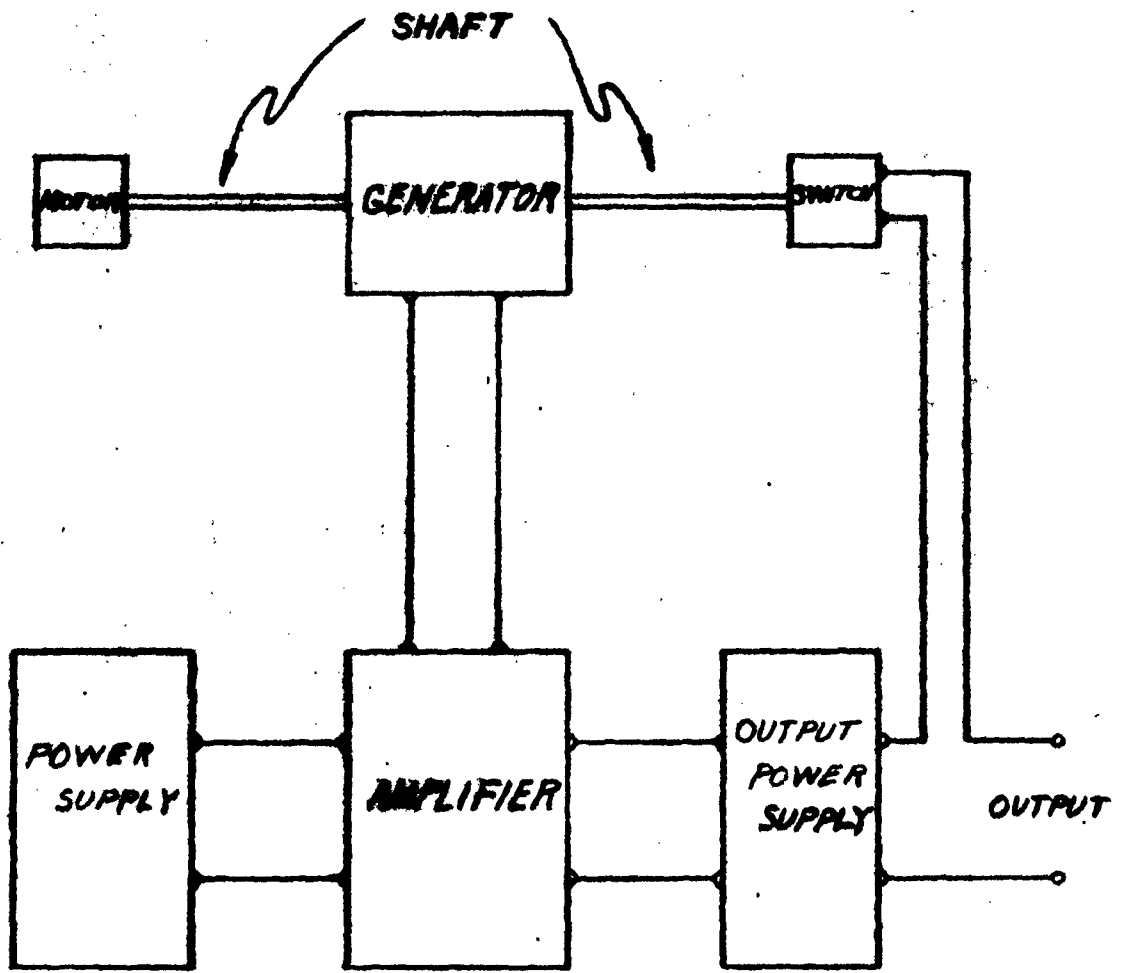


Fig. 14

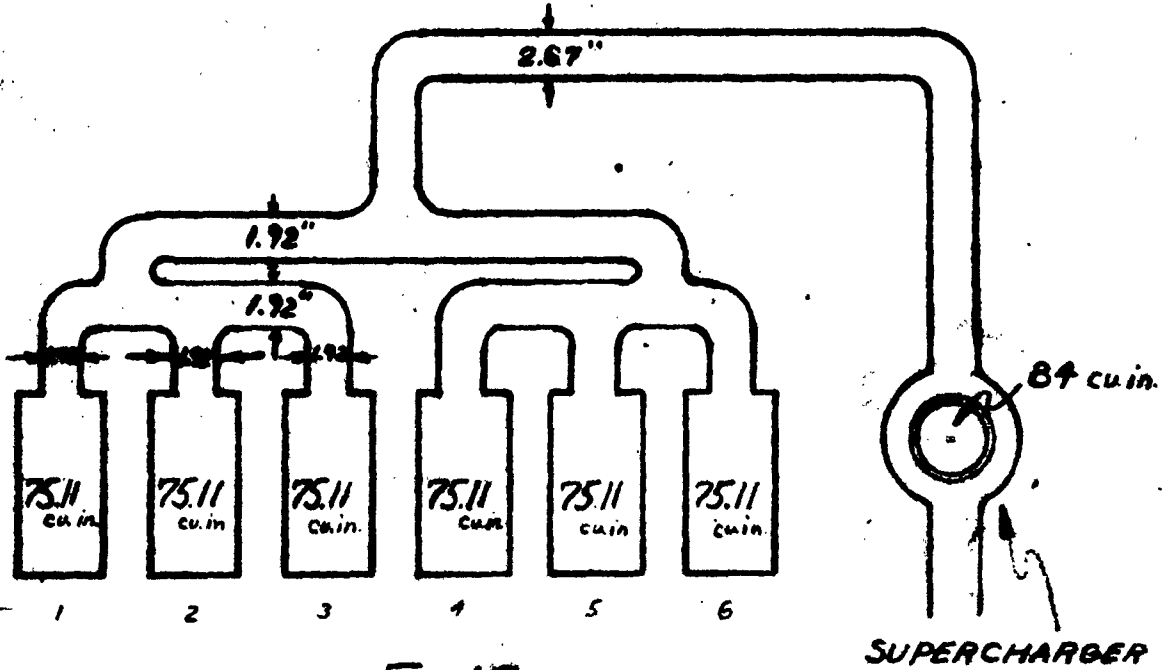


Fig. 19(a)

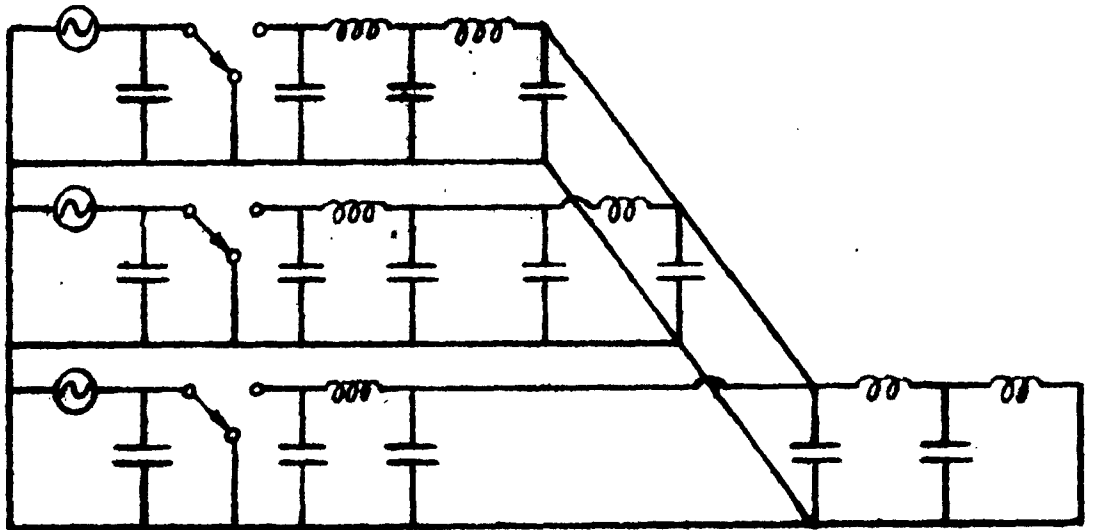


Fig. 19(b)

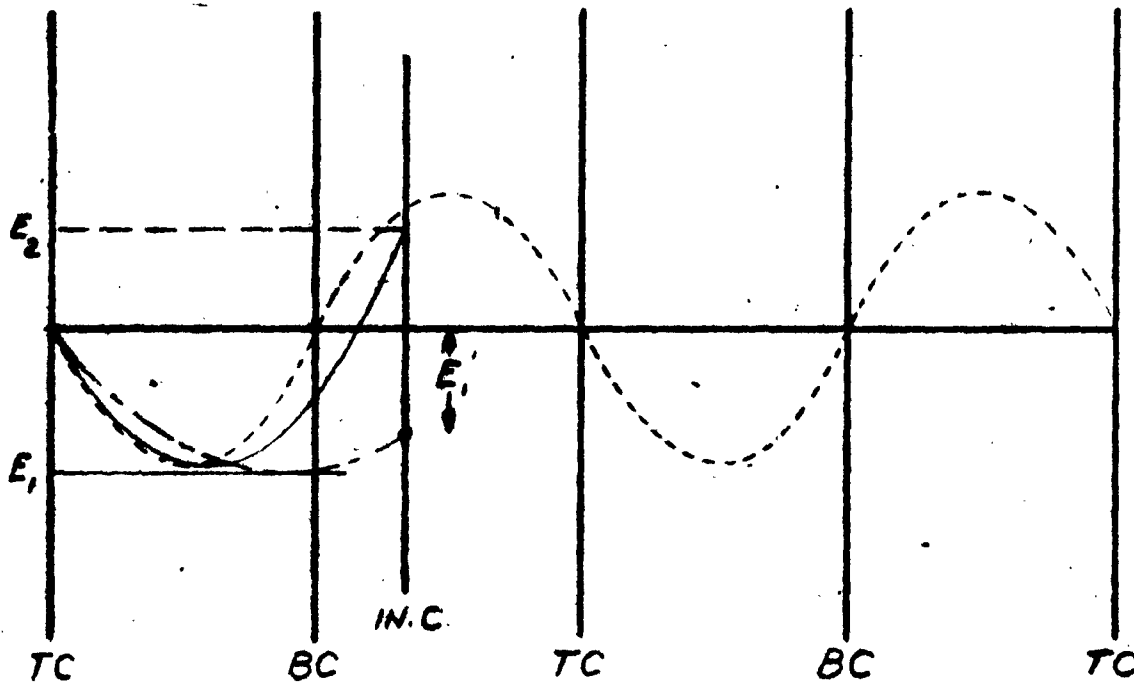


Fig. 20(a)

- Current representing piston velocity
- . - . - Voltage on cylinder condenser when pipe is disconnected,
- Voltage on cylinder condenser when pipe is connected

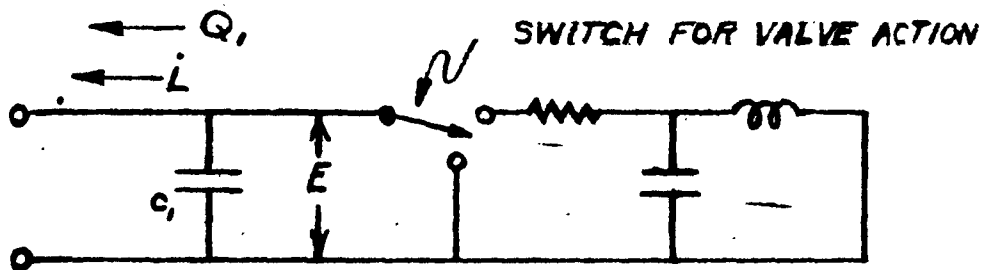
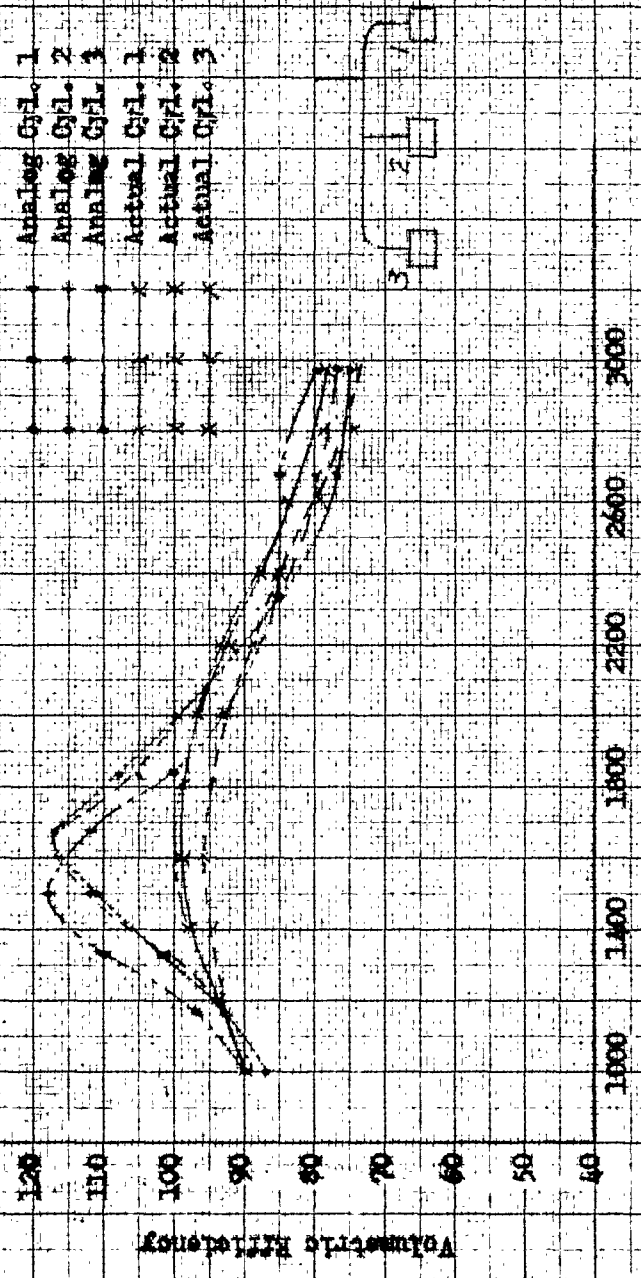


Fig. 20(b)

Comparison of Actual Volumetric Efficiencies with Analog Volumetric Efficiencies on Three Cylinder Engine

Valve friction too low



Engine Speed, RPM

Fig. 204

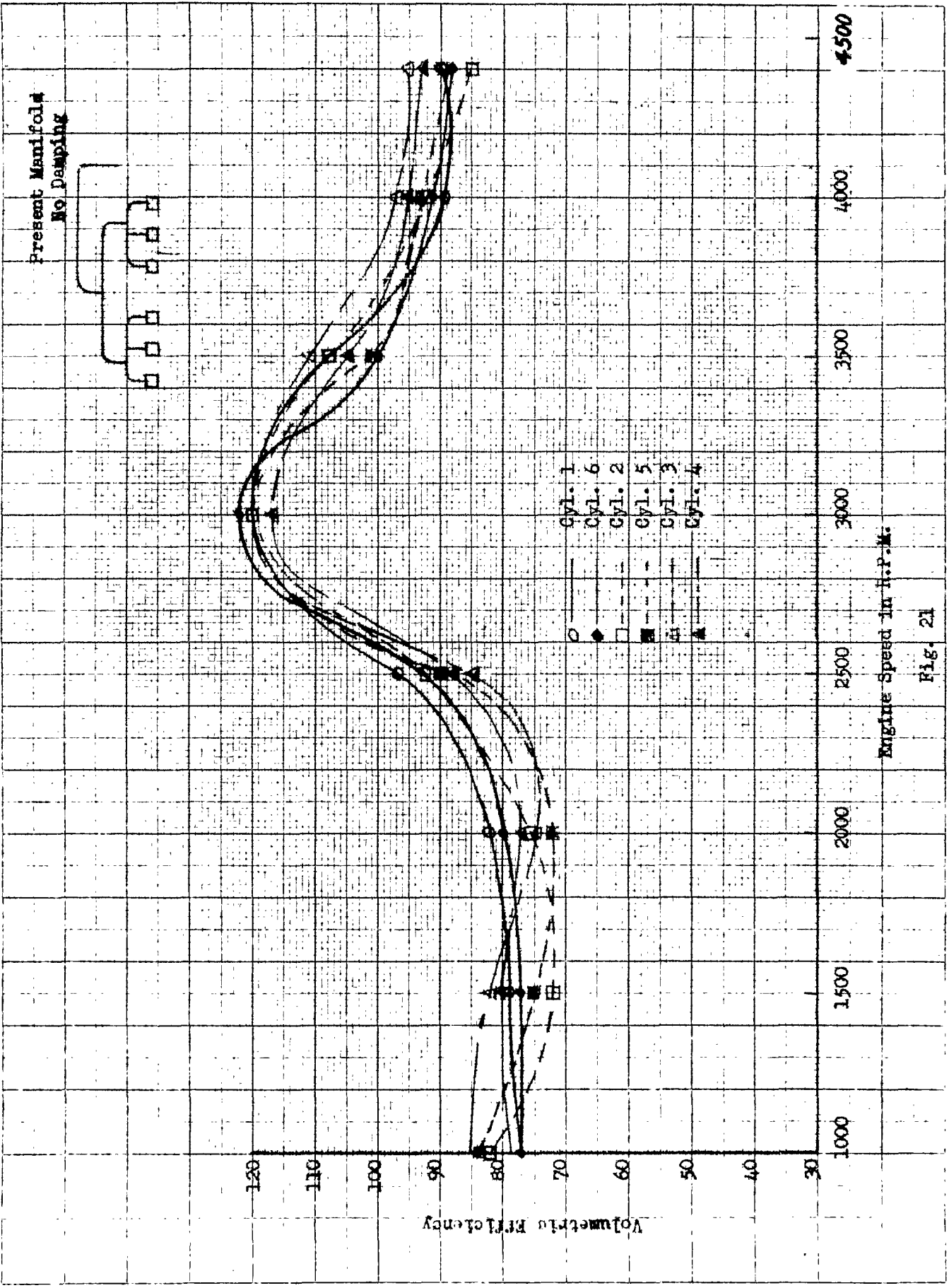
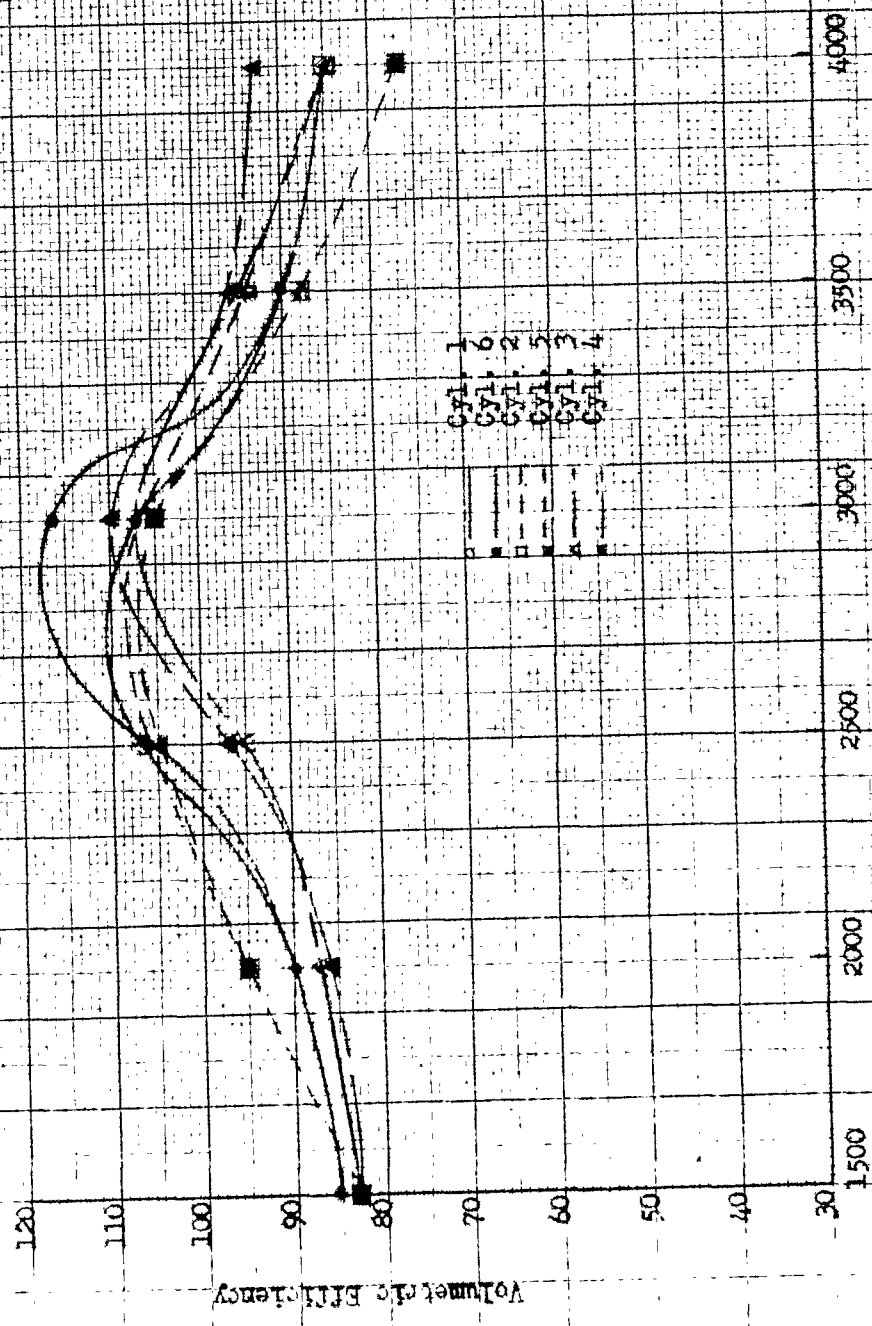
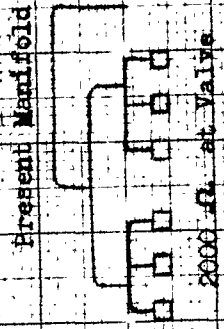


Fig. 21



Engine Speed in R.P.M.
Fig. 22

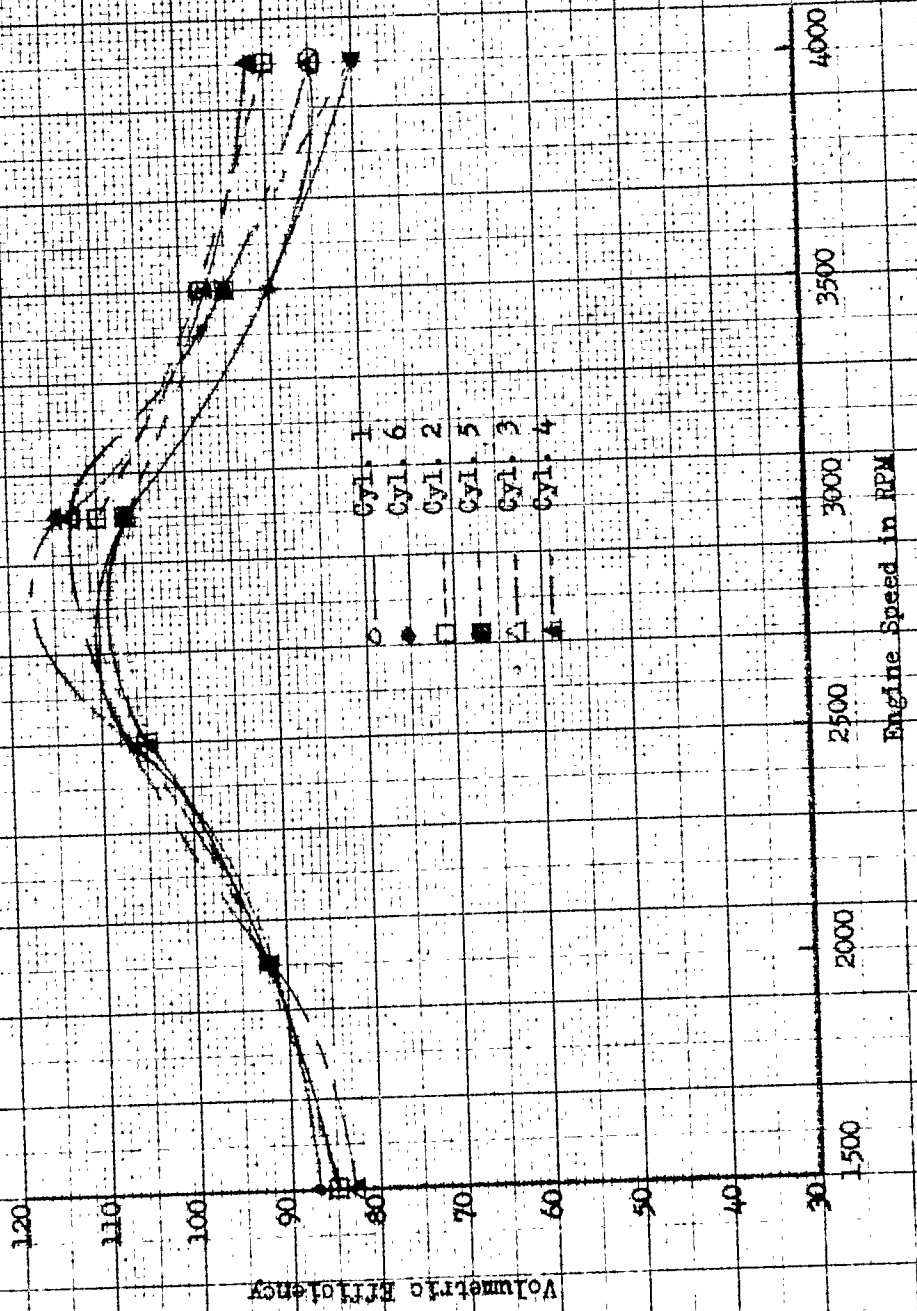
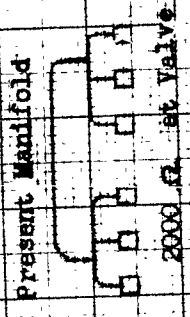


Fig. 23

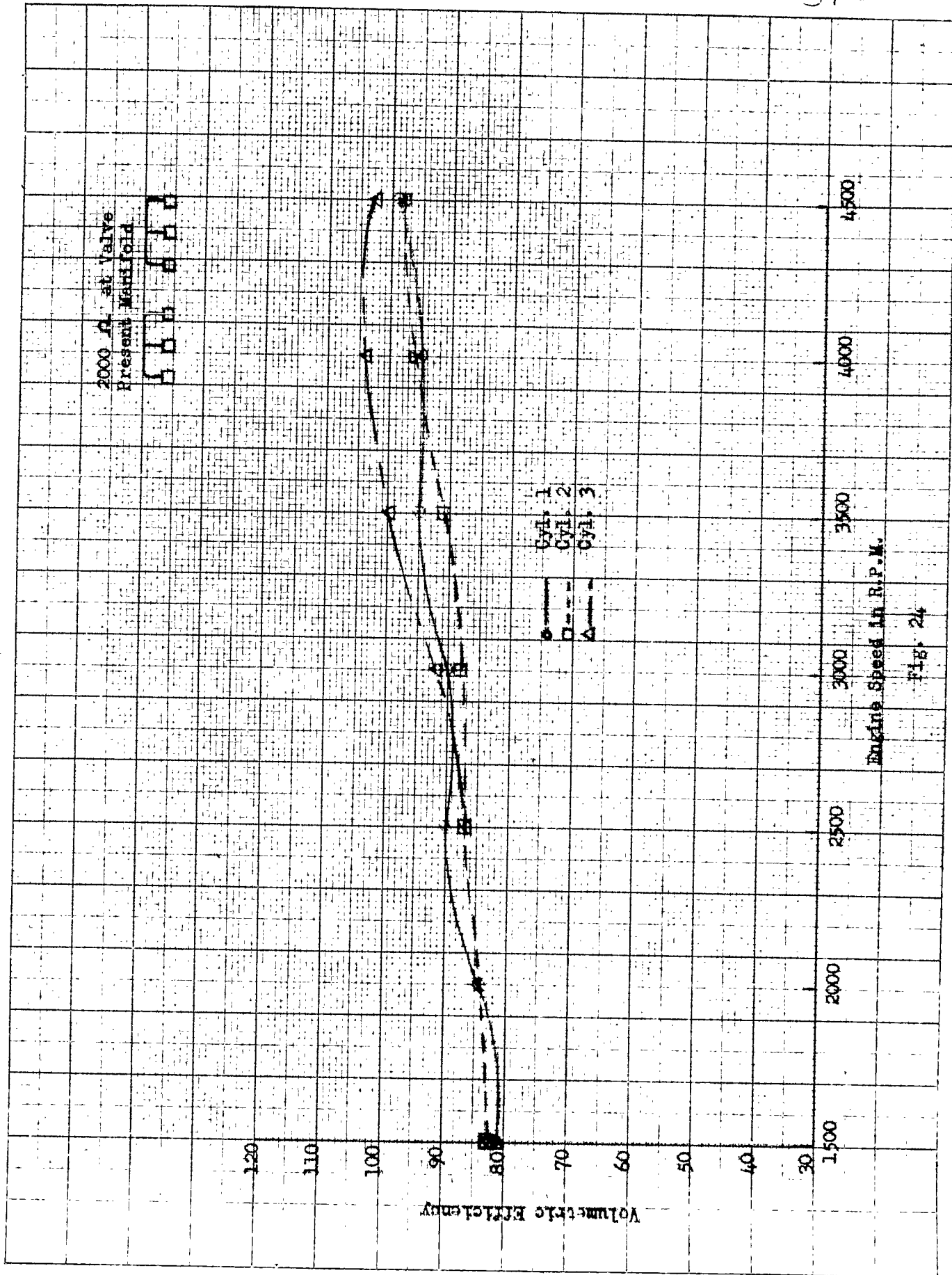


Fig. 24

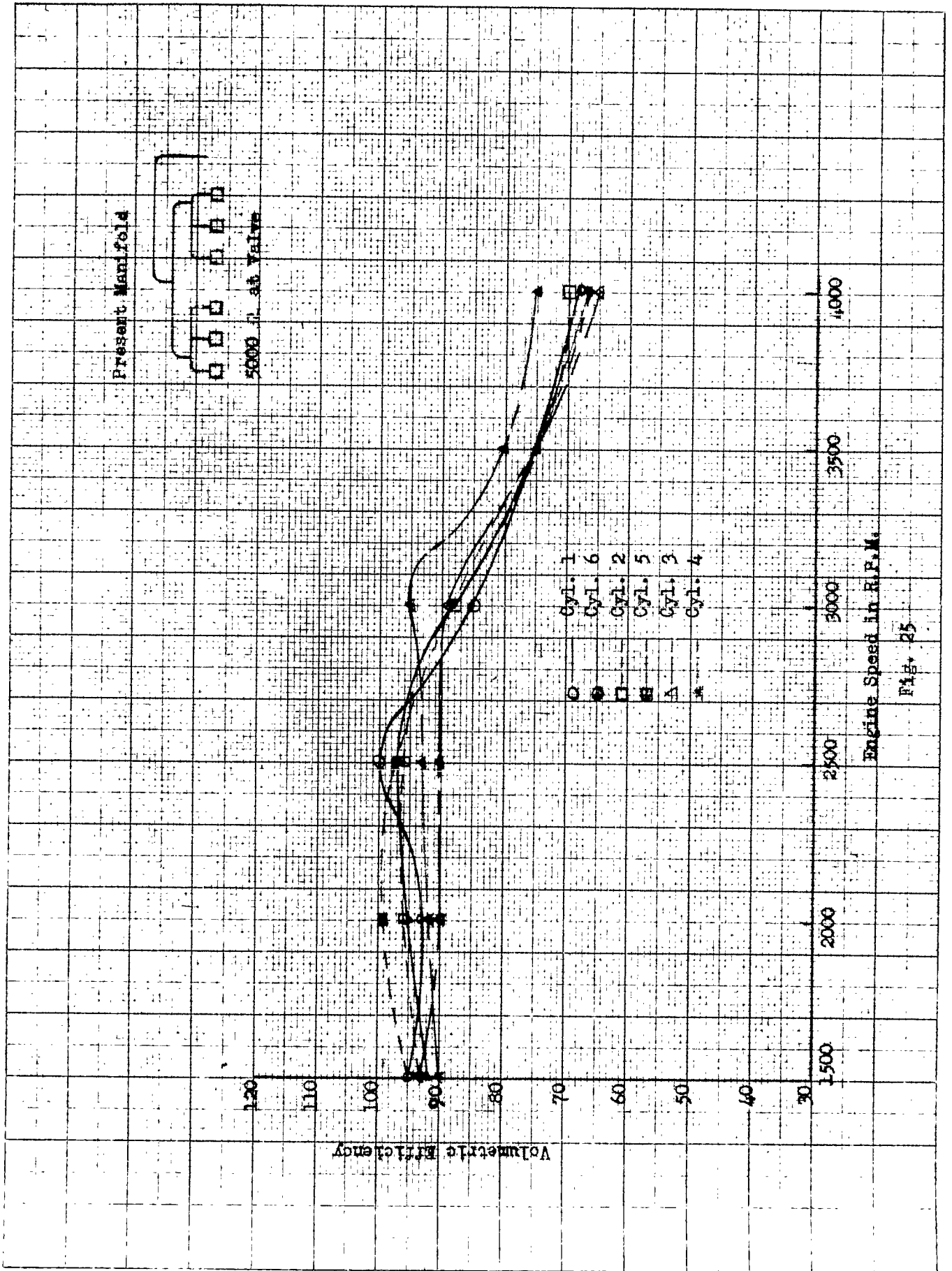


Fig. 25

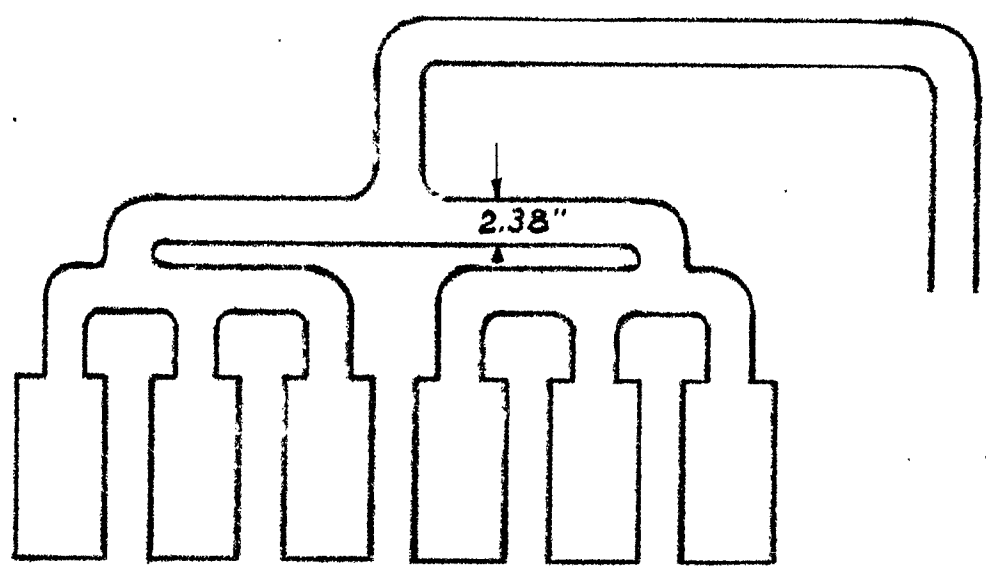


Fig. 26

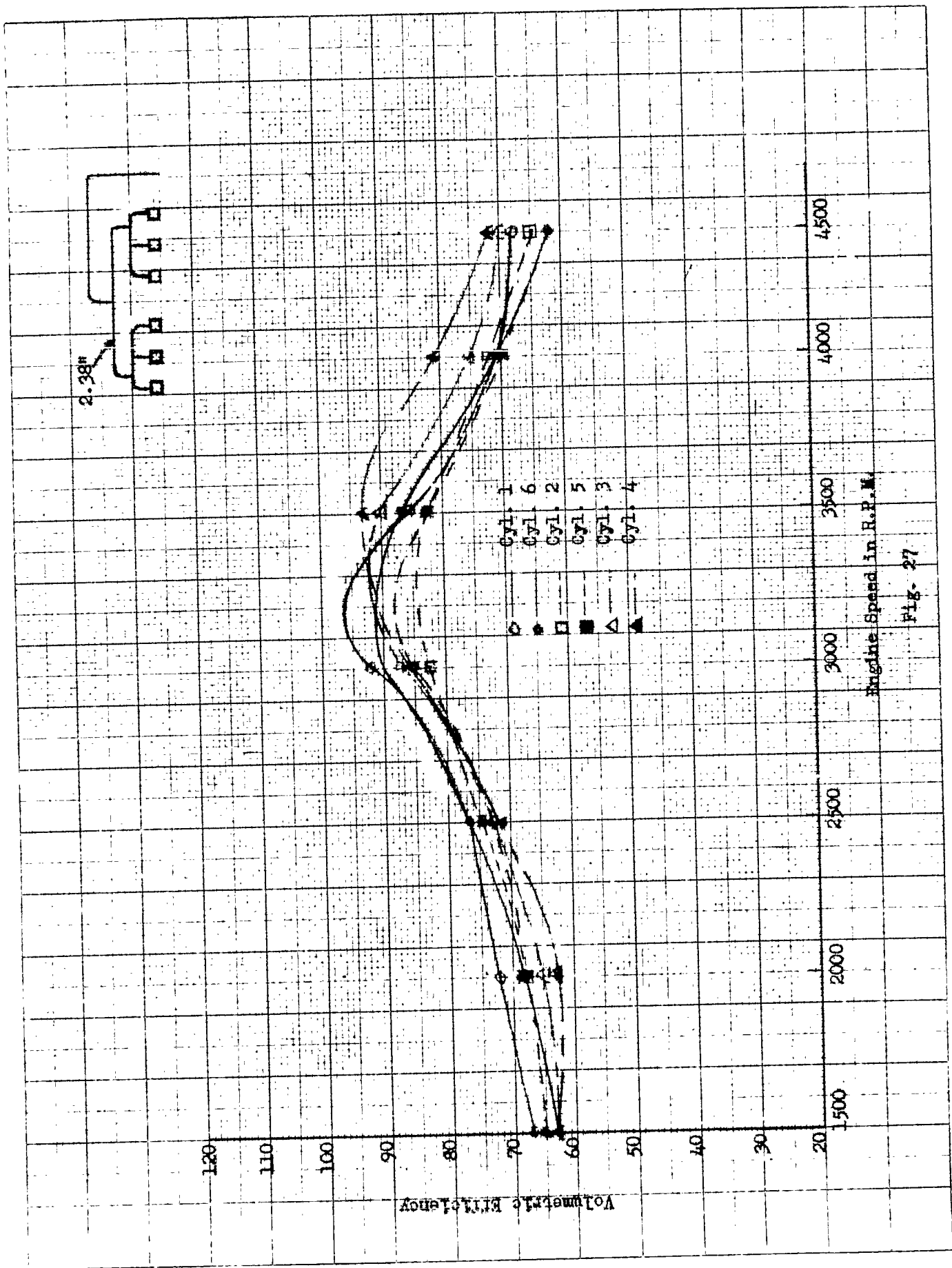
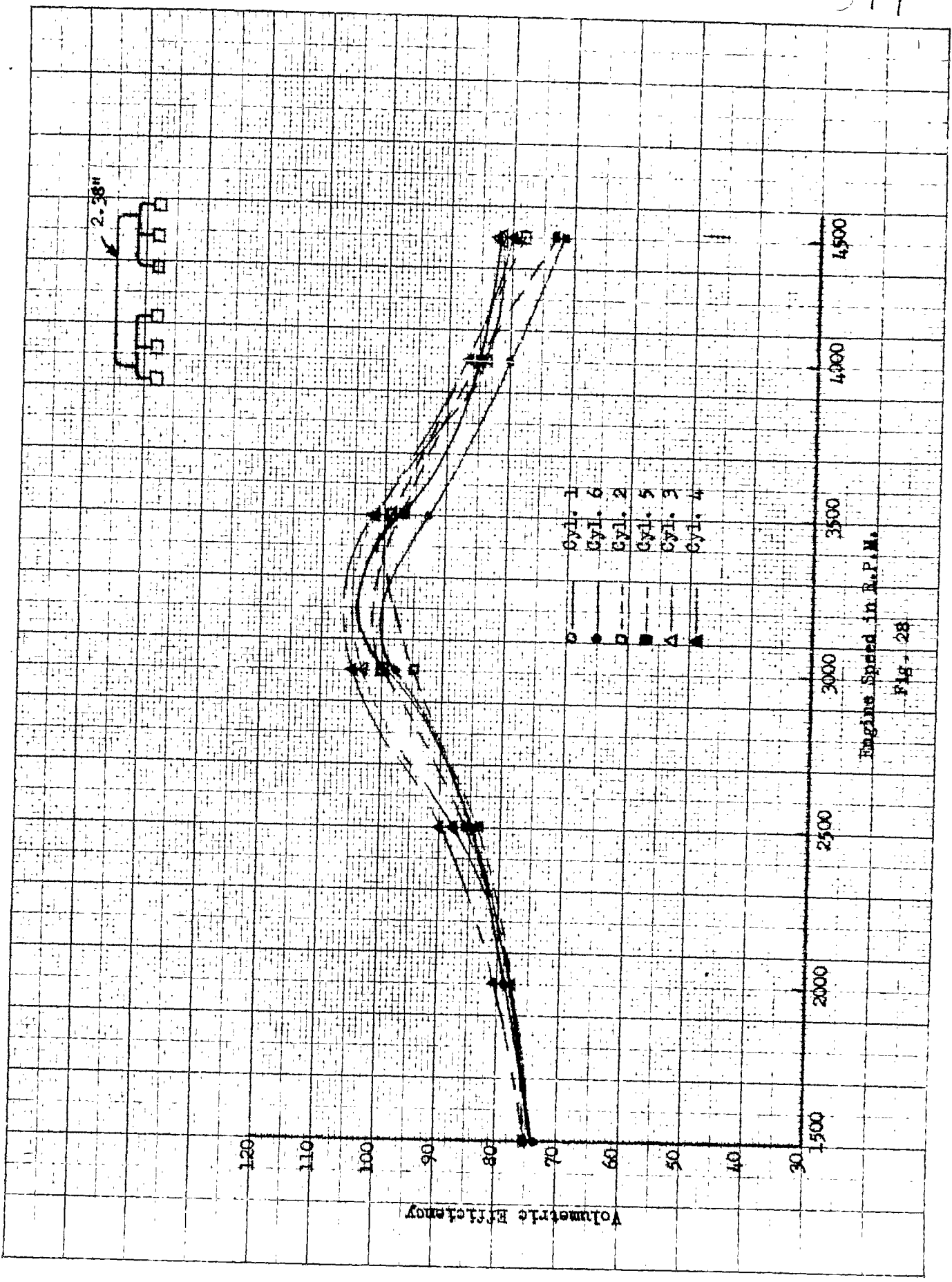


FIG. 27



Engine Speed in R.P.M.

Fig- 28

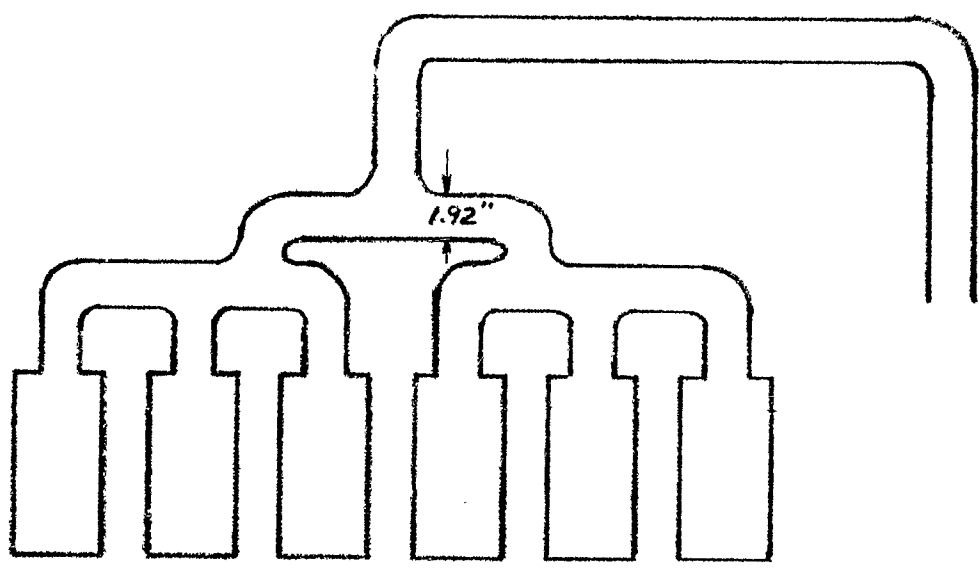


Fig 29

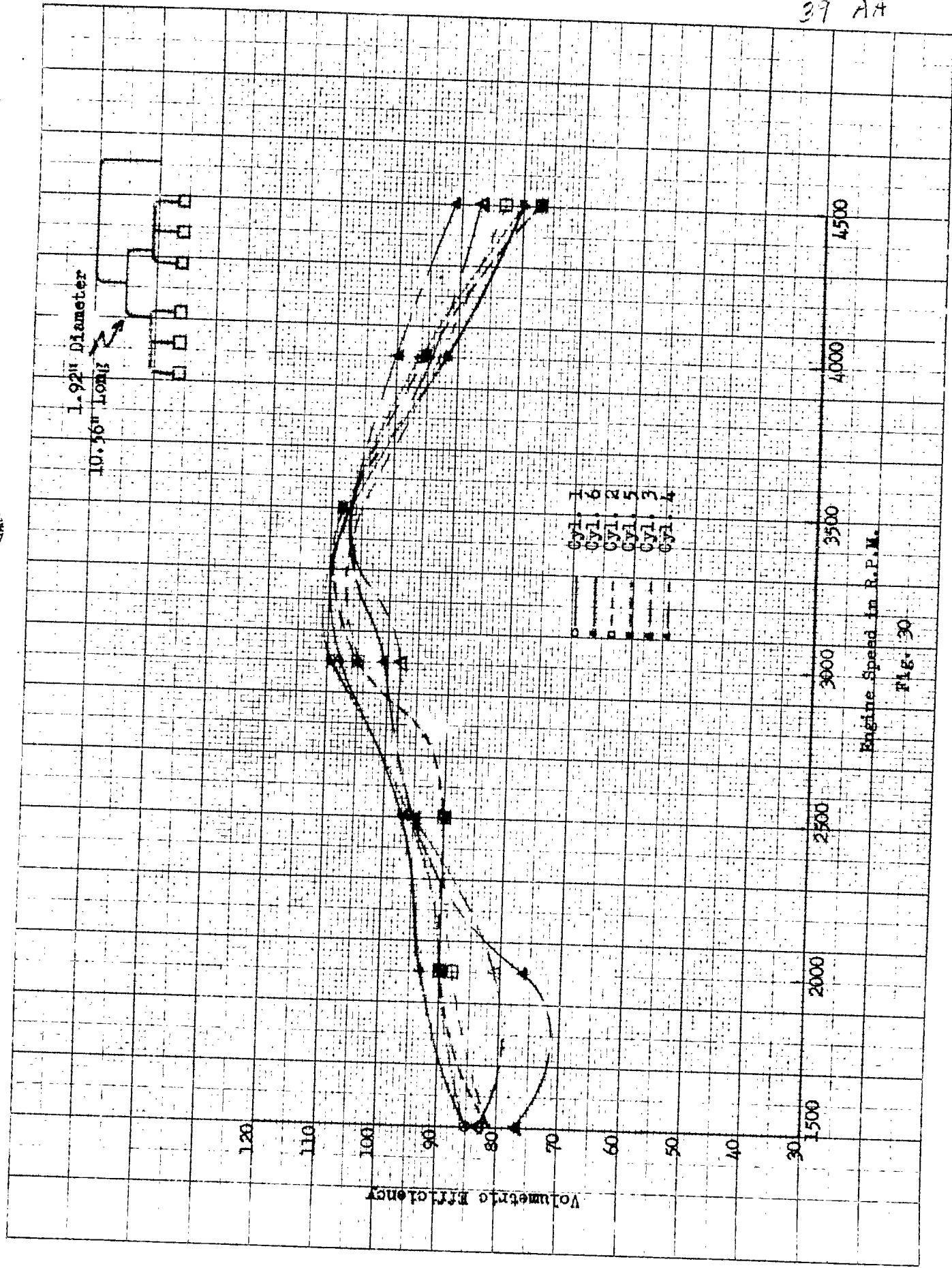


FIG. 30

Engine Speed in R.P.M.

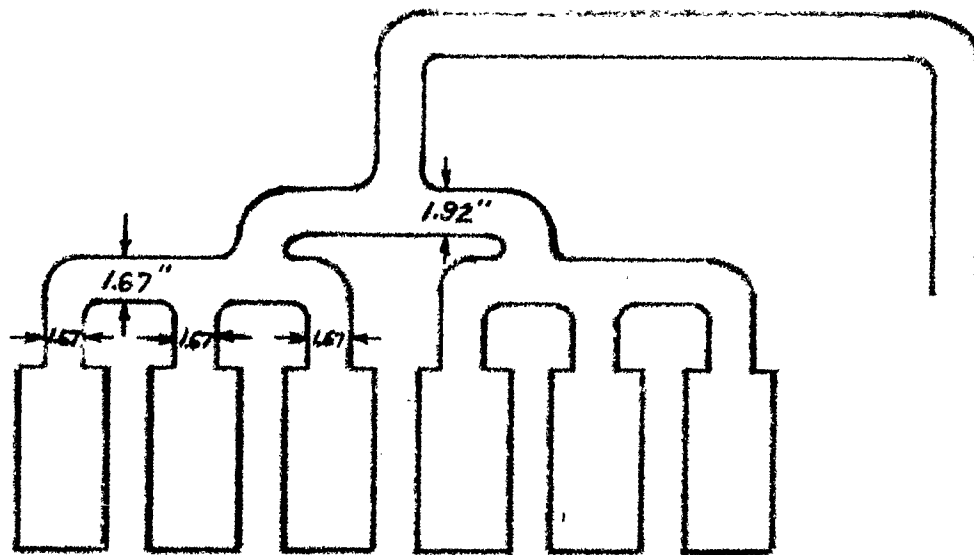
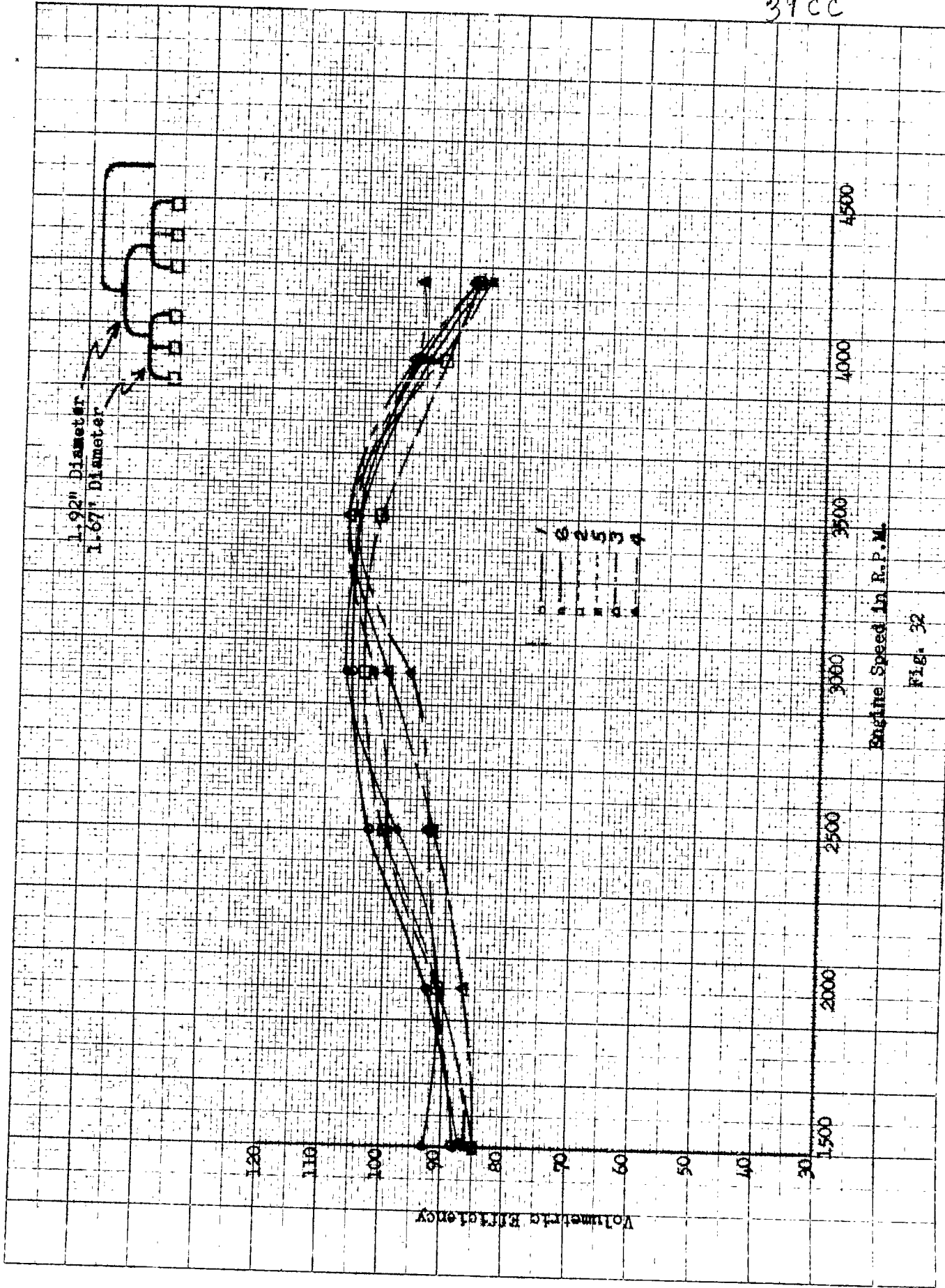
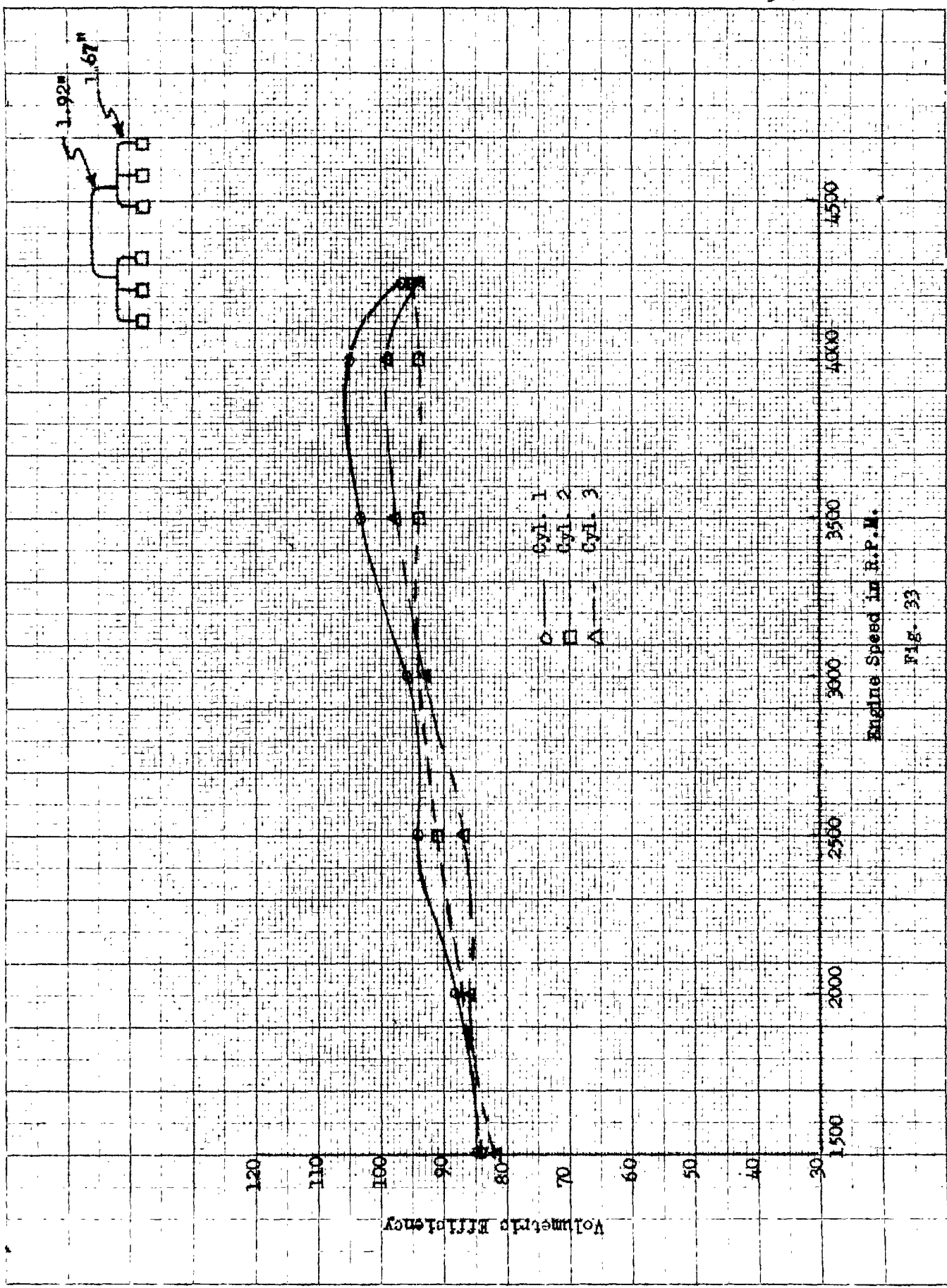


Fig 31



Engine Speed in R.P.M.

Fig. 32



Engine Speed in R.P.M.

FIG. 33

PART II.

I. Purpose

The experimental work for this report was done to obtain information concerning the effects of vibrations in intake manifolds on multi-cylinder engines of the six and twelve cylinder types. Most of the work was done on three cylinder groups that could be combined into six or twelve cylinder manifolds.

II. Experimental Apparatus

The engine used for the tests covered by this report was a six cylinder, Franklin, aircooled, automobile engine. This engine was used because it had individual intake ports which permitted the use of a wider variety of manifolds than would be possible with an engine having dual ports. The engine dimensions and an intake valve lift curve are given in Fig. 1. The valve lift on this engine was not great enough to permit high volumetric efficiencies to be obtained at high speeds. In order to study the effects of vibrations it was necessary to design many of the manifolds to give maximum vibration effects at relatively low speeds because high valve friction tended to prevent the vibrations from producing the desired effects at high speeds.

The engine was motored by another automobile engine (Fig. 2). The peak compression pressures obtained during motoring were used as a measure of relative volumetric efficiencies.

Compression pressures were measured with balanced pressure gages. Pressure diagrams in the various parts of the manifold were

obtained with magnetic pressure pick-ups used with a cathode ray oscillograph. Descriptions of the instruments and their calibration are given in a previous report on this project.*

Manifolds for the engine were made of standard pipe fittings welded together and drilled out so that they had uniform internal diameters. The pipe fittings used on the 1" diameter manifold were 3/4" pipe fittings with the threads drilled out so that the internal diameter was the same as that of 1" pipe (1.05"). 1" pipe fittings were used with 1-1/4" pipes.

Tests on a six cylinder manifold indicated that the flow through the common inlet for six cylinders was so uniform that vibrations of the air in the common inlet were small and of little importance. Because of this, most of the tests were run on three cylinder sections that might be used on six and twelve cylinder engines. The performance characteristics of a complete six or twelve cylinder manifold made up of sections of this type should be the same as those of one section. A picture and the dimensions of each manifold are shown with the performance data for the manifolds.

III. Theory

Figures 3 and 4 illustrate some features that are common to many multi-cylinder engine manifolds. There is a common inlet pipe leading to a Tee or header. Branch pipes lead from there into the

* "Progress Report on Study of Multi-Cylinder Engine Manifolds" by J. A. Hardy and E. N. Kemler, Army Air Forces Cooperative Research Project, M-125-1, Contract No. W535 ac-38886.

cylinders. On six and twelve cylinder engines of the inline or V type, the cylinders are often connected in groups of three. The intake strokes of these three cylinders are evenly spaced with respect to time so that there is little or no overlap of the valve opening periods on the different cylinders. In other words, during the intake stroke of one cylinder the valves on the other two cylinders are closed and the volumes of these cylinders are not connected to the manifold. The volume of the branch pipes leading to these cylinders, however, is still connected to the rest of the manifold and will influence the performance of the one cylinder under consideration.

During the intake period of any one cylinder, the air in the branch pipe for that cylinder and also the air in the common inlet pipe are accelerated during the first part of the intake period and decelerated during the last part of the intake period. The air in the other branch pipes does not move very much during this period and therefore does not contribute very much to the inertia effects of the system. The volume of these other branches, however, acts as a spring connected to the middle of the pipe leading to the active cylinder as shown in Fig. 4.

The deceleration of the air toward the end of the intake period is brought about by the stopping and reversal of the piston at the bottom of its stroke. Under some operating conditions the air may be decelerated and stopped before the intake valve closes. In this case some air may flow back out of the cylinder and less than maximum

charging effect will be obtained. Under different operating conditions the flow of air may not be stopped at the time of valve closing and the cylinder will be prevented from receiving a maximum charge as a result of the valve closing. In this case the valve itself finally stops the flow of air. The pressure at the intake port will be a maximum at the instant when the air flow in the pipe stops. Any reversal of flow will decrease the pressure.

The action of the air as described in the preceding paragraph will be called a ramming action. It produces high volumetric efficiencies under proper operating conditions by using the kinetic energy of the air in the intake pipe to compress the air in the cylinder. This is the only type of vibration of importance that exists when individual intake pipes leading from a common inlet such as a supercharger housing are used. The following equation will give the speed at which the maximum benefits can be obtained from ramming.*

$$N = C \frac{60}{2\pi} \sqrt{\frac{k}{m}} \quad (1)$$

where N = speed at which peak volumetric efficiency will occur, rpm

C = a constant which depends principally on the effective valve closing angle and on the amount of friction in the system.

It usually has a value between 0.6 and 0.7.

k = spring constant for the cylinder volume and a part of the manifold volume which acts as a spring in the vibrating system, lb/in.

* "Progress Report on Study of Multi-Cylinder Engine Manifolds", Army Air Forces Cooperative Research Project H-125-1, Contract No. W535 ac-38886.

~~44~~

m = effective mass of air entering into the "ramming" vibration,
lb/g or lb-sec²-in.⁻¹

This is the equation for the natural frequency of a simple vibrating system consisting of one mass and one spring with the constant, C , added. It is easy to apply to single cylinder intake pipes but it is sometimes difficult to use on multi-cylinder intake manifolds because it is difficult to determine what the effective mass and spring constant are. This equation is applied in analyzing experimental results given in this report. The equation can be put into a more convenient form by substituting for k and m in terms of engine dimensions. The equation will then be:

$$N = C \frac{60}{2\pi} \sqrt{\frac{a c^2}{V l}} \quad (2)$$

where a = cross-sectional area of intake pipe, in.²

V = effective volume = cylinder volume plus part of manifold volume, in.³

l = effective pipe length, in.

c = velocity of sound in air, in/sec = 13,900 in./sec for air at 100°F

The "ramming" vibration is not a resonant vibration, that is, it does not accumulate energy from one cycle to the next.

The best volumetric efficiency can be obtained when all, or nearly all, of the kinetic energy gained by the air in the branch pipe and inlet pipe during the first part of the intake process can

be used to compress the air in the cylinder toward the end of the intake stroke. The kinetic energy of the air in the branch pipe can be used quite advantageously, but the kinetic energy of the air in the inlet pipe must be partly used for compressing the air in the manifold volume and therefore is not as effective in increasing the volumetric efficiency. Generally the maximum pressure at the manifold toe which results from the deceleration of the air in the common inlet pipe will not be obtained until sometime after the maximum pressure at the port is obtained. This is due to the fact that the extra volume of the manifold connected to the inlet pipe acts as a reservoir for the air and even though the piston or valve stops the air in the branch pipe, the air in the inlet pipe can continue to flow into this volume until its kinetic energy is used up in compressing the air in the manifold. The extra volume of the manifold also prevents the air in the common inlet pipe from being accelerated as quickly as the air in the branch pipe during the first part of the intake stroke. The overall result is that the motion of the air in the common inlet lags behind the motion in the branch pipes.

The effect of the intake strokes of all three cylinders connected to this manifold is such that a steady state forced vibration of the air in the inlet pipe may exist. The frequency of this vibration is the same as the cyclic frequency of the engine ($3/2$ times the rpm.) The vibrating system consists of the mass of air in the inlet pipe and the volume of the manifold and one of the cylinders. Only one cylinder is connected to the manifold at any one time.

Such a system has a natural frequency of vibration. When the driving frequency is nearly the same as the natural frequency, small exciting forces will cause large amplitudes of vibration because energy is accumulated from one cycle to the next. When this condition exists the vibrating system is said to be in resonance.

The natural frequency of such a system is given by the same type of equation as was given for the speed for peak ramming effect:

$$f = \frac{60}{2\pi} \sqrt{\frac{a \cdot c^2}{V \cdot l}} \text{ cycles/min} \quad (3)$$

where a = area of inlet pipe, in.²

c = velocity of sound in air = 13,900 in./sec at 100° F

l = length of inlet pipe, in.

V = volume of manifold and one cylinder, in.³

When the driving frequency (3/2 times the rpm) is nearly equal to the natural frequency the amplitude of the pressures resulting from this vibration will be greatest. This high pressure amplitude, however, does not usually produce beneficially effects on the three cylinder systems because the air motion in the inlet pipe tends to be behind the motion in the branch pipes causing the pressure peaks to occur after the valve closes as was indicated earlier in this discussion. At driving speeds below the natural frequency some beneficial effects may be obtained even though the pressure amplitude is relatively low because the peak pressure will occur at the time of valve closing. At these low speeds the vibration is essentially a "ramming" vibration not a resonant vibration.

In general it does not seem likely that the vibration of the air in the common inlet pipe to three cylinders can be made to produce volumetric efficiencies as great as can be obtained by using individual intake pipes for all engine cylinders. A common inlet pipe to three cylinders sets up vibrations that waste energy in compressing air in the manifold. At speeds where a resonant effect carries energy over from one intake stroke to the next the pressure peaks occur too late (after valve closing) to produce beneficial effects.

The four cylinder manifolds discussed in the preceding report on this project showed that important beneficial effects could be obtained from a resonant vibration of the air in a common inlet pipe on a four cylinder manifold. The phase relation of the driving force on a four cylinder engine is such that the peak pressure occurs at the time of valve closing when the vibrating system is in resonance.

IV. Experimental Results

Single Cylinder Data

Some tests were run with pipes on one cylinder of the engine. The results of these tests are shown in Figures 5 and 6. The compression curves (Fig. 5) are typical of the curves that are obtained with most single cylinder intake pipes. The principal vibration is a ramming vibration as shown by Fig. 6. There is a large drop in pressure during the first part of the intake stroke. The pressure builds up at the end of the intake process due to deceleration of the

air in the pipe. The speed at which the peak volumetric efficiency occurs can be calculated from the equation given in the Theory. Calculated speeds at the peak and actual speeds at the peak are given in Table I. The value of C used for these calculations was 0.63. The actual and calculated peak speeds agree quite closely and thus check the theoretical reasoning.

Two Cylinder Manifolds

Tests on some two cylinder manifolds were given in the progress report on this project. Two additional modifications of the two cylinder manifolds were tested on the six cylinder engine. These manifolds had long branch pipes (26"). The first test was run with a short common inlet pipe. The results of this test are shown in Fig. 7. The speed for peak volumetric efficiency was 1700 rpm. The calculated speed based on the ramming action in the branch pipes is also about 1700 rpm (See Table I for 1-1/4" x 28.5" pipe). The maximum compression pressure, however, is lower than for a single cylinder inlet pipe of similar size (See Fig. 5). This is due largely to the extra friction in the Tee of the two cylinder manifold.

This manifold was also tested with a 30" inlet pipe attached. The results of this test are shown in Figures 8 and 9. The pressure diagrams taken at the Tee show that the vibration of the air in the inlet pipe increased in amplitude and became nearly sinusoidal at the high speeds indicating that a resonant vibration developed. At these high speeds, however, the pressure peaks occurred too late to produce

benefits. The principal vibration causing a high volumetric efficiency is a ramming action at low speeds. The mass of air in the common inlet pipe enters into the ramming action along with the air in the branch pipes. It is difficult to calculate the peak speed from the equations given in the Theory because of the uncertain effect of the extra manifold volume attached to the inlet pipe at the Tee.

Three Cylinder Manifolds, 1" Diameter

Figures 10 and 11 show the results of a test run on a 1" diameter manifold with long (25") branch pipes. No extra length of inlet pipe was used. The pressure diagrams show that the pressure amplitudes at the Tee are very small. This indicates that the vibration of the mass in the inlet pipe has only a small effect on the performance of the manifold. The volumetric efficiency should be affected principally by the ramming action in the branch pipes. The pressure diagrams taken at the intake port on cylinder 1 show the effects of ramming. There is a big pressure drop (Fig. 11) during the middle part of the intake stroke resulting from the acceleration of the air in the branch pipe. Toward the end of the stroke there is a pressure rise resulting from the deceleration of the air. The vibrations are almost identical to those in single cylinder intake pipes. The maximum volumetric efficiency should be obtained at the speed where the pressure at the time of valve closing is a maximum. Apparently the effective valve closing angle is somewhat earlier than that shown on the pressure diagrams, because the compression pressures reach a

maximum at about 1400 rpm while the pressure diagrams show that it should occur at a higher speed.

The important dimensions to be used in calculating the speed for peak volumetric efficiency calculated from equation 2 (Theory) are as follows:

Pipe length

length of branch pipe to header	25"
length of port	3"
inlet Tee to branch pipe	2.5"
total length	<u>31.5"</u>

Volume

volume of cylinder	60 in. ³
1/2 volume of pipe	<u>14 in.³</u>
total volume	74 in. ³

$$\text{area of pipe} = 0.868 \text{ in.}^2$$

Table I gives the actual and calculated speeds for peak volumetric efficiencies for a single cylinder intake pipe of about the same dimensions (33"). The calculated speed is 1560 rpm and the actual speed is 1500 rpm. The peak speed obtained on the multi-cylinder manifold is 1300 rpm. The lower speed at the peak obtained with the multi-cylinder engine is probably due to greater friction in the manifold. The lower peak pressure (about 117 psi) obtained with the multi-cylinder manifold compared with the value obtained with a single cylinder pipe (127 psi) is also the result of greater friction in the multi-cylinder manifold.

Figures 12 and 13 show the effect of adding a 13" inlet pipe to the manifold with 25" branch pipes. The compression pressure curves (Fig. 12) show that the additional length of inlet pipe had very little effect on the volumetric efficiency. The shape of the curves and the pressures are the same as without the inlet pipe. The speed for peak volumetric efficiency (1300 rpm) is the same.

The pressure diagrams taken at the inlet Tee show that a resonant type of vibration of the mass in the inlet pipe does develop. It reaches a maximum amplitude at about 1800 rpm. The phase relation of this vibration is such that very little beneficial effect is obtained. The pressure at the Tee at the time of valve closing never becomes much greater than atmospheric. Since the compression pressure curves were unaffected by the inlet pipe, it may be concluded that the inlet pipe did not have an appreciable effect on the ramming action.

Figures 14 and 15 show the effect of adding a 33" inlet to the manifold. This pipe had an important effect on the compression pressures as shown in Fig. 14. The peak occurred at about 1100 rpm and the curves are nearly flat from 1500 rpm to 2000 rpm.

The pressure diagrams help to explain the factors affecting the shape of the compression pressure curves. The pressure diagrams obtained at the inlet Tee (Fig. 15) show that a resonant vibration of the air in the inlet pipe developed and reached a maximum amplitude at about 1400 rpm. At speeds below 1400 rpm the phase relation of this vibration was such that a pressure greater than atmospheric existed

at the Tee at the time of valve closing. At speeds above 1400 the pressure at the Tee at the time of valve closing were below atmospheric. This vibration should, therefore, increase volumetric efficiencies at the low speeds. The compression pressure curves show evidence of this. The effect of ramming in the branch pipes was not greatly changed but the compression pressures were modified by the vibration of the air in the intake pipe.

15" branch pipes were used with the 1" diameter manifold. The results of a test with this manifold and no inlet pipe attached are shown in Figures 16 and 17. The principal vibration affecting the volumetric efficiency, as in the case of the 25" branch pipes, is the ramming action. The peak volumetric efficiency occurs at 1450 rpm. This speed is lower than the speed calculated from equation (2) because of the high friction of the multi-cylinder manifold. The pressure diagrams taken at the inlet Tee show that the pressure amplitudes due to vibration of the air in the short 3" inlet were very low and should have a negligible effect on volumetric efficiency. The pressure diagrams taken at the intake port have the typical shape of pressure curves resulting from ramming.

Figures 18 and 19 show the results of a test run with 15" branch pipes and a 13" inlet pipe on the 1" diameter manifold. The peak compression pressures occur at 1400 rpm almost the same as the speed that was obtained without the 13" inlet pipe. The pressure diagrams obtained at the inlet Tee show that the vibration of the air in the inlet pipe should aid the ramming action at 1400 rpm because the

pressure at the Tee is above atmospheric at the time of valve closing.

Tests were run with short, 4" branch pipe lengths, on the 1" diameter manifold. On the first of these tests a 13" inlet pipe was used. The results of this test are shown in Figures 20 and 21. The peak compression pressures occur at 1500 rpm. The pressure diagrams obtained at the inlet Tee show a rather steep rise in pressure at the time of valve closing for speeds above 1000 rpm. This indicates that the air in the inlet pipe is slowed down rapidly by the stopping of the piston and the valve closing. The effect is similar to ramming in the branch pipes. It is more predominant when short branch pipes are used because the manifold volume is small and does not have a "soft" enough spring action to permit the air in the intake pipe to vibrate in the normal manner. The air in the inlet pipe therefore produces a significant ramming action along with the air in the branch pipes. Any attempt at calculating the speed for peak ramming action in the branch pipes on this manifold is complicated by the indeterminate ramming effect of the air in the inlet pipe. The combined effects of ramming in the branch pipes and ramming in the inlet pipe causes the peak volumetric efficiency to occur at a lower speed than it would for either of these effects separately.

A 33" intake pipe was attached to the 1" manifold with 4" branch pipes. The results of a test run on this manifold are shown in Figures 22 and 23. The compression pressure curves show that the peak volumetric efficiency was obtained at 1300 rpm. The pressure diagrams, Fig. 23, show that the pressures at the port are generally

not greatly different from those obtained at the inlet Tee. This indicates that the vibration of the air in the inlet pipe produces the principal effect. At the speed where the peak compression pressure occurs the vibration is principally a ramming action of the air in the inlet pipe.

1-1/4" Manifolds

A manifold made of 1-1/4" pipe was tested. The first test run on this manifold was made with short (3") branch pipes and a short (2.5") inlet pipe. The results of this test are shown in Figures 24 and 25. This manifold did not produce any very important vibrational effects. The pressure diagrams, Fig. 25, show that the pressures at the Tee were always very close to atmospheric pressure. The pressures obtained at the valve port show a significant pressure drop during the intake stroke but very little pressure rise at the end of the stroke. The pressure drop is apparently largely due to friction in the manifold. The small pressure rise is to be expected because the pipes are too short to produce important ramming effects at the speeds used for the test.

The compression pressure curves show a small rise up to 1900 rpm and a decrease beyond that speed. The small rise is due to the small amount of ramming that is obtained in the manifold. The decrease is due to high friction in both manifold and the engine valves. The speed for peak compression pressure is much lower than would be expected for a manifold with such short pipes. This particular engine apparently has too much valve friction to permit obtaining

benefits from vibrations at high speeds.

Figures 26 and 27 show the results of a test run with a 19" inlet pipe on the 1-1/4" manifold. The addition of the inlet pipe caused vibrations of significant amplitude to exist within the speed range for the test. The pressure diagrams obtained at the Tee show that a resonant vibration tends to develop at the high speeds. At the speeds where the pressure peak occurs early enough to produce an increase in volumetric efficiency the vibration is principally a ramming vibration. The pressure diagrams obtained at the valve port are similar in shape and amplitude to the diagrams obtained at the Tee indicating that the principal effect is produced by the vibrations of the air in the inlet pipe. There is some evidence of ramming produced by the air in the branch pipe.

The theoretical speed for peak ramming effect assuming the effect of ramming in the branch pipe to be negligible is as follows:

manifold and port volume	42 in. ³
1/2 of inlet pipe volume	13.5 in. ³
cylinder volume	60.0 in. ³
Total volume	<u>115.5 in.³</u>

pipe length = 19 in.

pipe area = 1.49 in.²

$$C = 0.63$$

$$N = C \frac{60}{2\pi} \sqrt{\frac{a c^2}{V l}}$$
$$= .63 \frac{60}{2\pi} \sqrt{\frac{1.49 \times 13,900^2}{115.5 \times 19}} = 2100 \text{ rpm}$$

The compression pressure curves show that the peak occurs at 1800 rpm instead of 2100 rpm. This is probably due to the fact that the high manifold and valve friction tend to reduce the peak speed and also due to the effect of inertia in the branch pipes which would tend to retard the development of the vibration in the inlet pipe.

14" branch pipes and a short inlet pipe used on the 1-1/4" manifold. The results of a test on this arrangement are shown in Figures 28 and 29. The pressure diagrams obtained at the Tee show that the vibrations of the air in the short inlet pipe produce negligible pressure effects. The principal vibration is, then, a ramming action of the air in the branch pipes. The peak compression pressures were obtained at 1800 rpm. This speed is somewhat lower than the theoretical speed for ramming with the branch pipe length used. This is probably due to friction in the multi-cylinder manifold.

Six Cylinder Manifold

Some tests were run on a six cylinder manifold as shown in Fig. 30. Tests were run both with and without the carburetor attached. Figures 30, 31, and 32 show the results of a test run without the carburetor. The pressure diagrams obtained at the Tee where the riser from the carburetor joins the header are shown in Fig. 31. The pressure amplitudes obtained at this point are very small, indicating that the effects of vibration of the air in the riser were negligible. The principal factor affecting the volumetric efficiency appears to be the ramming action of the air in the branch pipes leading from the

header to the individual cylinders. These branch pipes are short (6" plus 3.5" port length) and should produce maximum ramming action at speeds higher than those used in the test; however, the high valve friction on this engine prevented the utilization of the vibrations at high speeds.

Fig. 30 shows the compression pressure curves for the first three cylinders. The last three cylinders are symmetrical with the first three and should have identical curves. These curves show the tendency for the compression pressures to rise with speed but at high speeds the high valve friction prevents the continued rise in pressure.

The data obtained with the carburetor attached are shown in Figures 33, 34, and 35. The results are almost identical to those obtained without the carburetor indicating that the carburetor did not modify the vibrations. The compression pressures are slightly lower because of a small increase in friction due to the carburetor.

V. Conclusions

Manifolds on six and twelve cylinder engines are often arranged so that the cylinders are connected in similar groups of three. The vibrational effects of the manifold as a whole should be the same as that of one three cylinder group because when two of these groups are connected together at a common inlet the air flow in the common inlet is so nearly steady that no new vibrational effects are introduced.

The vibrations in the three cylinder manifold can be divided into two principal types: (1) a ramming vibration and (2) a resonant vibration. Simple equations given in this report show the effects of engine and manifold dimensions on these vibrations and help to explain the performance of the manifolds.

The ramming type of vibration has the most important effect on the volumetric efficiency. The total ramming action includes the effect of the mass of air in the common inlet pipe to the three cylinder group, together with the ramming action in the branch pipes. The ramming action of the air in the common inlet is less effective than the ramming action from the air in the branch pipes. This is due to the fact that kinetic energy of the air in the common inlet pipe is partly used in compressing air in the manifold volume rather than ramming air into the cylinder.

Resonant vibrations of the mass of air in the common inlet do occur but they are not effective in increasing the volumetric efficiency of a three cylinder group. When the system is in resonance the pressure peaks occur too late (after valve closing) to produce beneficial effects. Beneficial resonant vibrations in four cylinder manifold sections may be obtained as was indicated in a previous report on this project.

The tests indicate that the highest volumetric efficiencies can be obtained with individual pipes to each cylinder from a common inlet for all cylinders. The pipe dimensions necessary to produce maximum volumetric efficiency at any speed can be calculated quite

closely by using equation 2 in this report.

Some two cylinder manifolds were tested but the results of the tests indicated that single pipes were better whenever they can be used.

The tests show that excess friction in the valves or manifold prevent vibrations from developing and producing beneficial effects. Tests run at high speeds where the valve friction was excessive showed that very short pipes gave results as good as those obtained with pipes tuned for these high speeds.

59A

TABLE I.

Actual and Calculated Speeds for Peak Volumetric
Efficiency for Single Cylinder Intake Pipes

Pipe Size	Actual Speed, RPM	Calculated Speed, RPM *
1½" x (28.5 + 3.5)	2000	1980
1" x (44 + 3.5)	1300	1260
1" x (30 + 3.5)	1550	1560
1" x (20 + 3.5)	1800	1920

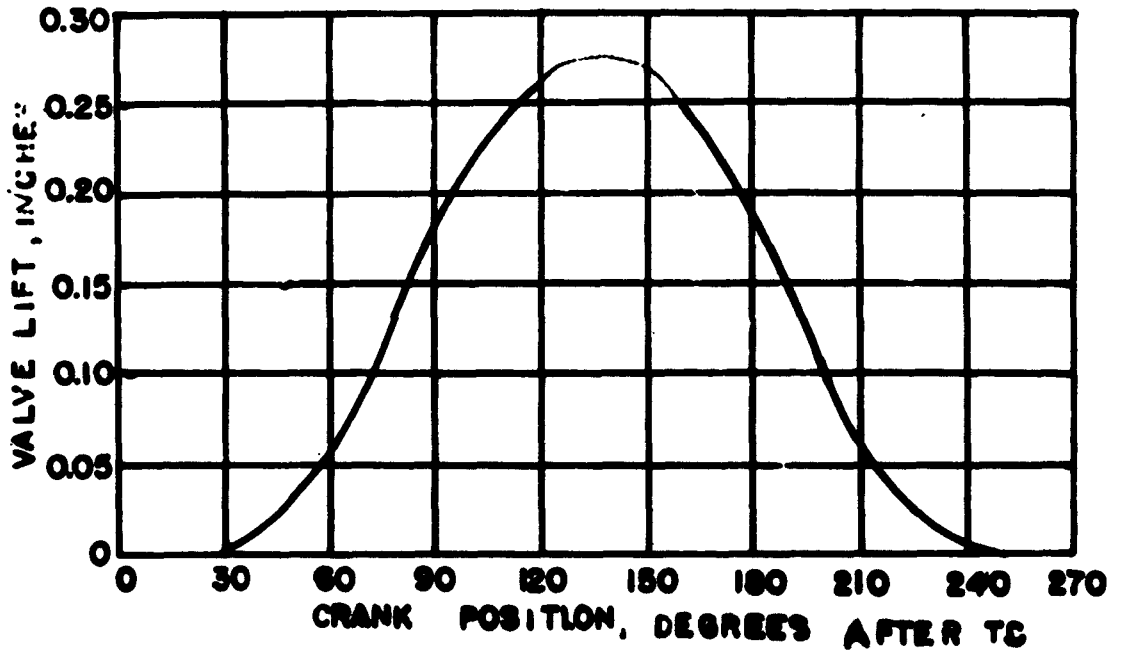
* Equation 2 of the theory was used for these calculations.
V was taken as the maximum cylinder volume plus one-half of
the pipe volume. c was taken as 0.65.

59B

FIG. 1 - ENGINE DATA

NO. OF CYLINDERS	6
BORE	3.5"
STROKE	5.0"
DISPLACEMENT	48.0 CU IN. PER CYL.
INTAKE VALVE PORT DIAMETER	1.375"
COMPRESSION RATIO	4.7
FIRING ORDER	1-4-2-6-3-5

INTAKE VALVE LIFT CURVE



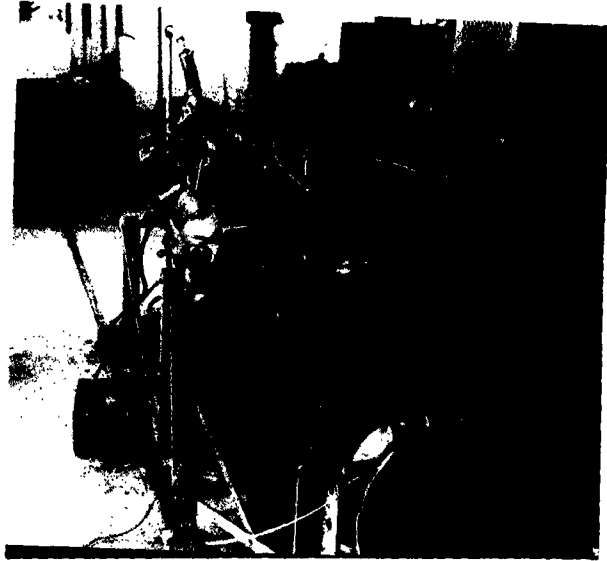


Fig. 2 -- Experimental Engine With
Motoring Engine

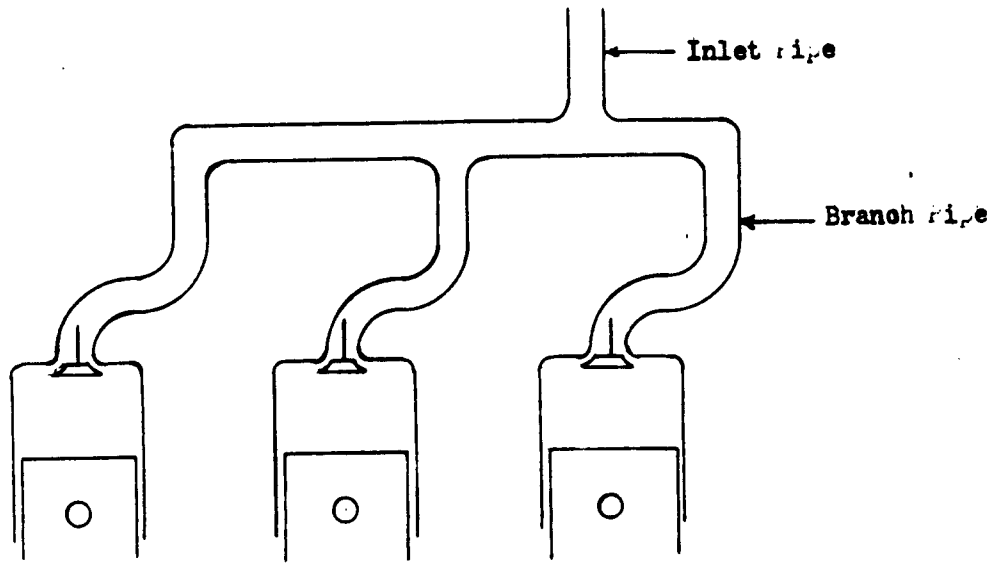


Fig. 3

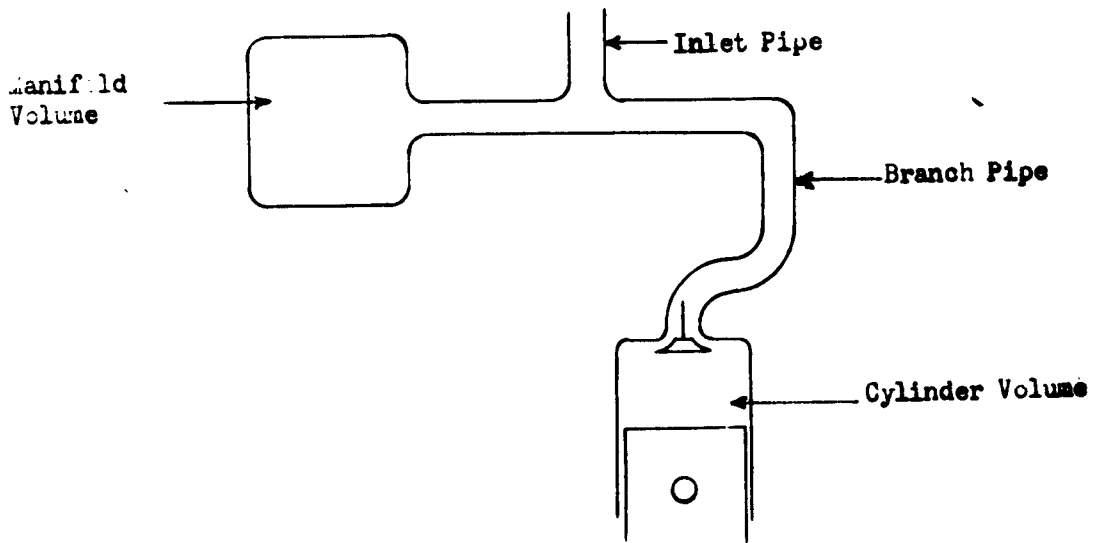
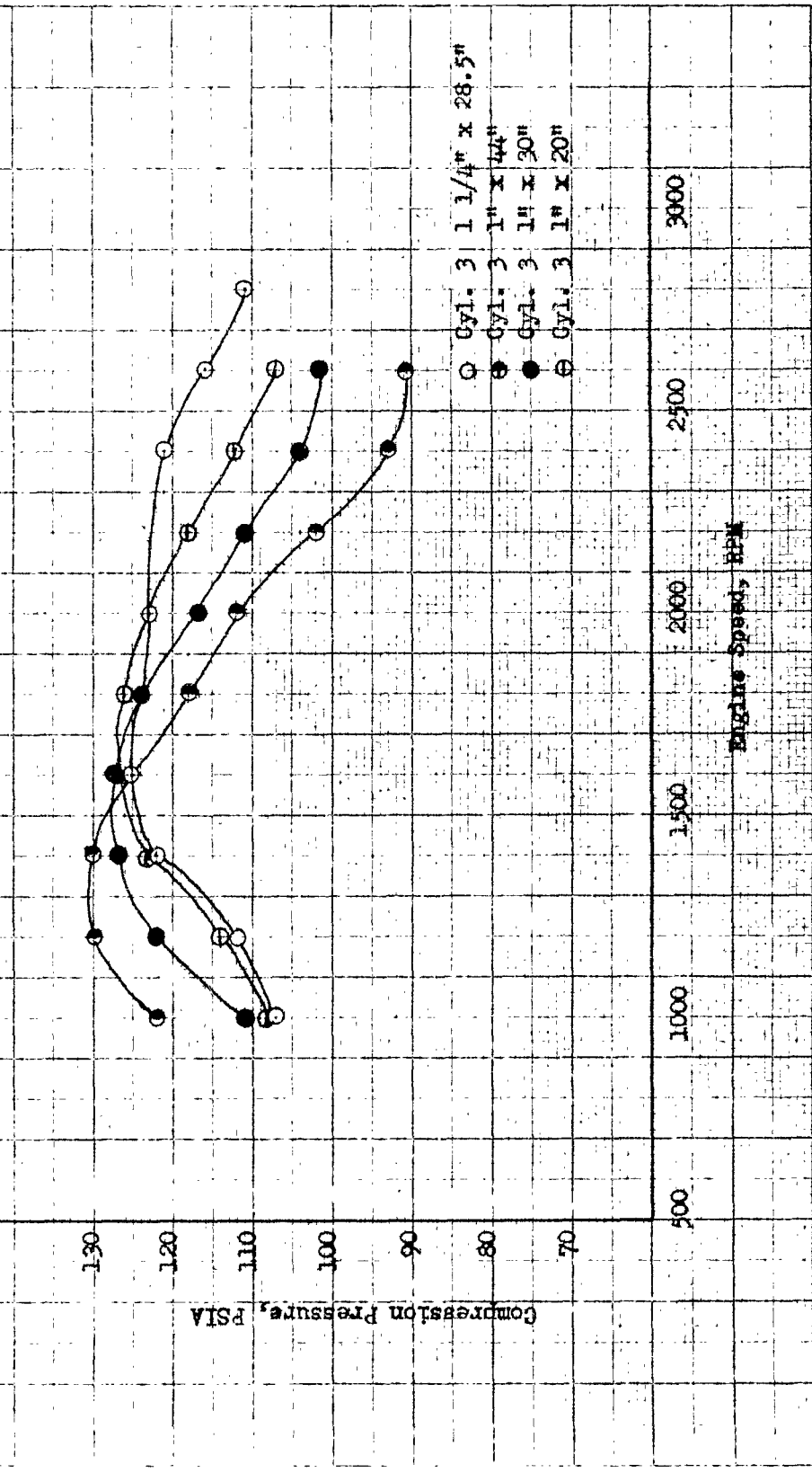


Fig. 4



Fig. 5 - Compression Pressures, Single Cylinder Manifolds



Compression Pressure, PSIA

500

1000

1500

2000

2500

3000

Engine Speed, RPM

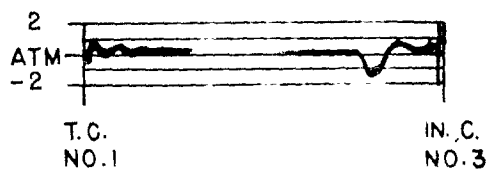
○ Cyl. 3 1 1/4" x 28.5"
□ Cyl. 3 1" x 44"
● Cyl. 3 1" x 30"
△ Cyl. 3 1" x 20"

Fig. 6 - Pressure Diagrams, Single Cylinder Manifolds

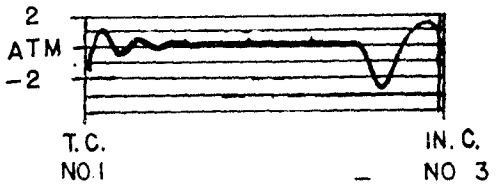
R.P.M.

CYLINDER. 3

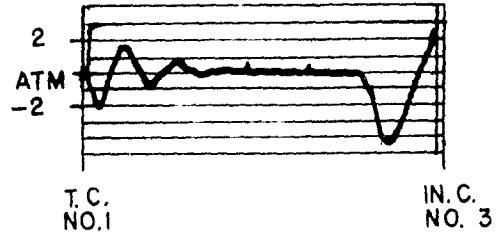
600



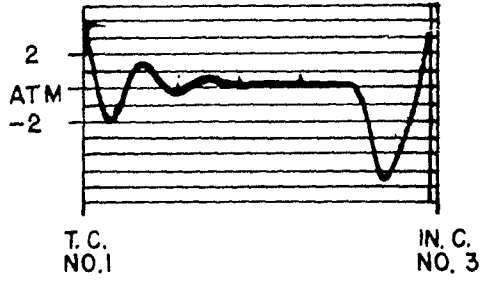
1000



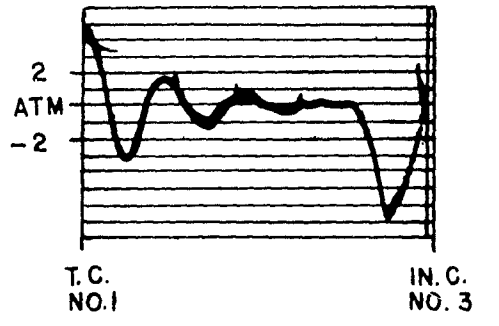
1400



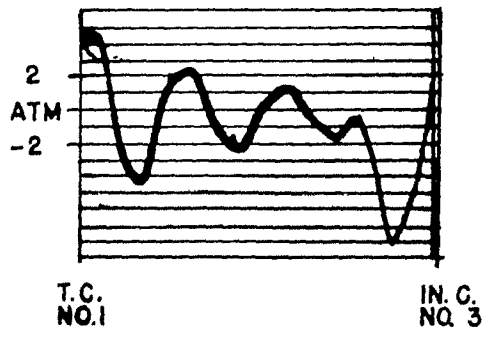
1800



2200



2600



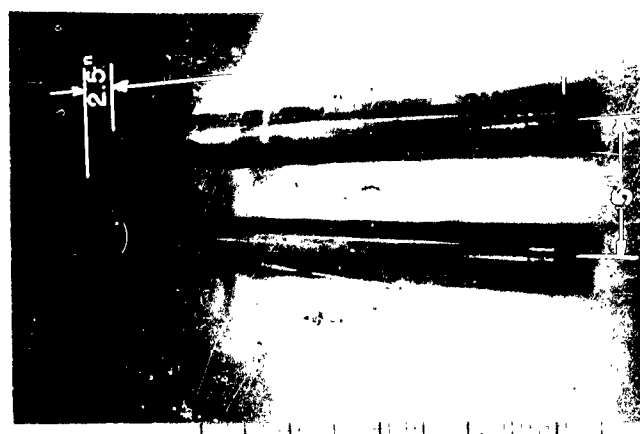
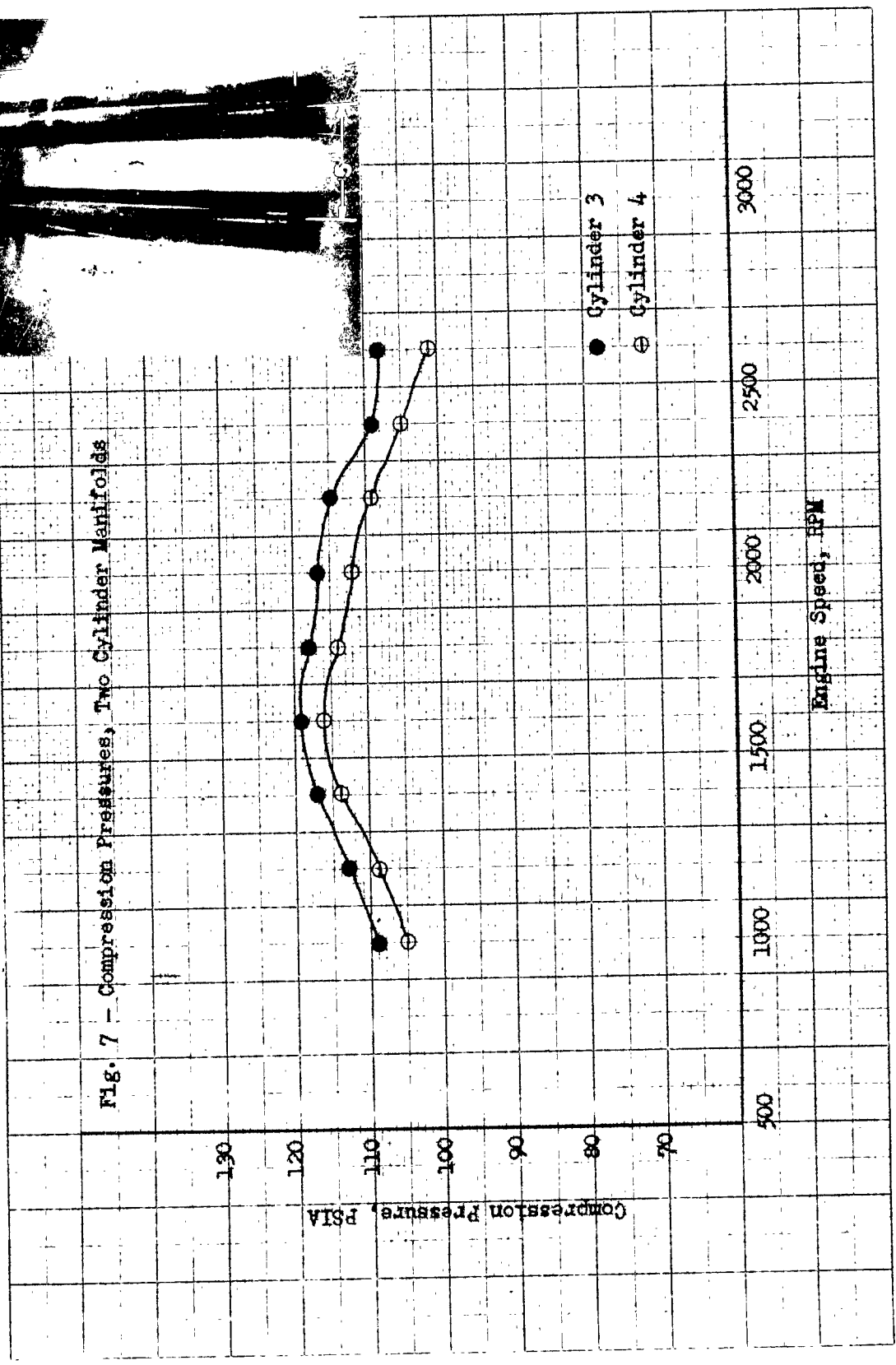


Fig. 7 - Compression Pressures, Two Cylinder Manifold





57H

Fig. 8 - Compression Pressures, Two Cylinder Manifolds

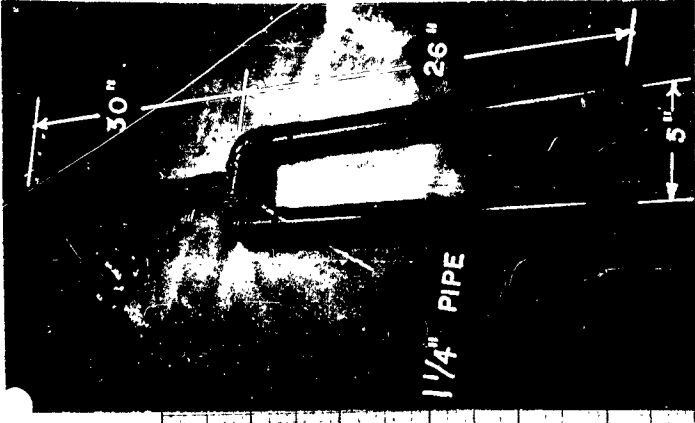
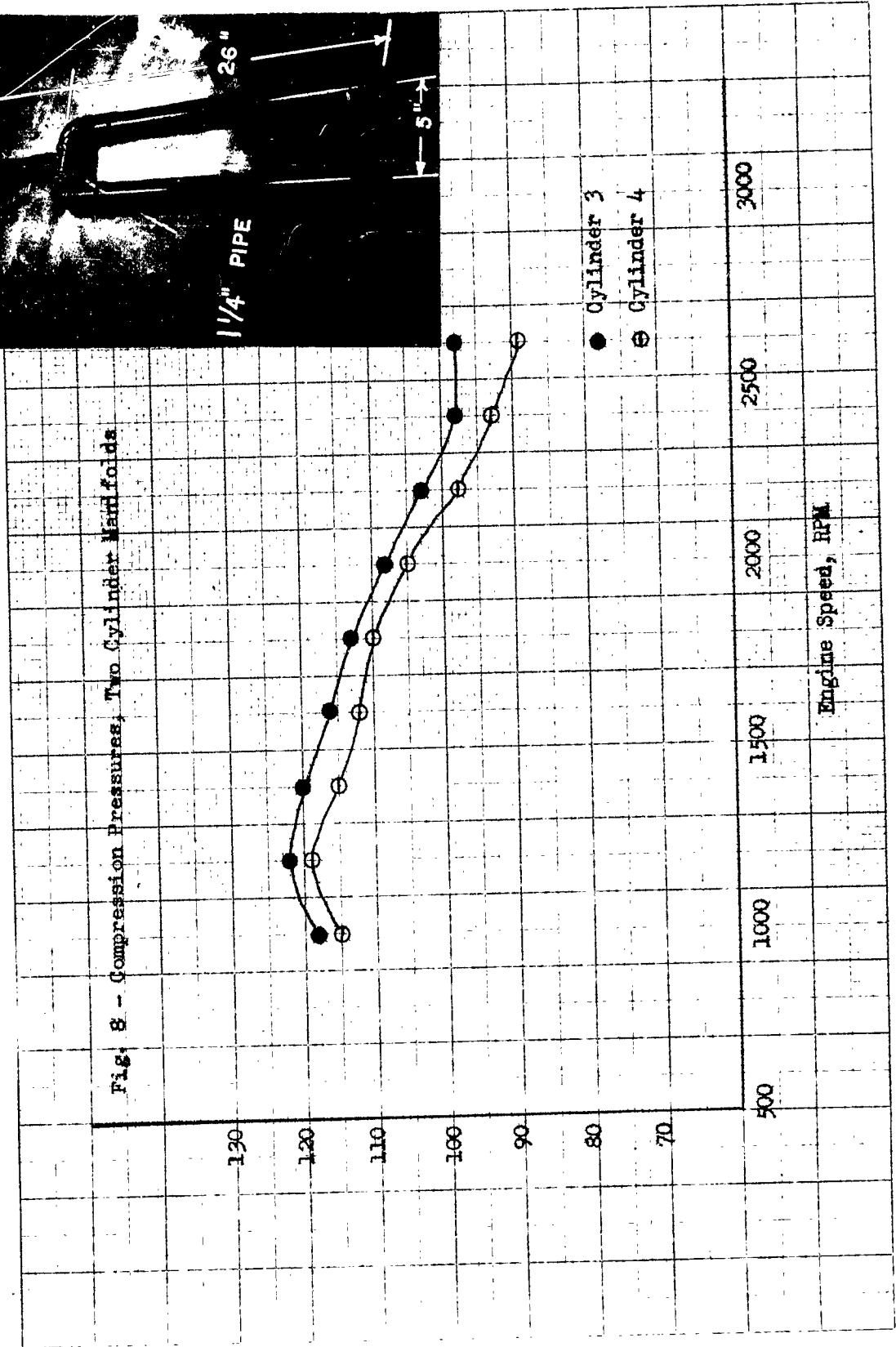


Fig. 9 - Pressure Diagrams, Two Cylinder Manifolds

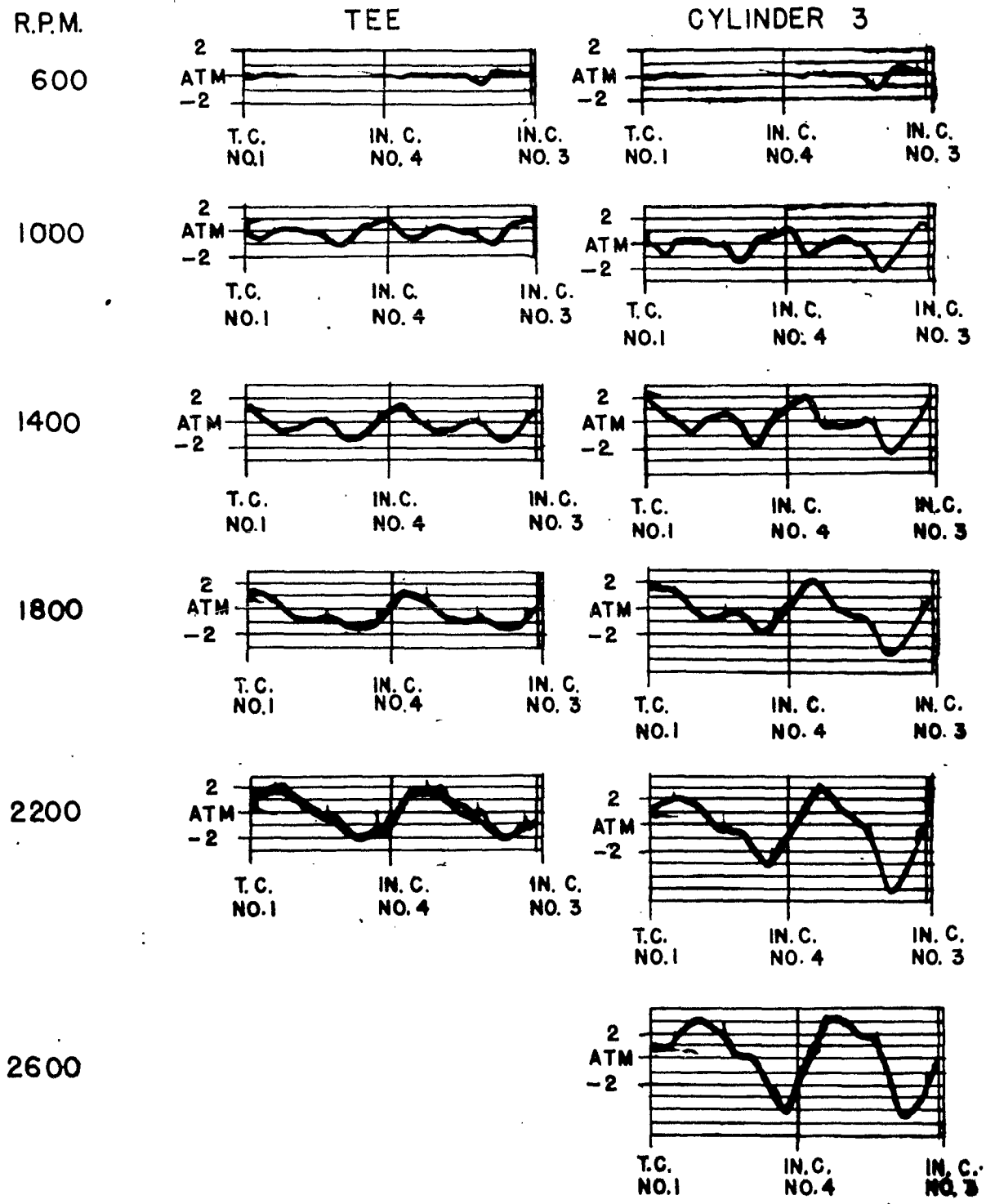
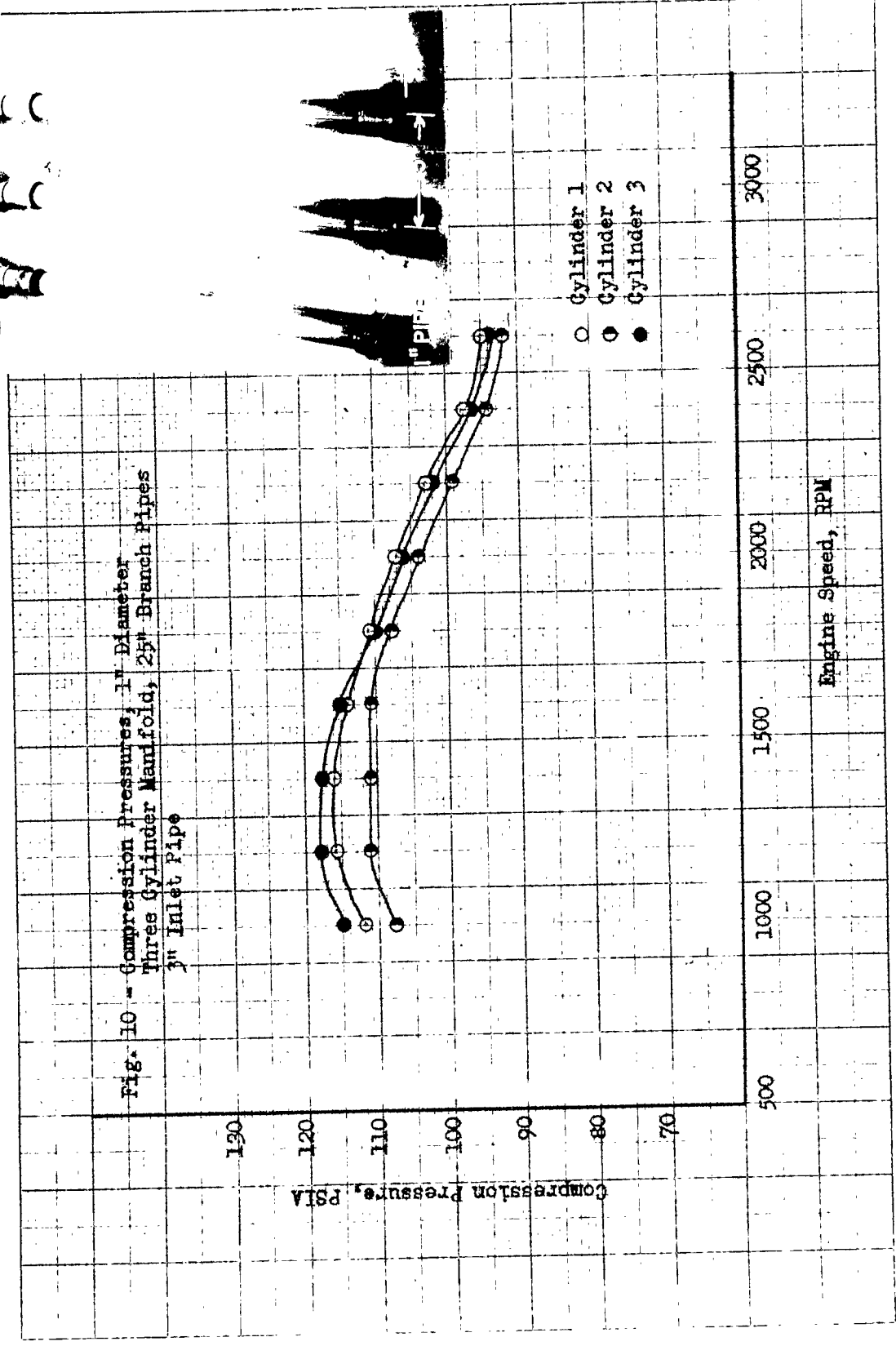




Fig. 10 - Compression Pressures, 1" Diameter Three Cylinder Manifold, 2 1/2" Branch Pipes 3/4" Inlet Pipe



51J

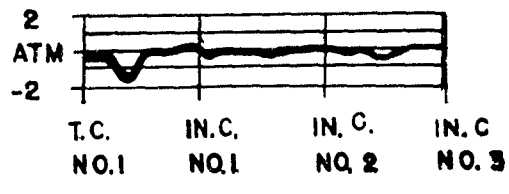
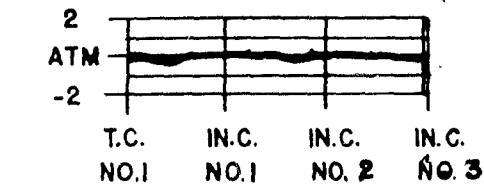
Fig. 11 - Pressure Diagrams, 1" Diameter Three Cylinder Manifold, 2 1/2" Branch Pipes, 3" Inlet Pipe.

R.P.M.

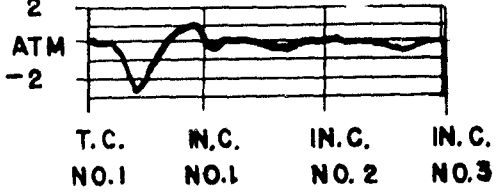
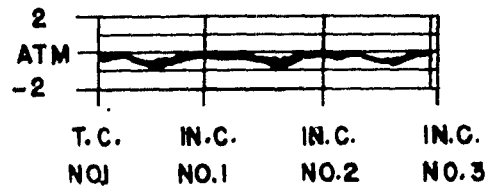
TEE

CYLINDER 1

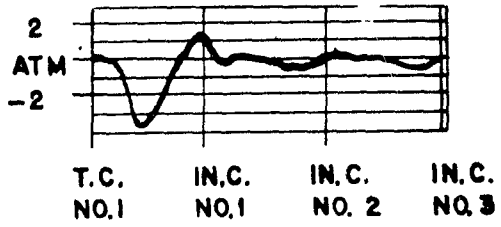
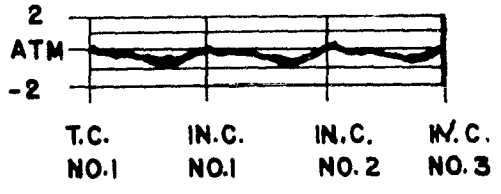
600



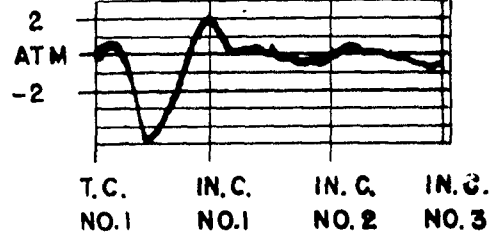
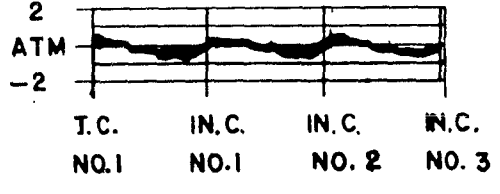
1000



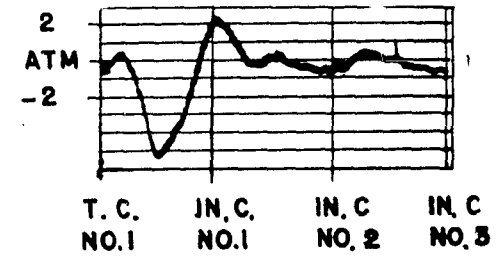
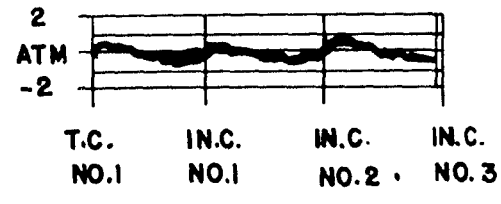
1400



1800



2200



2600

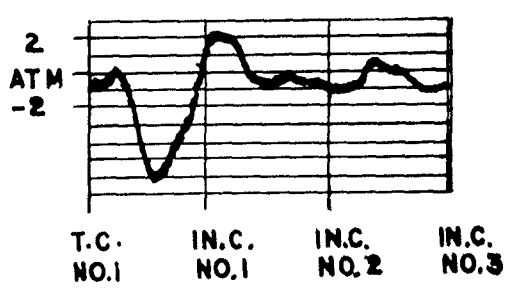
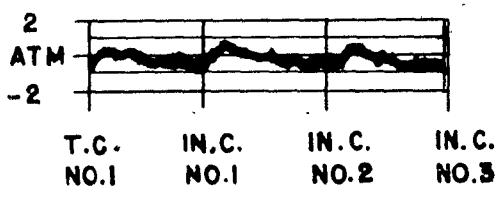




Fig. 12 - Compression Pressures, 1" Diameter
Three Cylinder Manifold, 25" Branch Pipes
1 3/4" Inlet Pipe

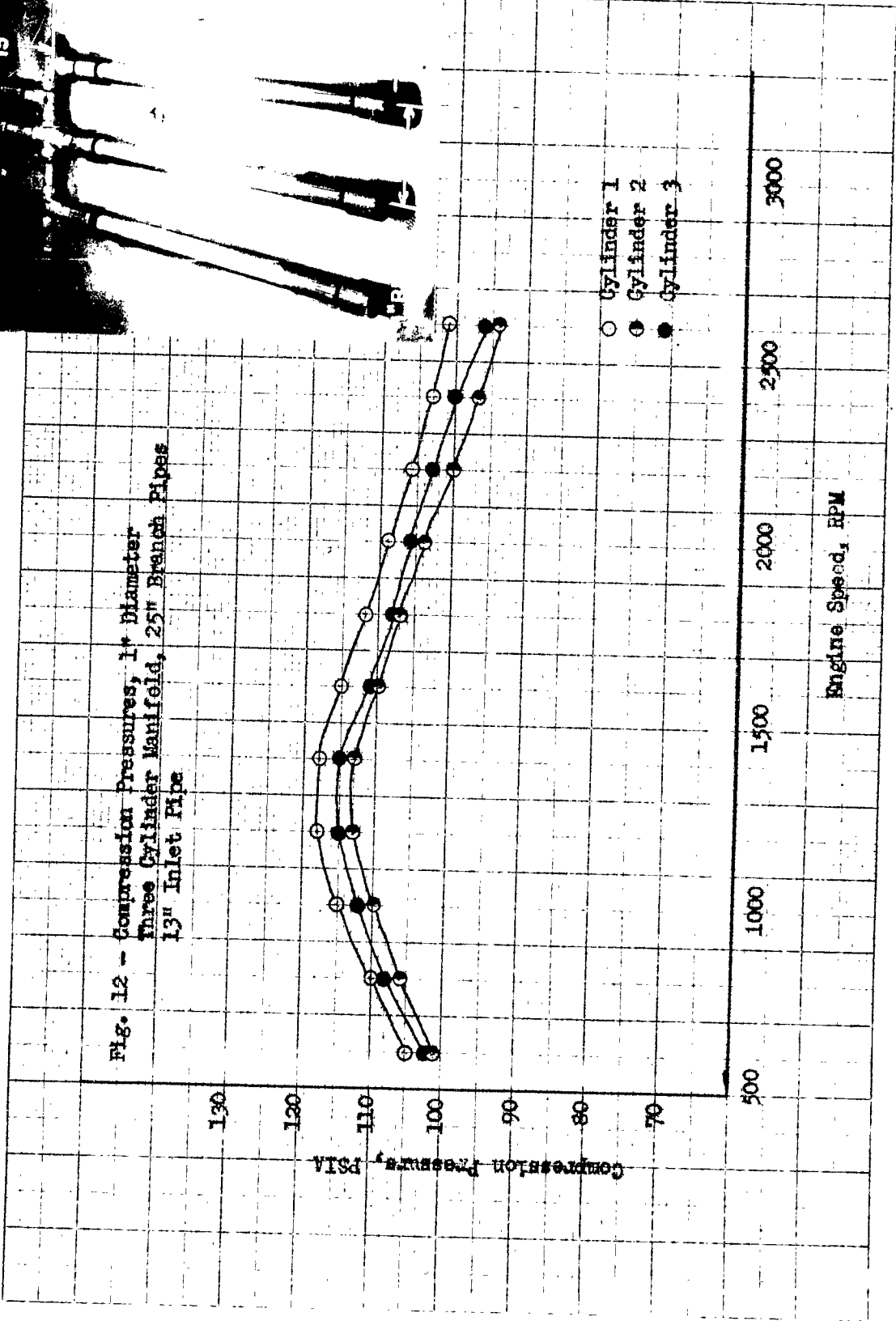
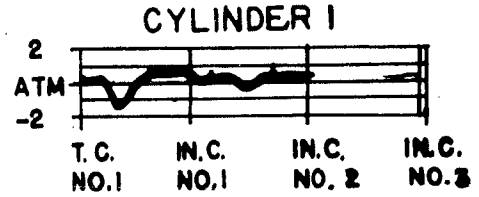
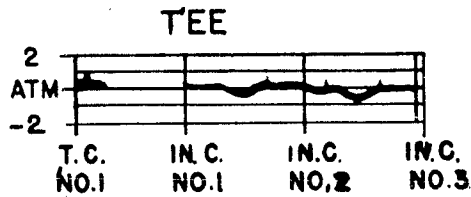


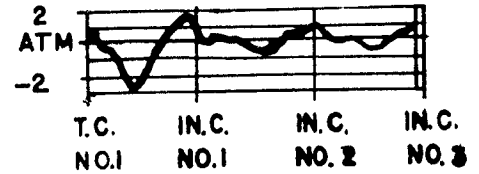
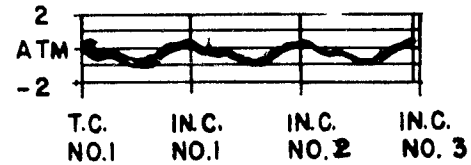
Fig. 13 - Pressure Diagrams, 1" Diameter
 Three Cylinder Manifold, 25" Branch
 Pipes, 13" Inlet Pipe.

R.P.M.

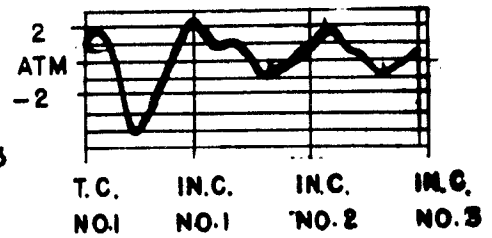
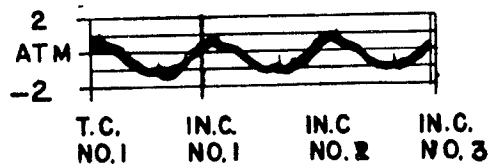
600



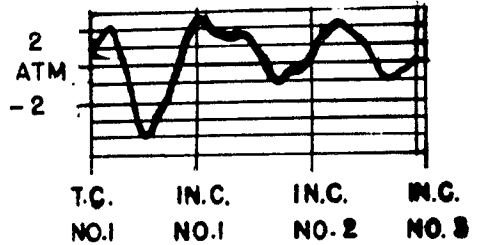
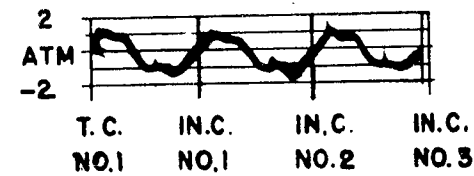
1000



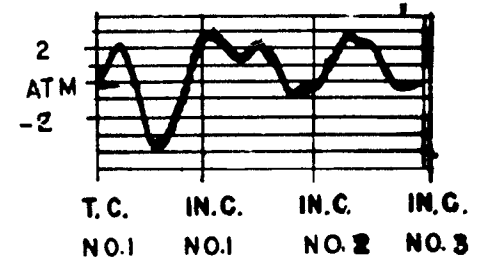
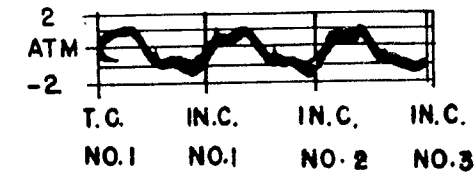
1400



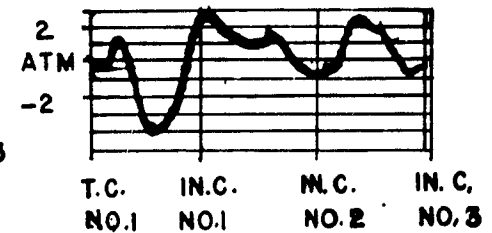
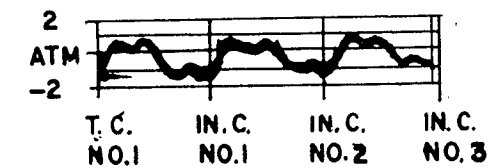
1800



2200



2600



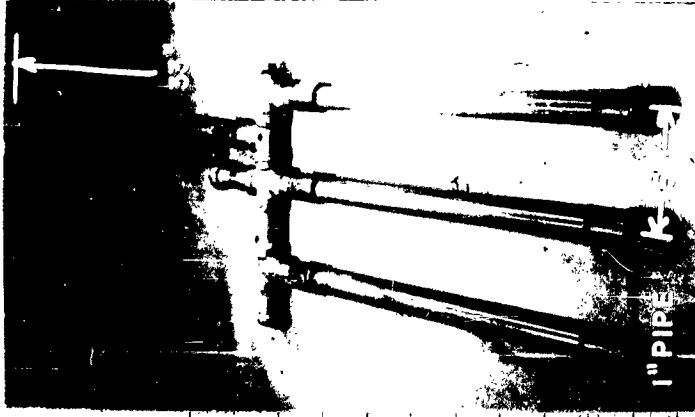
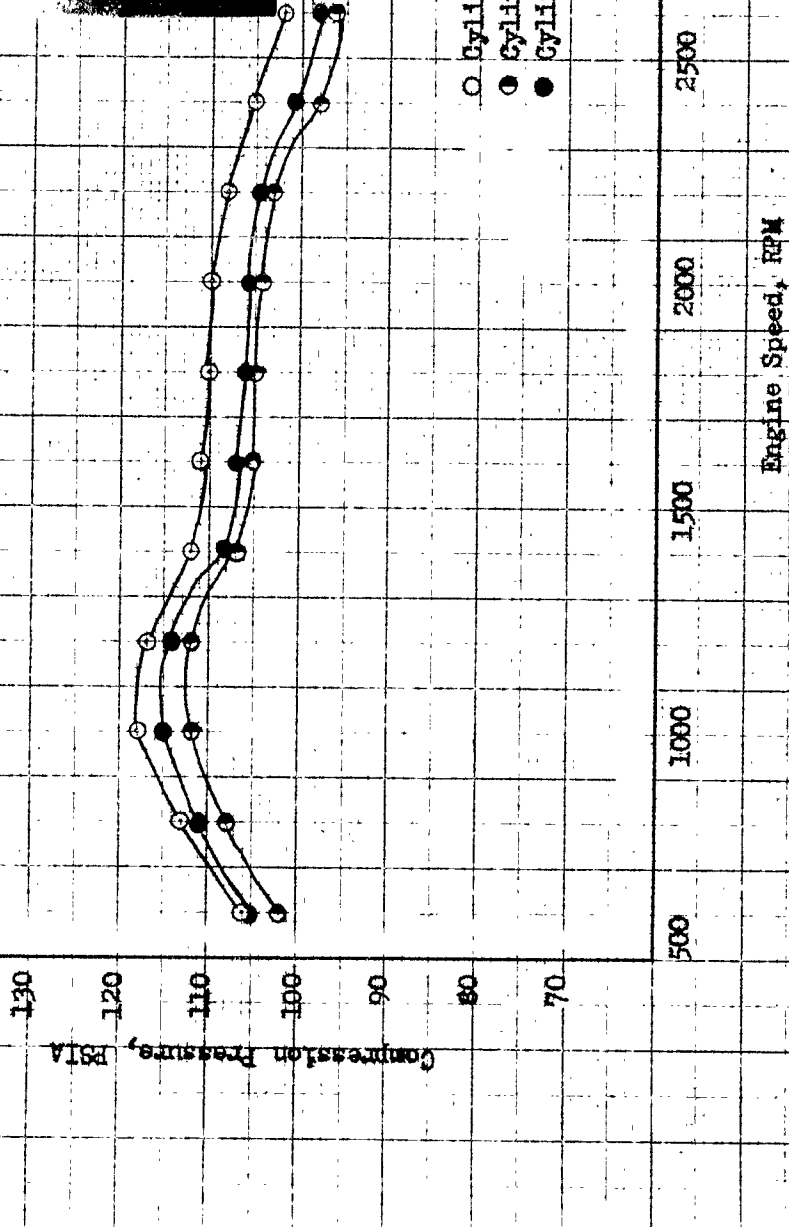


Fig. 14 - Compression Pressures, 1" Diameter, Three Cylinder Manifold, 2 1/2" Branch Pipes, 3/4" Inlet Pipe



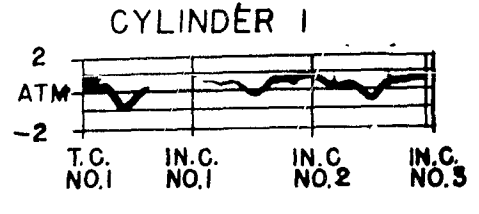
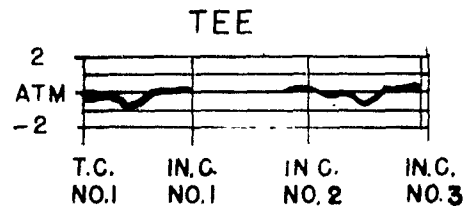
9M

5-11

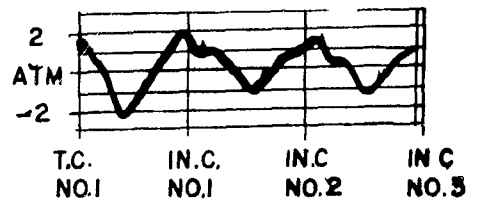
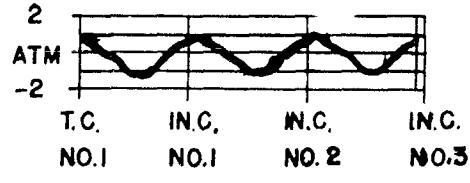
Fig. 15 - Pressure Diagrams, 1" Diameter
Three Cylinder Manifold, 25" Branch
Pipes, 33" Inlet Pipe

R.P.M.

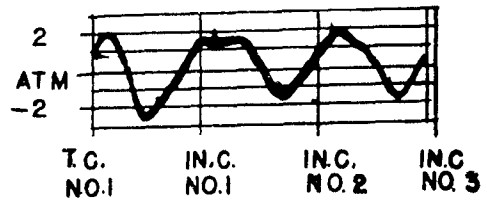
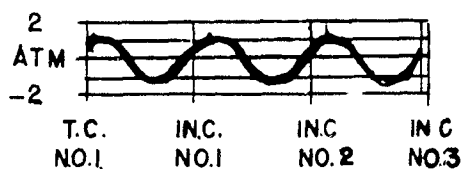
600



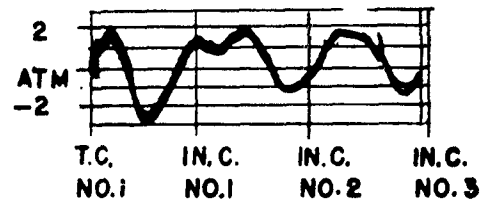
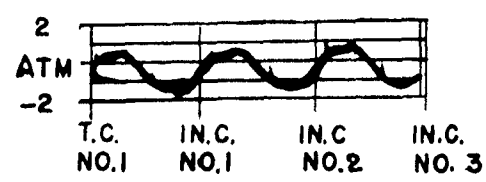
1000



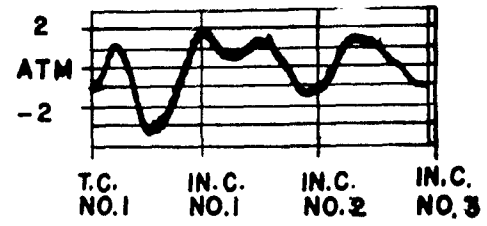
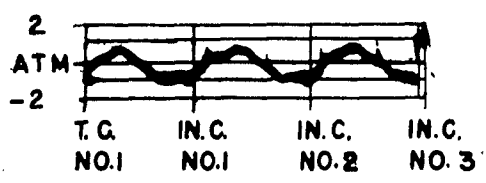
1400



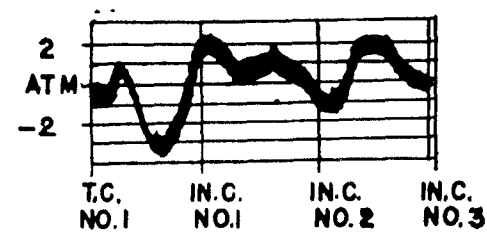
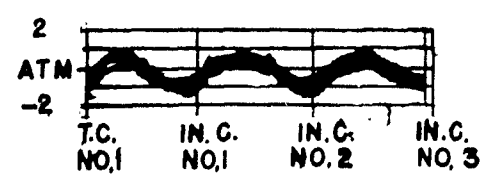
1800



2200



2600



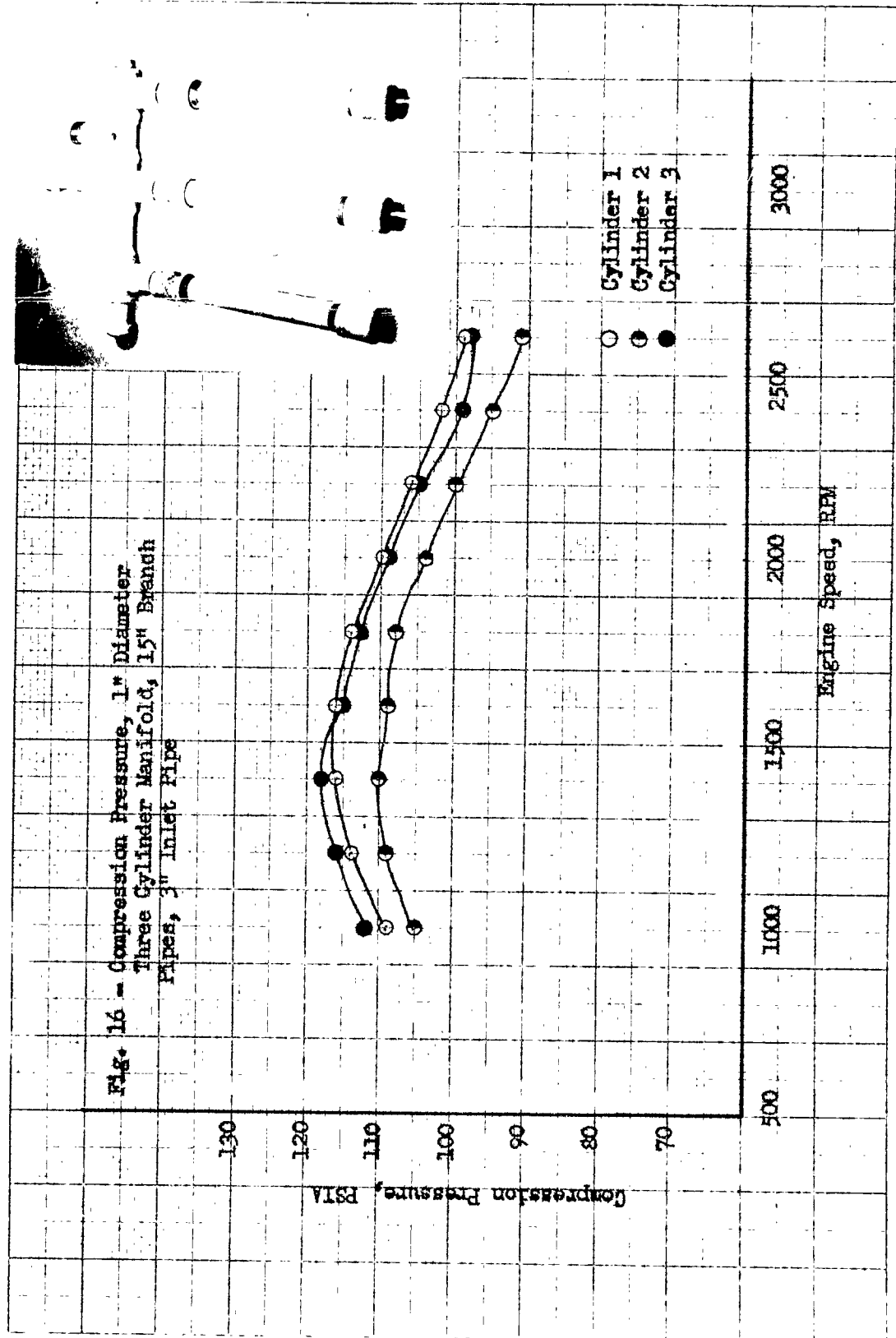
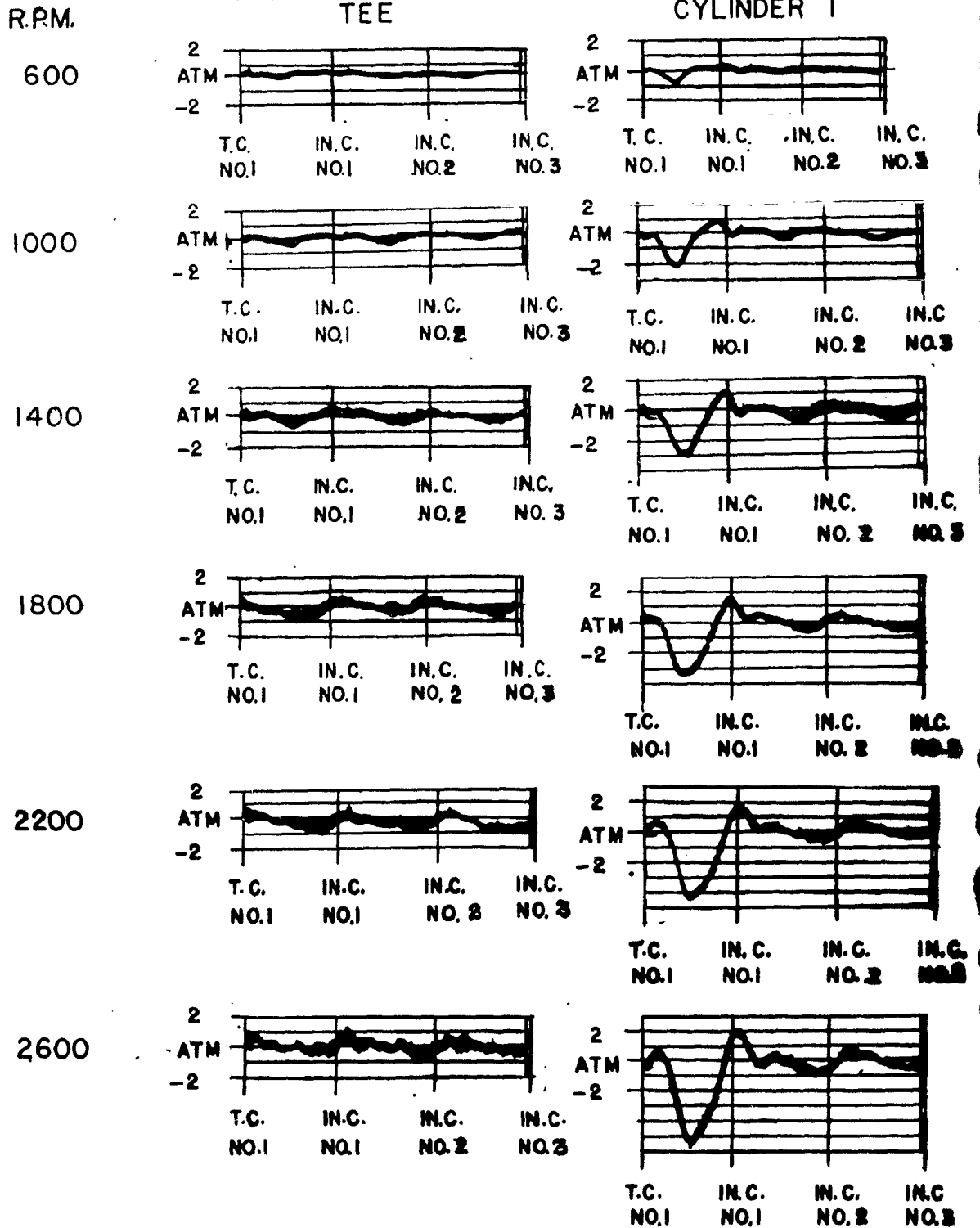


Fig 17

Fig. 17 - Pressure Diagrams, 1" Diameter
Three Cylinder Manifold, 15" Branch
Pipes, 3" Inlet Pipe



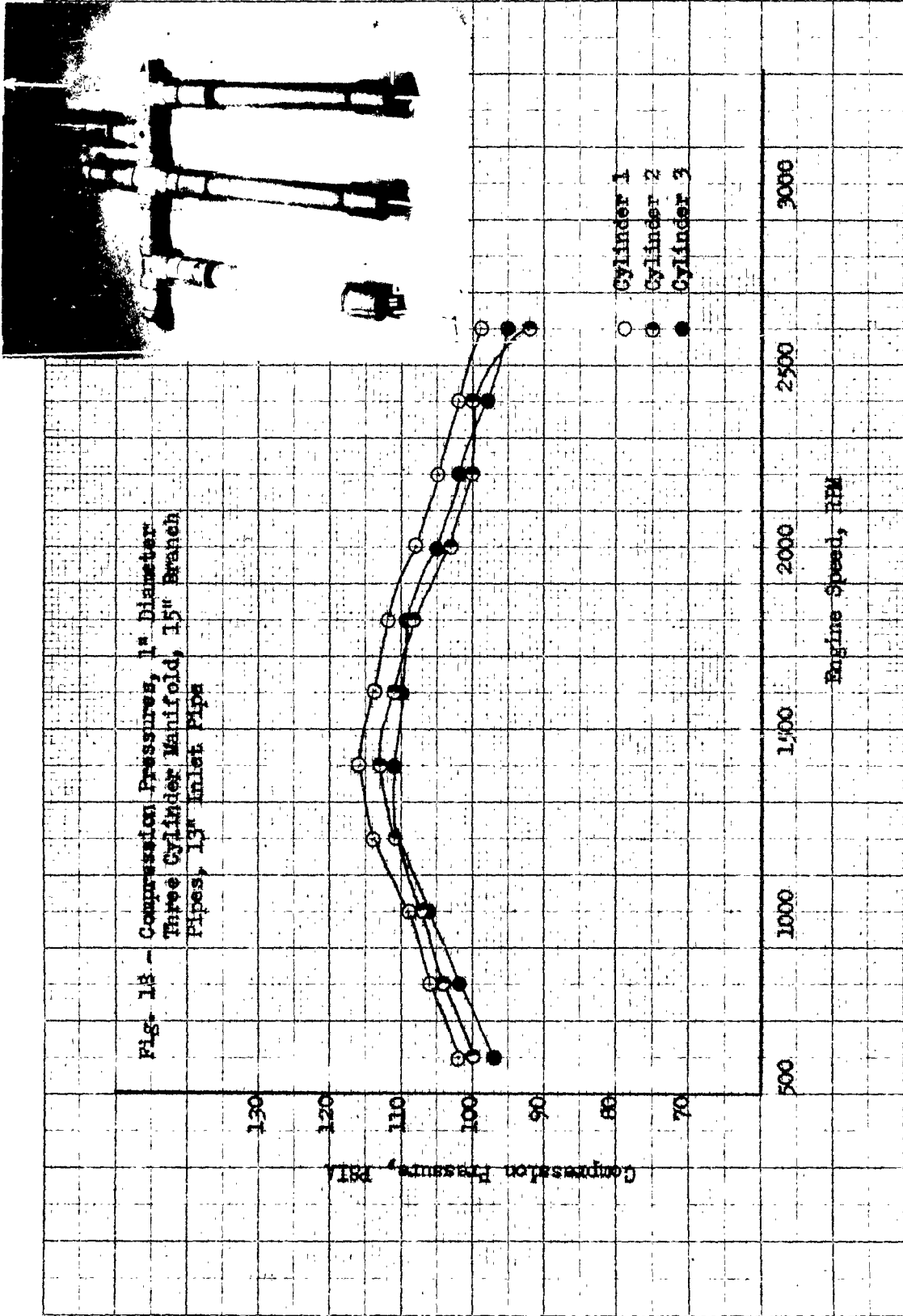


Fig. 19. Pressure Diagrams, 1" Diameter Three Cylinder Manifold, 15" Branch Pipes, 13" Inlet Pipe

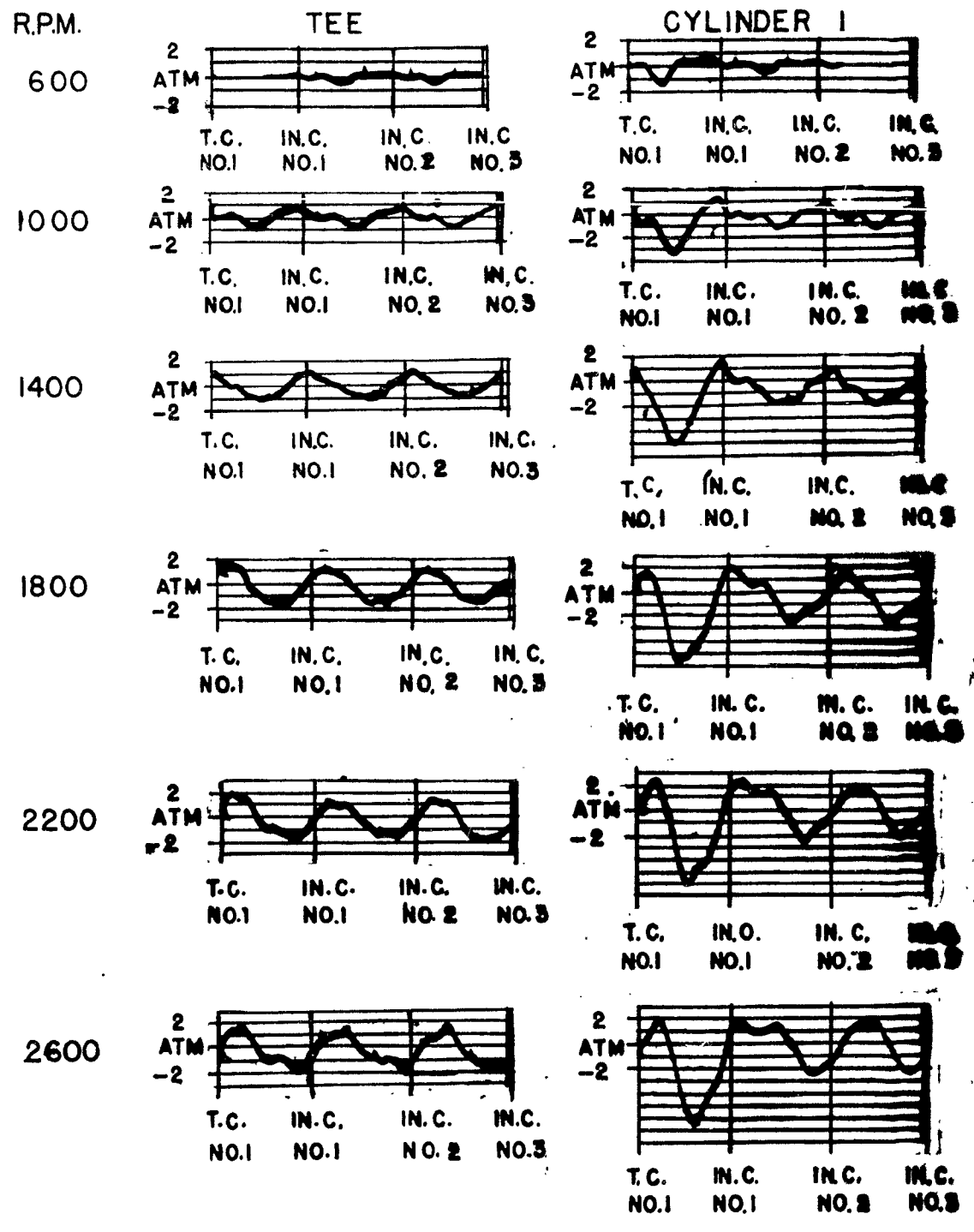
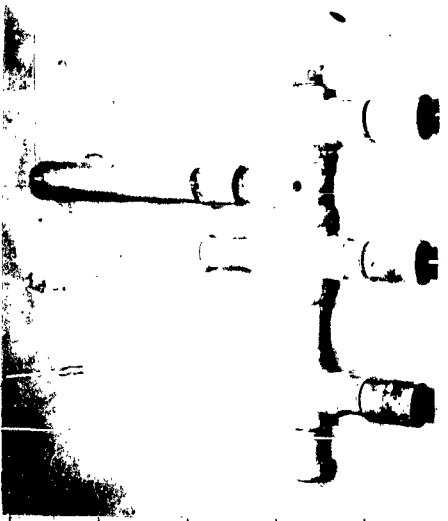
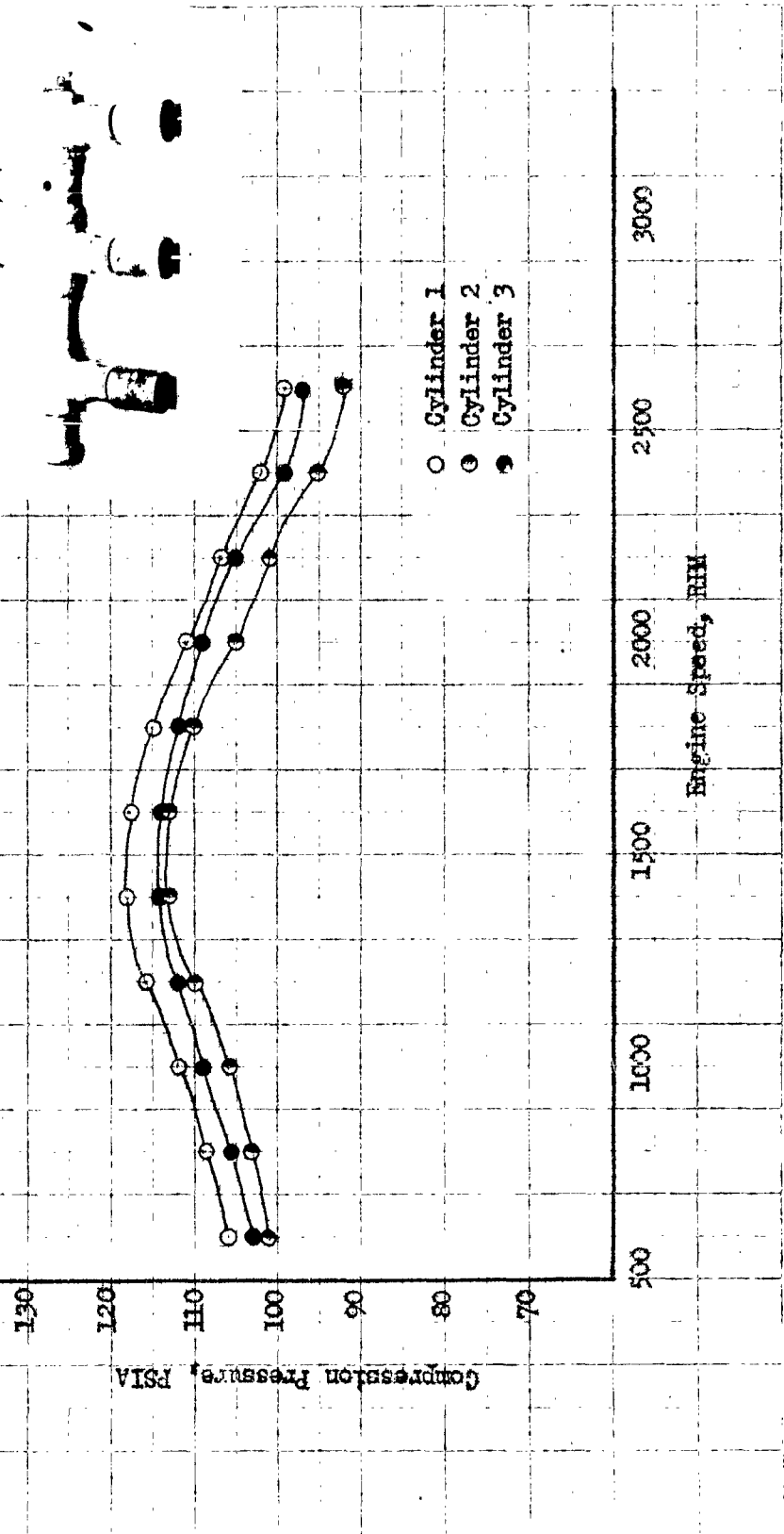




Fig. 20 - Compression Pressures, 1" Diameter Three Cylinder Manifold, 4" Branch Pipes, 1 3/8" Inlet Pipe

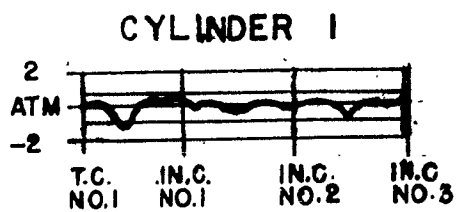
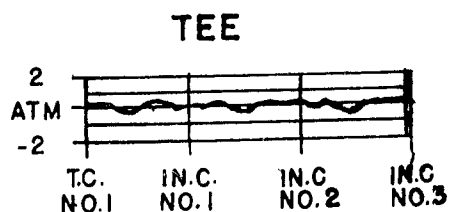


517

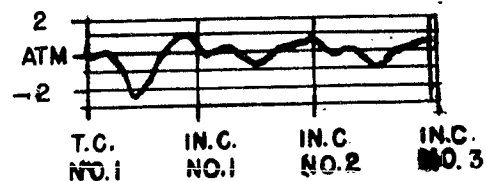
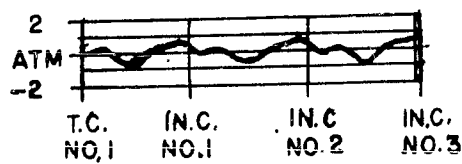
Fig. 21 - Pressure Diagrams, 1" Diameter
Three Cylinder Manifold, 4" Branch
Pipes, 13" Inlet Pipe

R.P.M.

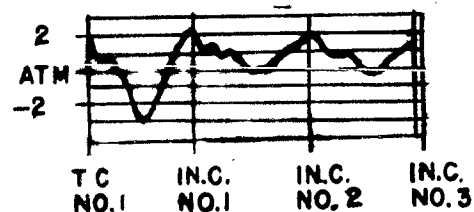
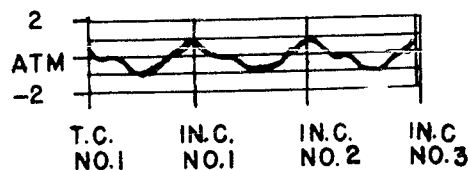
600



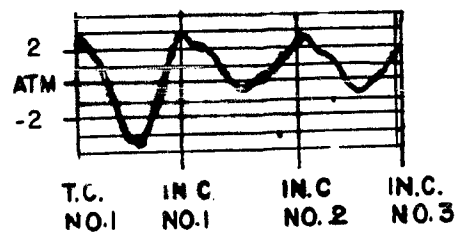
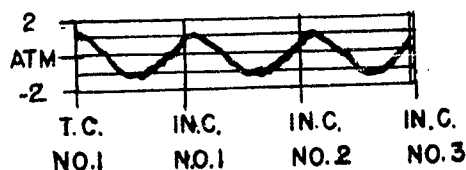
1000



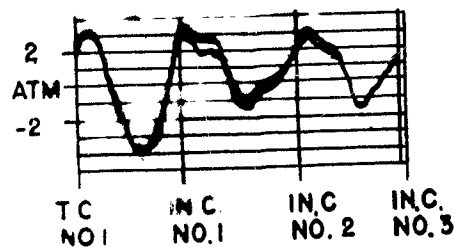
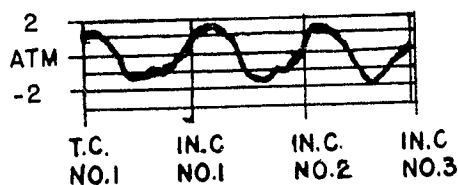
1400



1800



2200



2600

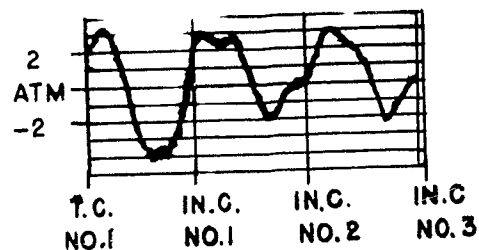
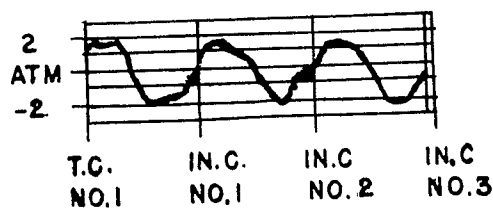




Fig. 22 - Compression Pressures, 1" Diameter Three Cylinder Manifold, 4" Branch Pipes, 3/8" Inlet Pipe

Compression Pressure, PSIA

130
120
110
100
90
80
70

500

1000

1500

2000

2500

3000

Engine Speed, RPM

- Cylinder 1
- ◐ Cylinder 2
- Cylinder 3

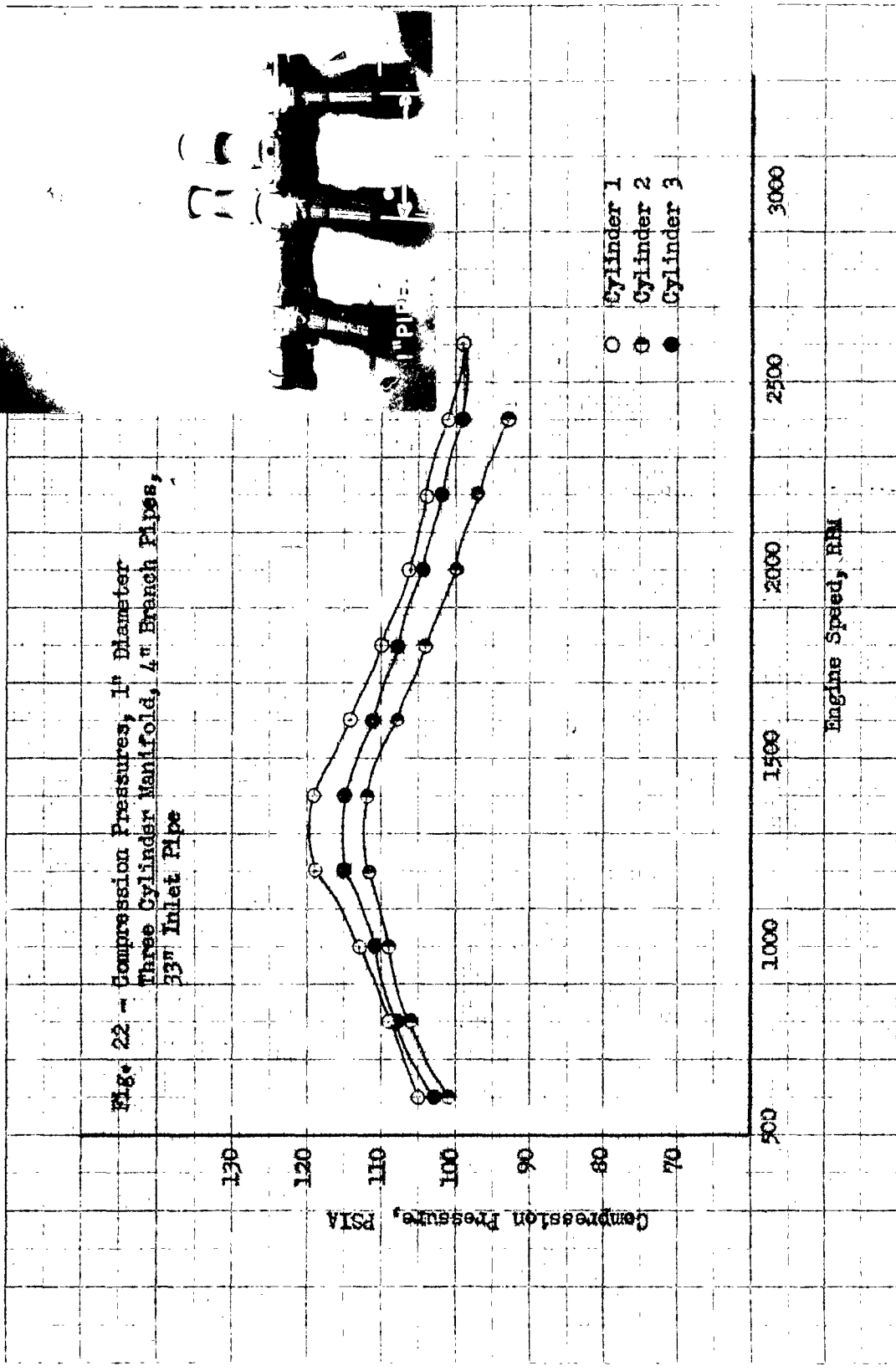
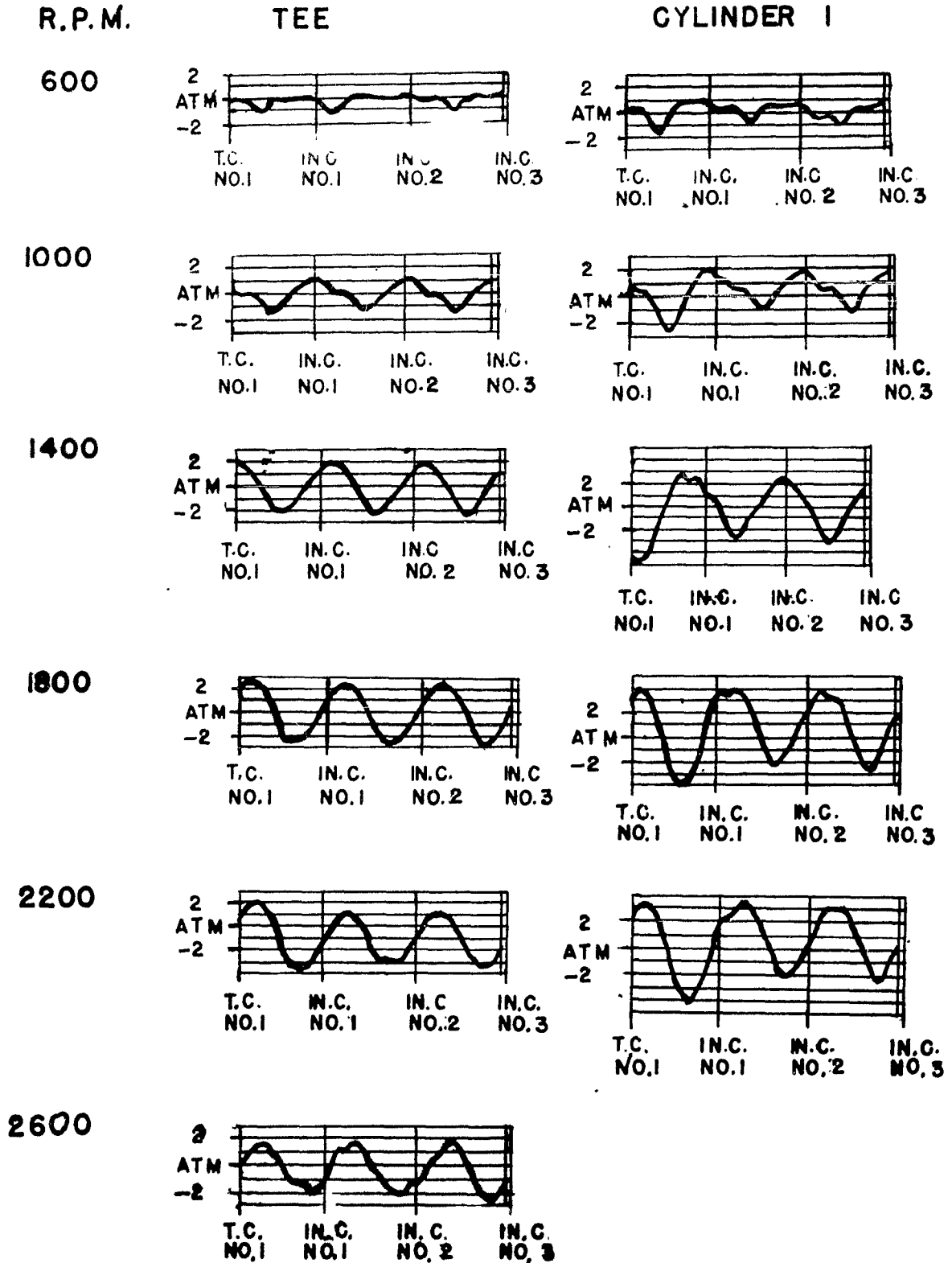
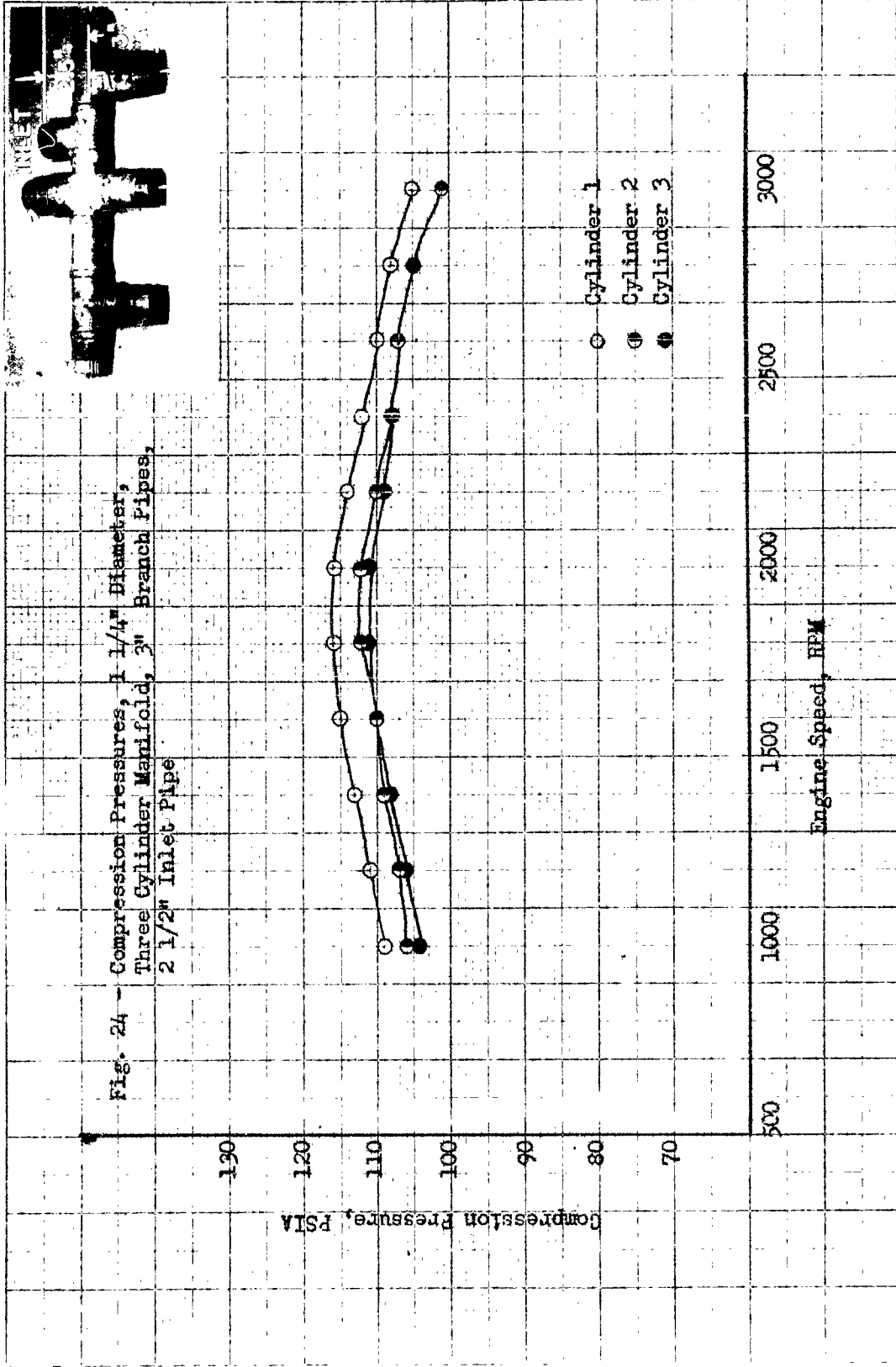


Fig. 23 - Pressure Diagrams, 1" Diameter, Three
Cylinder Manifold, 4" Branch Pipes,
33" Inlet Pipe

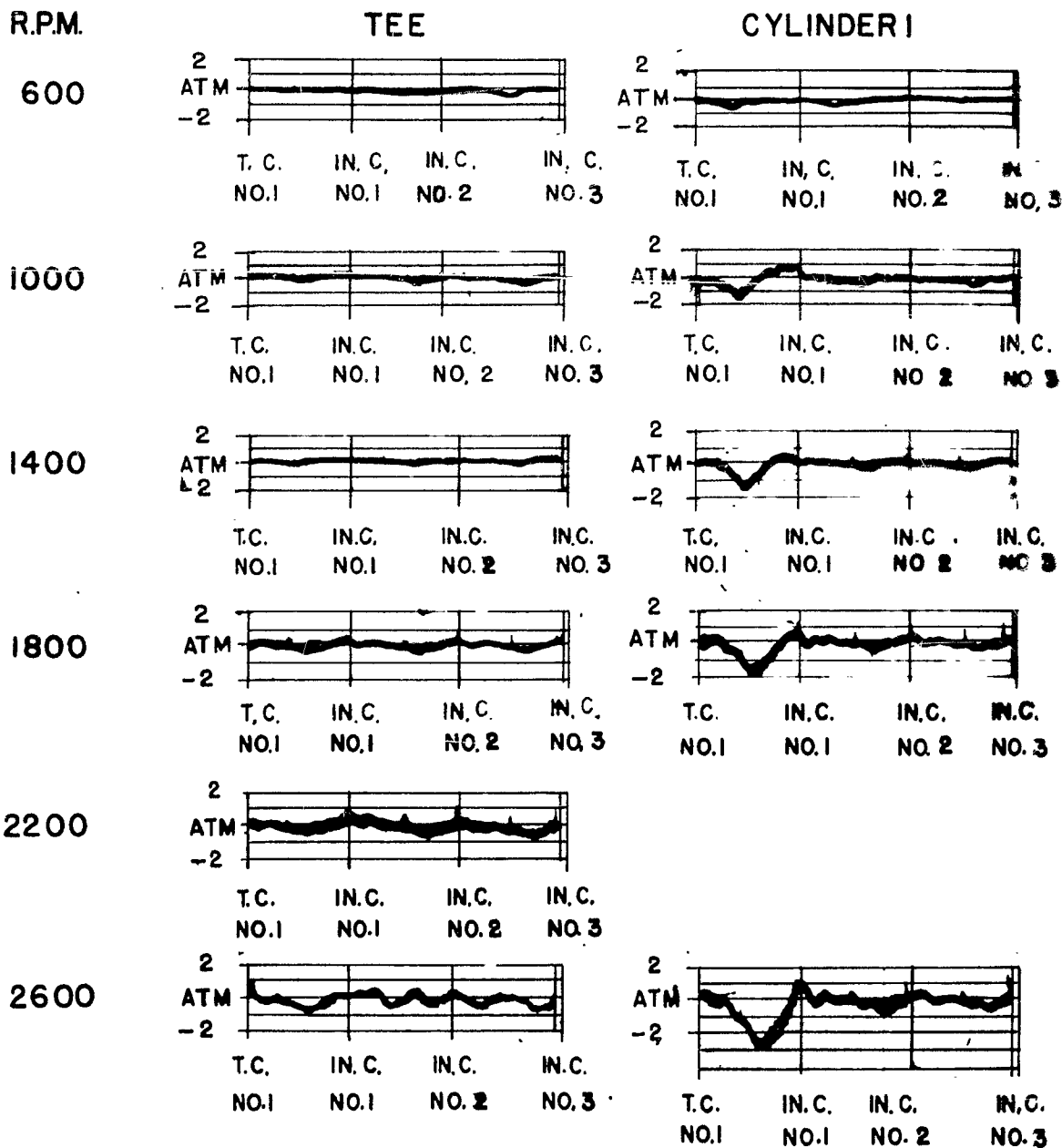


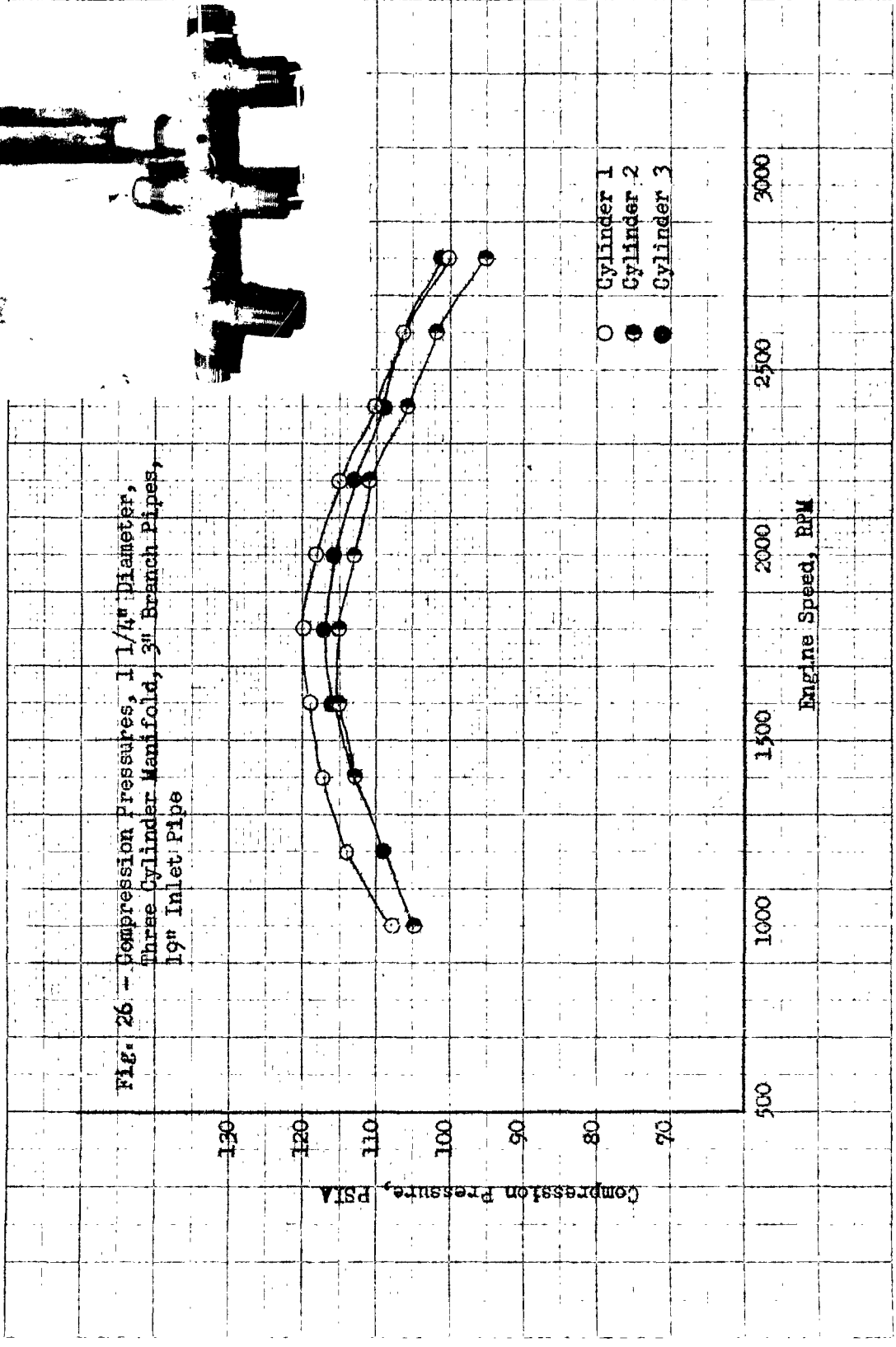


57 W

51X

Fig. 25 - Pressure Diagrams, 1 1/4" Diameter,
Three Manifold, 3" Branch Pipes,
2 1/2" Inlet Pipe





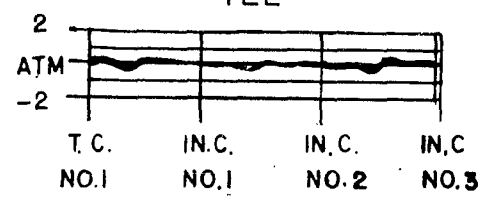
577

Fig. 27 - Pressure Diagrams, 1 1/4" Diameter,
Three Cylinder Manifold, 3" Branch
Pipes, 19" Inlet Pipe

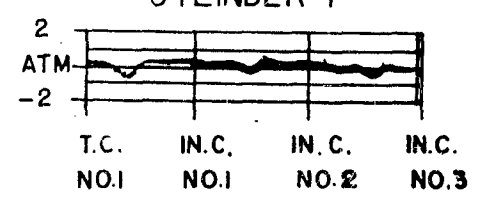
R.P.M.

600

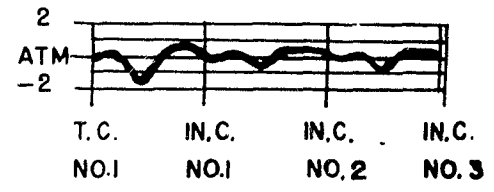
TEE



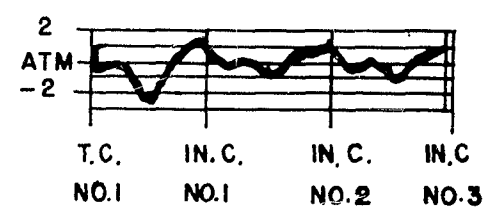
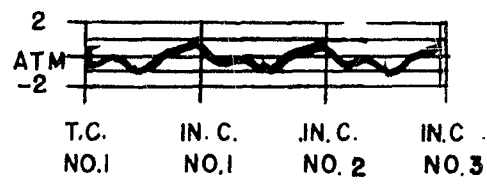
CYLINDER 1



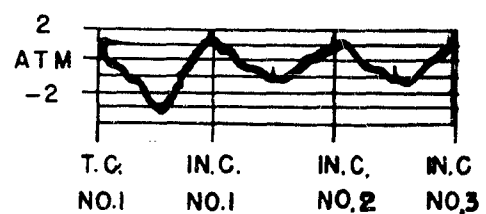
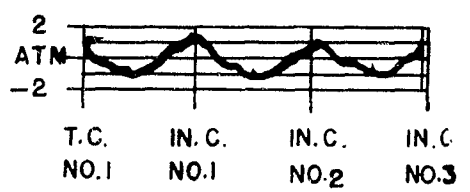
1000



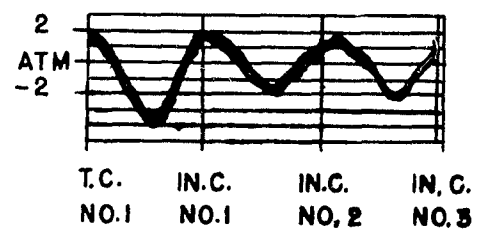
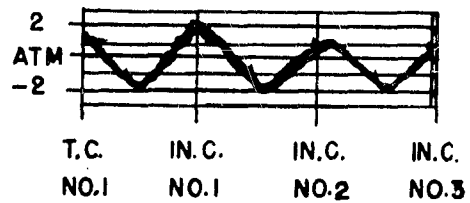
1400



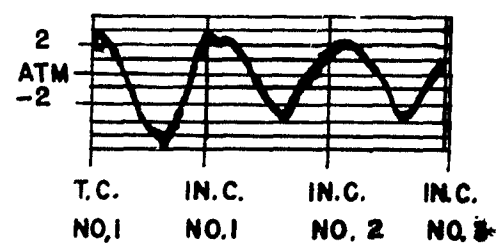
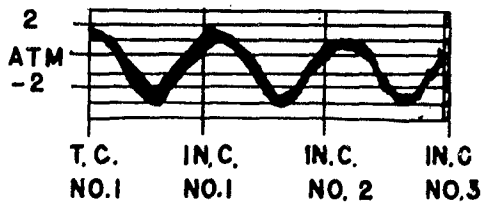
1800



2200



2600



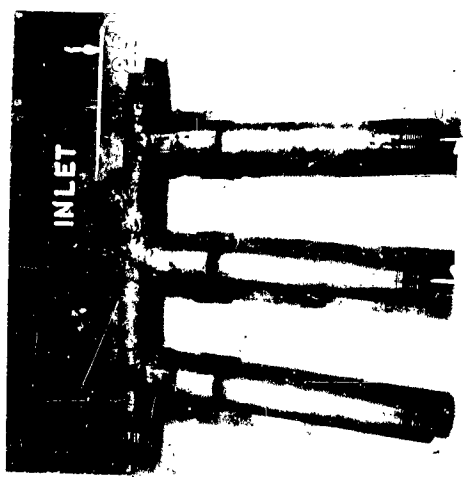
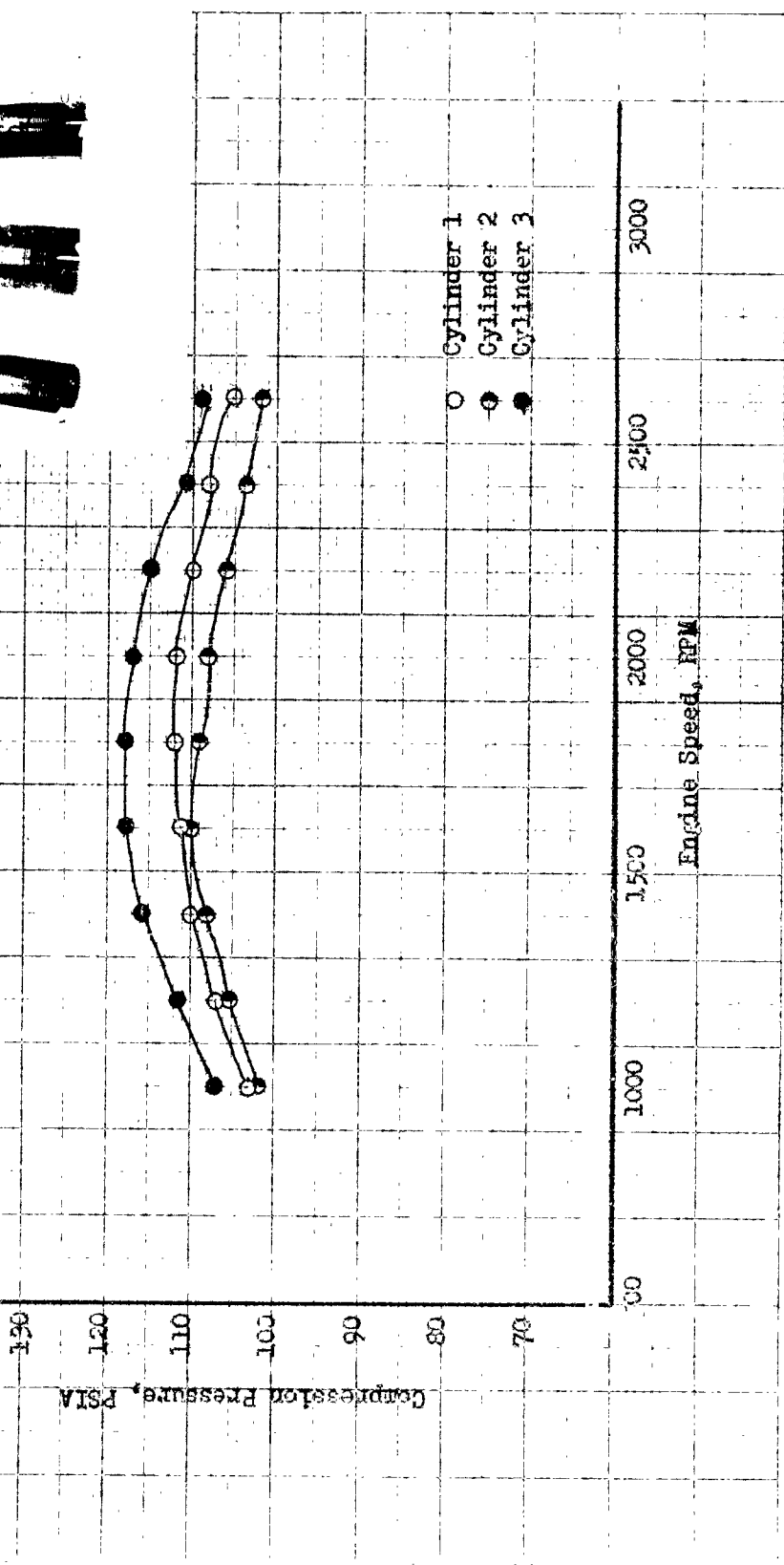


Fig. 28 - Compression Pressures, 1 1/4" Diameter,
Three Cylinder Manifold, 1/4" Branch Pipes,
2 1/2" Inlet Pipe

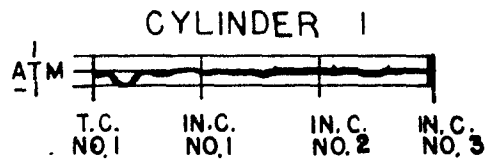
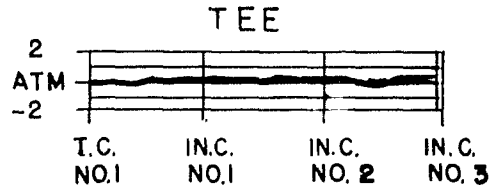


51A

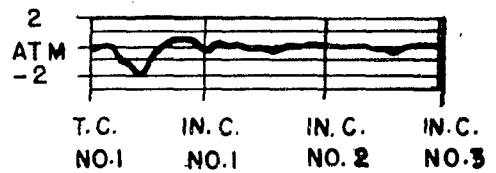
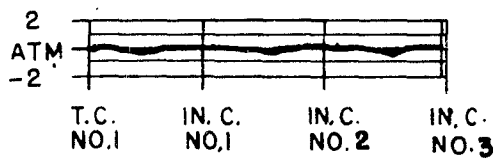
Fig. 29 - Pressure Diagrams, 1 1/4" Diameter,
 Three Cylinder Manifold, 14" Branch
 Pipes, 2 1/2" Inlet Pipe

R.P.M.

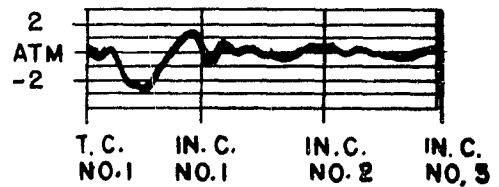
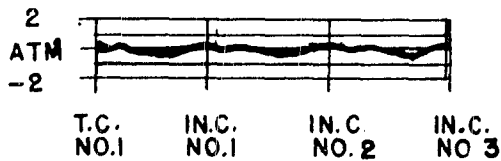
600



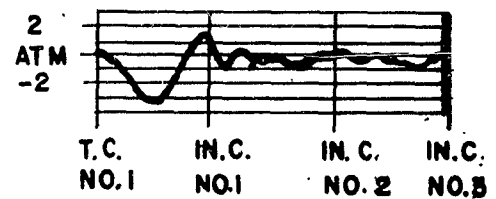
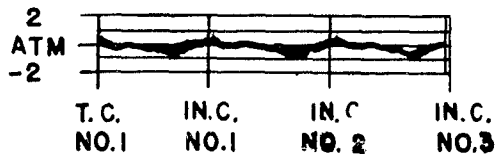
1000



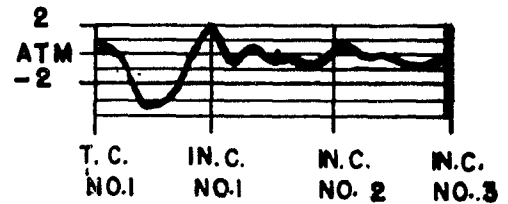
1400



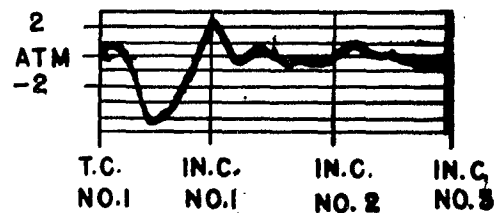
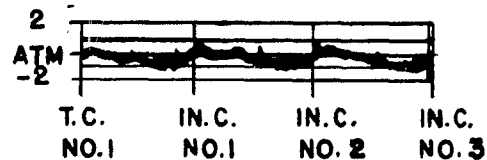
1800



2200



2600



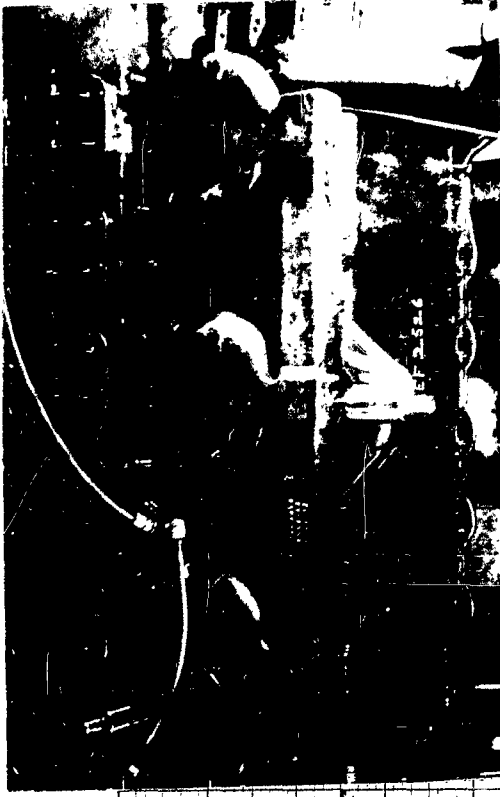
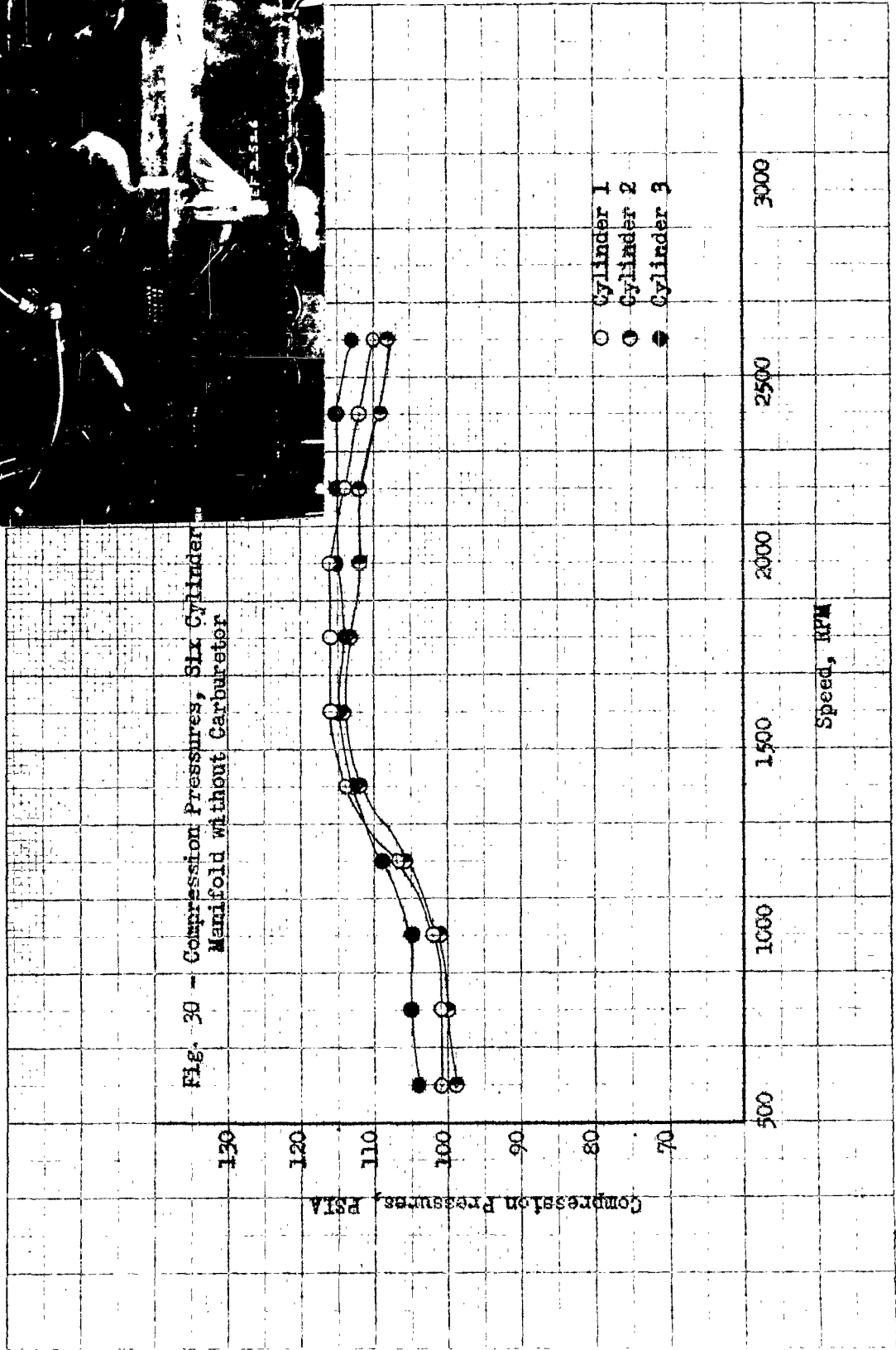
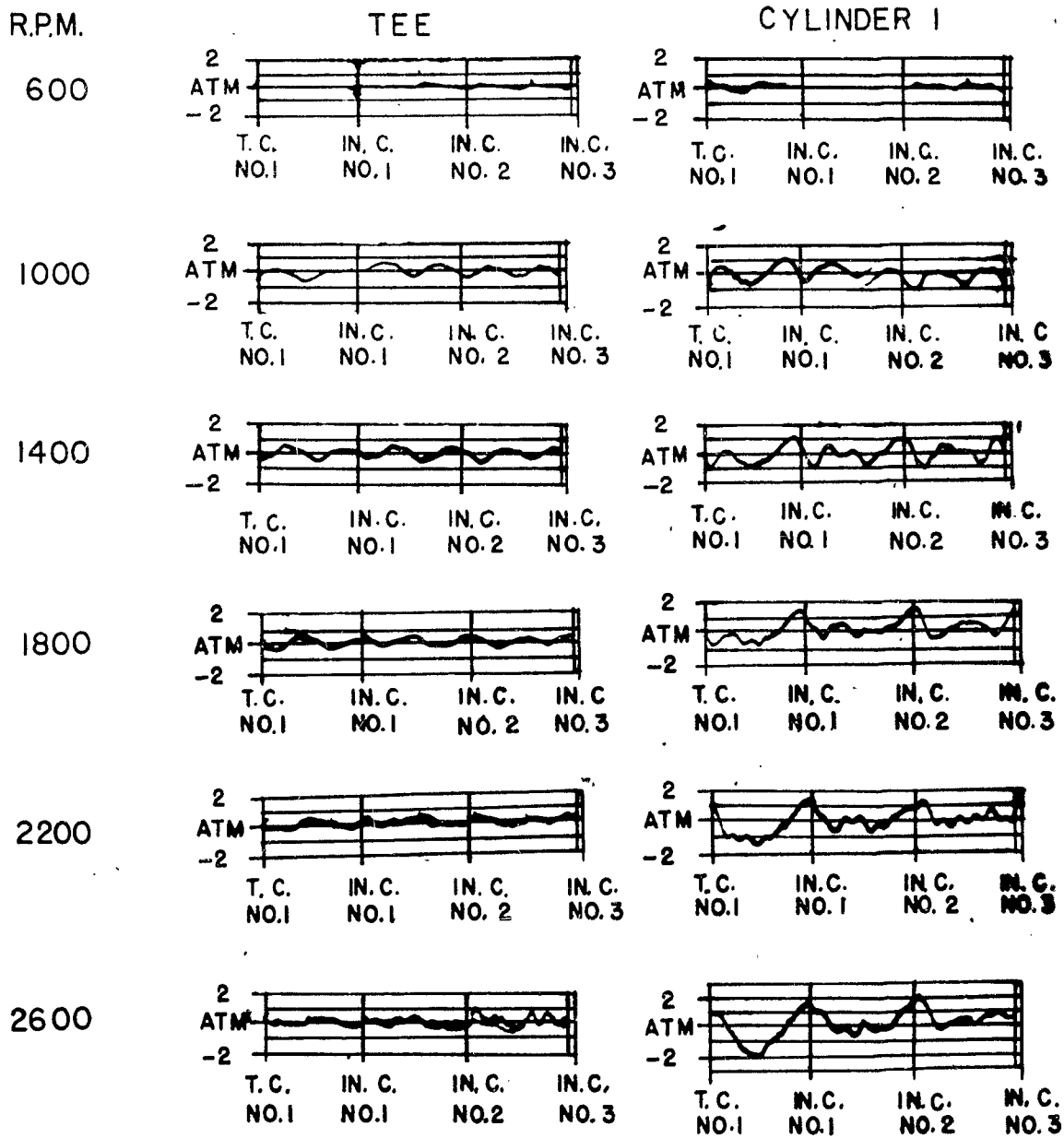


Fig. 30 - Compression Pressures, Six Cylinder Manifold without Carburetor



51 DD

Fig. 31 - Pressure Diagrams, Six Cylinder Manifold Without Carburetor



111 F

Fig. 32 - Pressure Diagrams, Six Cylinder
Manifold Without Carburetor

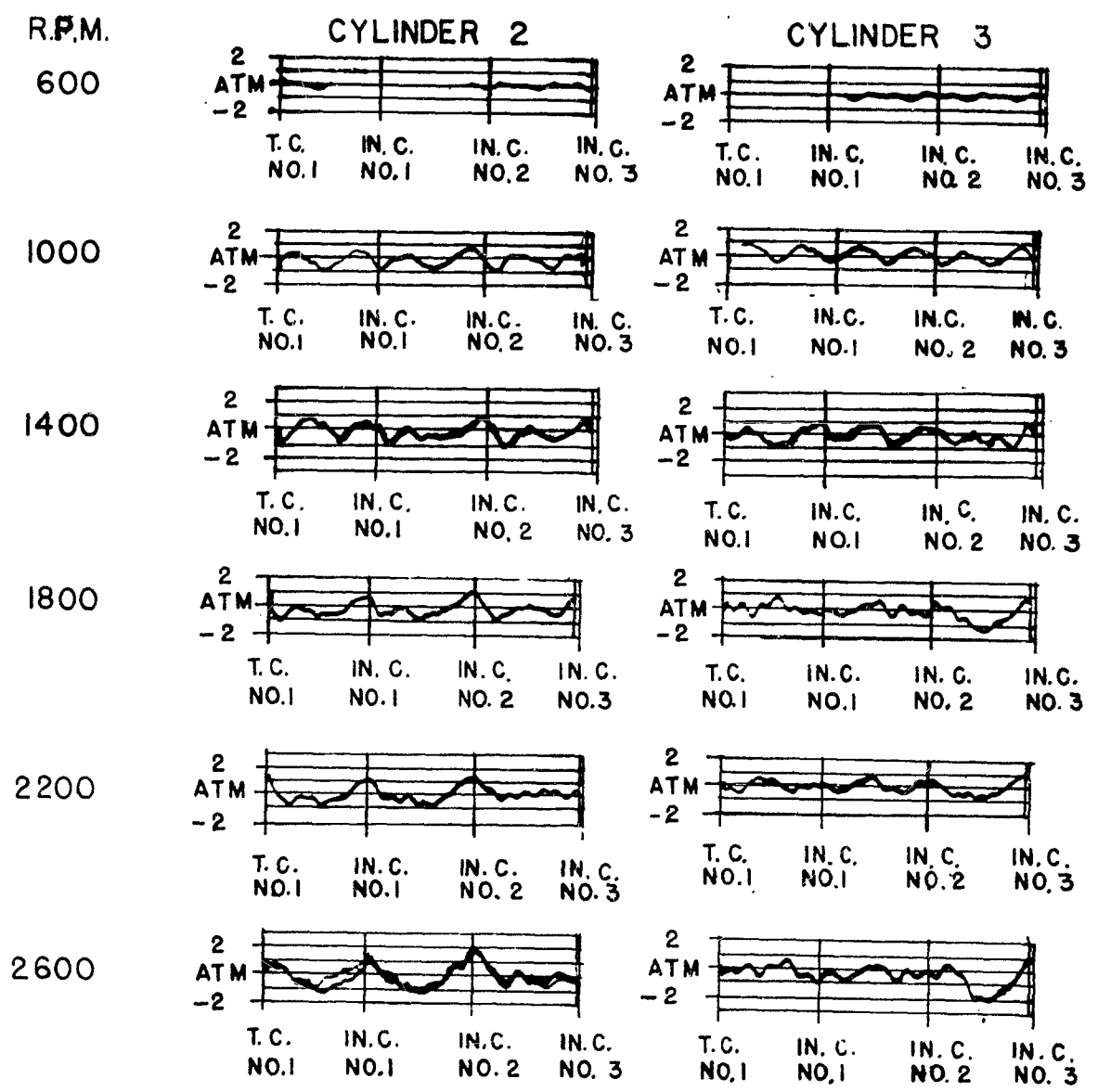
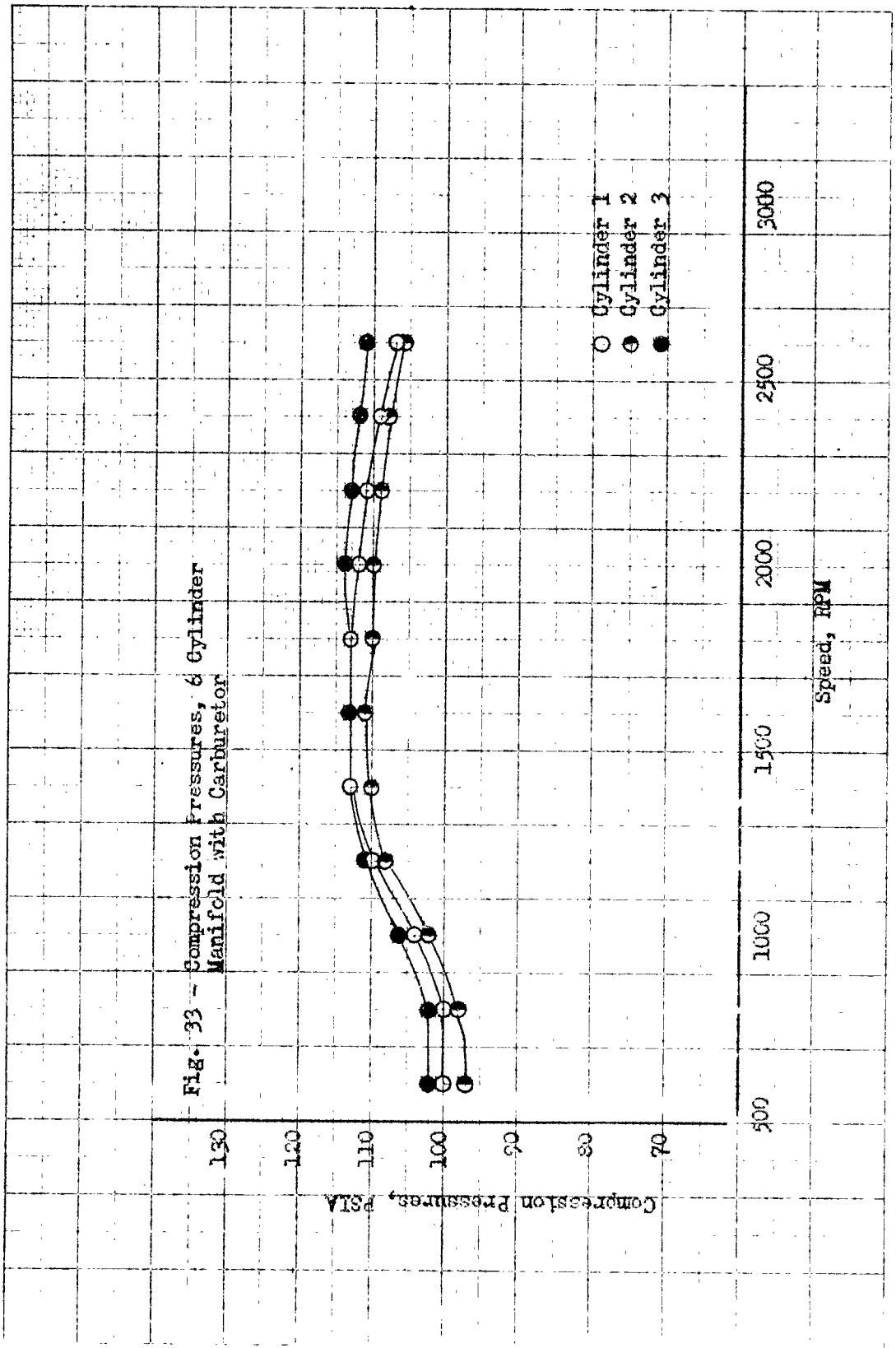


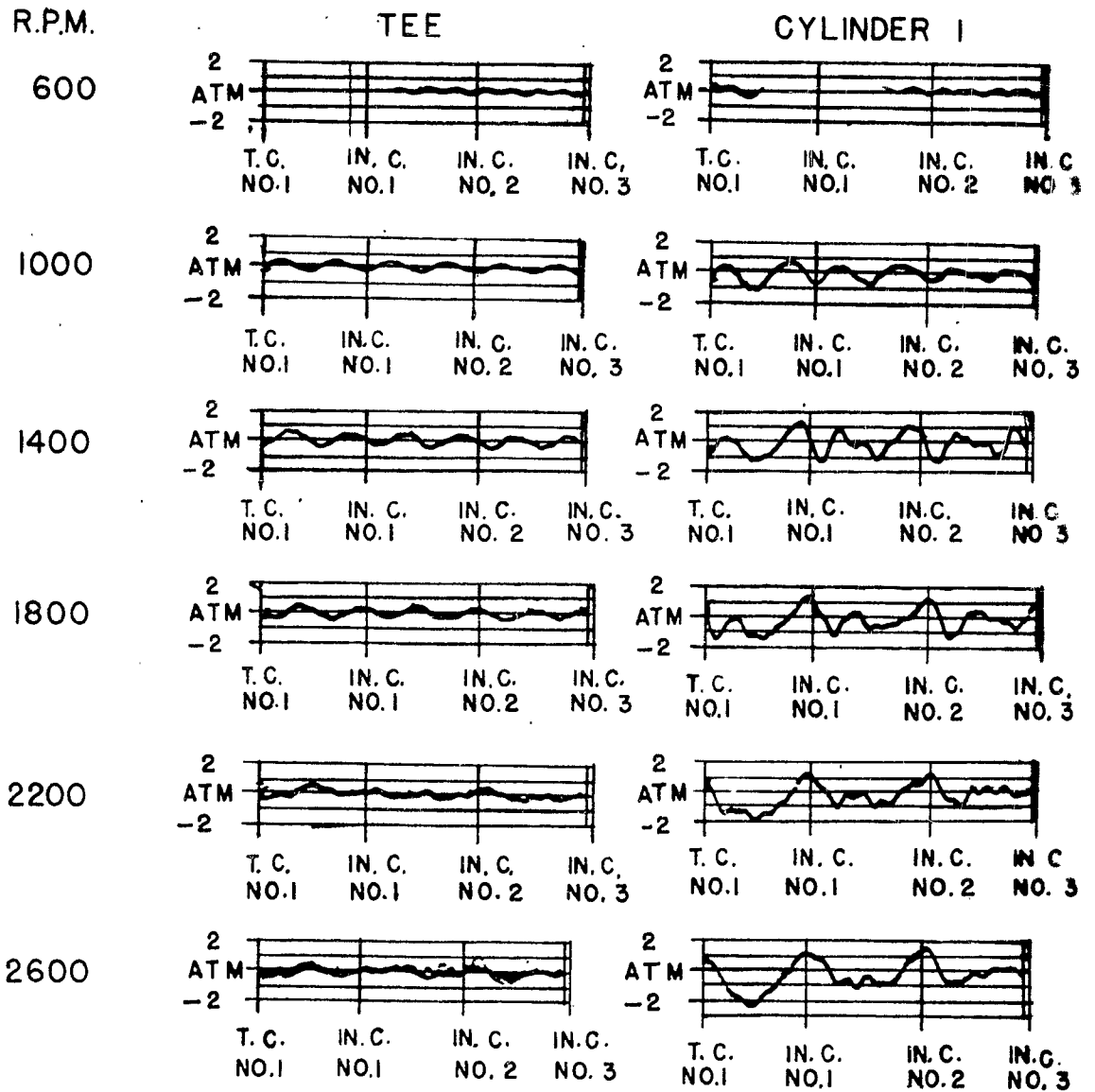


Fig. 33 - Compression Pressures, 6 Cylinder
Manifold with Carburetor



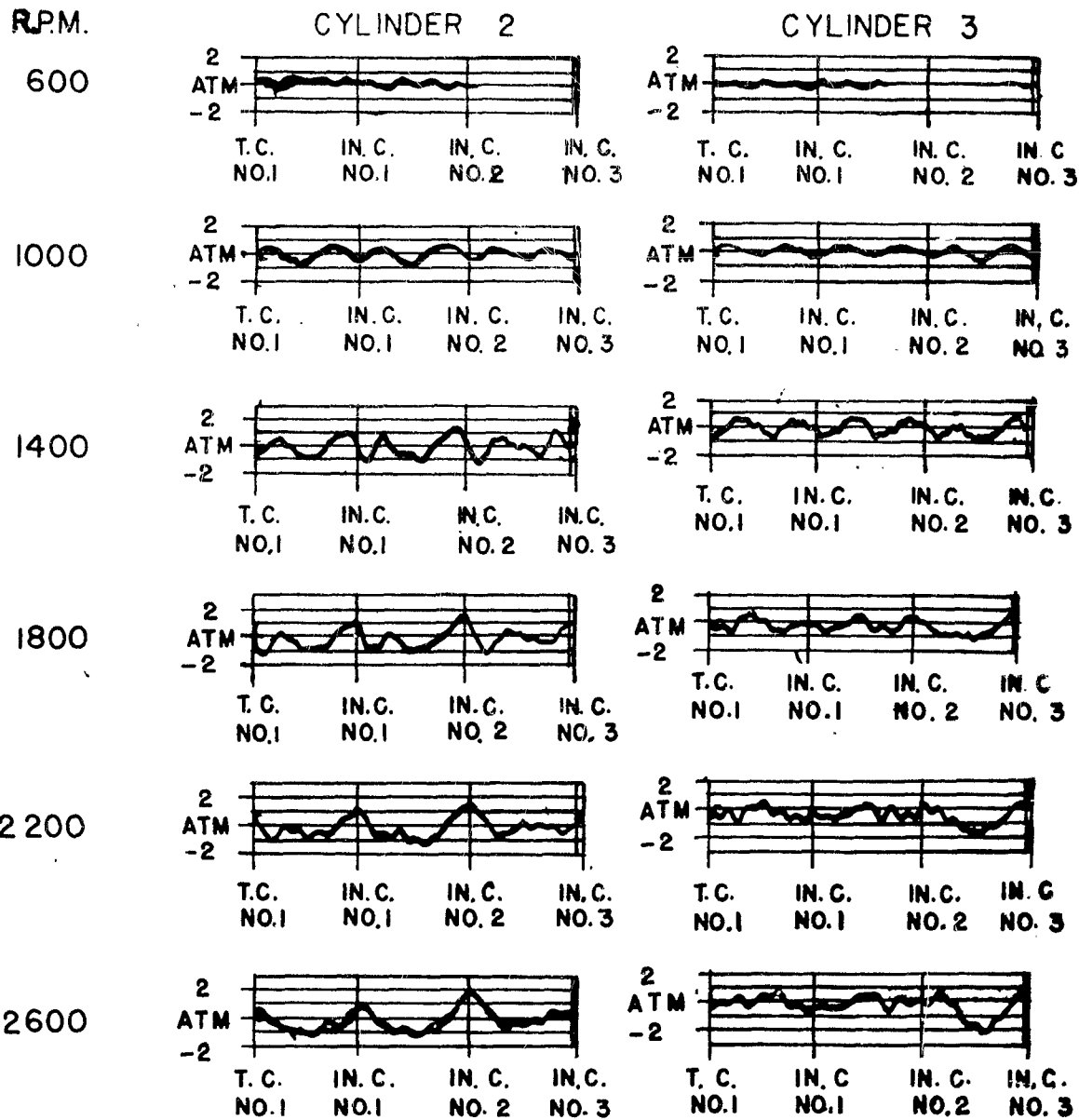
51FF

Fig. 34 - Pressure Diagrams, Six Cylinder
Manifold with Carburetor



51HH

Fig. 35 - Pressure Diagrams, Six Cylinder Manifold with Carburetor





**DEPARTMENT OF DEFENSE
WASHINGTON HEADQUARTERS SERVICES**
1155 DEFENSE PENTAGON
WASHINGTON, DC 20301-1155



Defense Technical Information Center
Attention: William B. Bush
8725 John J. Kingman Road, Ste 0944
Ft. Belvoir, VA 22060-6218

Subject: OSD MDR Case 09-M-0020, DTIC Case No. DTIC-BC

Dear Mr. Bush:

We reviewed the enclosed documents in consultation with the Department of the Air Force and have granted them in full. The information you requested is provided in the table below:

Document Number	Current Controlling Agency	Current Releasing Authority	Current Distribution Control Statement & Reason	Export Control Status
ADB804447	WHS	OSD Records Official	A/Approved for public release; distribution unlimited	A
ADB805158	WHS	OSD Records Official	A/Approved for public release; distribution unlimited	A
ADB815161	WHS	OSD Records Official	A/Approved for public release; distribution unlimited	A
ABD815958	WHS	OSD Records Official	A/Approved for public release; distribution unlimited	A

If you have any questions, contact me by phone at 703-696-2197 or by e-mail at storer.robert@whs.mil or robert.storer@whs.pentagon.smil.mil.

Robert Storer
Chief, Records and Declassification Division

Enclosures:

1. DTIC request
2. MDR request
3. Documents ADB804447, ADB805158, ADB815161, and ABD815958



UNCLASSIFIED / ~~LIMITED~~

ADB804447

Study of Multi-Cylinder Engine Manifolds

PURDUE UNIV LAFAYETTE IN

31 OCT 1944

Distribution authorized to DoD only; Administrative/Operational Use; 03 MAR 1999. Other requests shall be referred to Air Force Materiel Command, Wright-Patterson AFB, OH 45433-6503. Document partially illegible.

Page determined to be Unclassified
Reviewed Ch RDD, WHS

Date: APR 10 2009
IAW EO 12958 Section 3.5

UNCLASSIFIED / ~~LIMITED~~

09-17-0020
DOC 1